Experimental Load Rating of Posted Bridges

by

Michael Chajes
Dennis Mertz
Harry Shenton
Victor Kaliakin
Geoffrey Reichelt
Jonathan Reid

Department of Civil and Environmental Engineering
University of Delaware

December 2002

DELAWARE CENTER FOR TRANSPORTATION

University of Delaware
355 DuPont Hall
Newark, Delaware 19716
(302) 831-1446

Experimental Load Rating of Posted Bridges

by

MICHAEL CHAJES
DENNIS MERTZ
HARRY SHENTON
VICTOR KALIAKIN
GEOFFREY REICHELT
JONATHAN REID

Department of Civil and Environmental Engineering
University of Delaware
Newark, Delaware 19716

DELAWARE CENTER FOR TRANSPORTATION
University of Delaware
Newark, Delaware 19716

This work was sponsored by the Delaware Center for Transportation and was prepared in cooperation with the Delaware Department of Transportation. The contents of this report reflect the views of the authors who are responsible for the facts and accuracy of the data presented herein. The contents do not necessarily reflect the official views of the Delaware Center for Transportation or the Delaware Department of Transportation at the time of publication. This report does not constitute a standard, specification, or regulation.

The Delaware Center for Transportation is a university-wide multi-disciplinary research unit reporting to the Chair of the Department of Civil and Environmental Engineering, and is co-sponsored by the University of Delaware and the Delaware Department of Transportation.

Delaware Center for Transportation
University of Delaware
Newark, DE 19716
(302) 831-1446

Experimental Load Rating of Posted Bridges

Final Report

Report Prepared by:

Michael Chajes
Dennis Mertz
Harry Shenton
Victor Kaliakin
Geoffrey Reichelt
Jonathan Reid.

Department of Civil and Environmental Engineering
University of Delaware

Table of Contents

Report

Appendices

EXECUTIVE SUMMARY

Bridges have traditionally been evaluated and rated using rather simple analytical methods and without the use of site-specific data. It has been found that estimates of a bridges load-carrying capacity made in this manner are typically conservative. Because of the deterioration of our nations bridges, and the growing number of bridges that are being classified as "deficient," it is more important than ever that the estimate of a bridge's capacity be as accurate as possible. In the case of posted bridges, unwarranted postings can impose an unnecessary hardship on the traveling public. Even when a bridge is not posted, low ratings can present a major problem when superloads (permit vehicles) need travel over the bridge.

When it comes to determining a safe and accurate load-carrying capacity for a bridge, the best model of the bridge is the bridge itself. During design of a bridge, we do not have the luxury of utilizing this resource. Fortunately, during subsequent evaluation, we can utilize it. In effect, a field test has been underway since the bridge was opened to traffic. The results of this extended test should be used in assessing the need to restrict loads, retrofit, or replace the bridge. If the bridge remains serviceable after years of service, we should "listen" carefully to the bridge before we decide to restrict traffic or rehabilitate it. By carefully field testing a bridge, we may find that traffic restrictions or repairs are not necessary. By further monitoring of the bridge, we can have a better idea of how "healthy" it is, and whether or not its "health" has changed (i.e., deterioration has occurred).

The primary objective this project was to implement the findings of an initial project titled "Evaluation of Experimental Load Rating of Posted Bridges" to develop a systematic procedure for load rating of Delaware's bridges using field test results. The procedure was developed using results from a prior bridge load test conducted under the

initial project (Bridge 1-138). To demonstrate the procedure, three additional bridges (Bridge's 1-704, 1-788, and 1-791) were selected with the help of DelDOT's Bridge Management Engineers Dennis O'Shea and Darrin Sobota. While none of these bridges are posted, all three are on Interstate-95 and their current load ratings limit the weight of superloads (permit vehicles) allowed to pass through the state on this major route. The field test results of these three bridge tests were used to determine new load ratings for these bridges, thereby illustrating the procedure.

ACKNOWLEDGMENTS

The authors would like to acknowledge the financial support of the Delaware Department of Transportation and the Delaware Transportation Institute for this work. Special thanks to Dennis O'Shea and Darrin Sobota from the Delaware Department of Transportation for their help with this project.

DISCLAIMER

INTRODUCTION

Under the supervision of the four University of Delaware faculty investigators, and with help from Dennis O'Shea and Darrin Sobota from the Delaware Department of Transportation, University of Delaware civil engineering graduate students Geoffrey Reichelt and Jonathan Reid performed much of the experimental and analytical work. This work formed the basis for both of these students M.S. theses. This report is therefore divided into four parts.

First, a consise summary of the load rating procedure and the resulting load rating of Bridges 1-704, 1-791, and 1-788. For completeness, Bridge 1-138, tested in a prior project, is also rated in a similar manner.

Second, in Appendix A, the load rating method is elaborated upon in through a detailed presentation of the method as published in an article by the investigators in the ASCE Bridge Journal. This work is based on the test results for Bridge 1-138.

Third, in Appendix B, the details of the bridge tests on bridges 1-704 and 1-791 are presented in the M.S. thesis of Jonathan Reid.

Finally, in Appendix C, details of the rating of bridges 1-704 and 1-791 based on the field test results are presented in the M.S. thesis of Geoffrey Reichelt.

a summary of the method for experimentally rating bridges based on load tests is presented, followed by the results from The report that follows contains an introduction to the capacity evaluation of bridges in Chapter 1. In Chapter 2, traditional load rating techniques are reviewed. Chapter 3 presents details of diagnostic load testing and how bridge parameters needed for rating can be estimated based upon load test results. Bridge 1-138 is used as an example for this presentation. Chapter 4 presents methods for evaluating bridge load carrying capacity based on load test results. Again,

Bridge 1-138 is used as an example. Chapters 5, 6, and 7 present the complete load test results and bridge capacity evaluation for bridges 1-704, 1-791, and 1-788 respectively. Finally, conclusions are presented in Chapter 8. Included in the conclusions is a discussion of how the results from the testing of a single span can be used to evaluate adjacent spans or parallel "sister" bridges.

SUMMARY OF RATING PROCEDURE AND TEST RESULTS

The following portion of this report contains a consise summary of the load rating procedure and the resulting load rating of Bridges 1-704, 1-791, and 1-788. For completeness, Bridge 1-138 is also rated in a similar manner.

Summary of Capacity Evaluation Based on Load Test Data

Traditional bridge ratings are based upon simplified non-site specific analytical models of a bridge. By conducting a field test, several of the assumed parameters used to define the bridges structural response can be directly evaluated and incorporated into the existing analytical model being used for bridge rating. In Delaware, the analytical model used in rating girder bridges (the mnodel used in BRASS) a simple beam. The follwoing steps represent the suggested procedure for capacity evaluation of girder bridges based on load test data. Other bridge types should also be abale to be handled in an analogous manner.

Step-1) A load test is performed in which a pre-weighed vehicle (or vehicles) is driven very slowly (no impact) across an instrumented bridge and the bridge response is recorded.

Step-2) Immediately following a bridge test, one can determine whether or not a bridge has a higher capacity than currently predicted. This is done by comparing the peak live load stress caused by the test truck (as determined from the peak live load strain measured) to the value predicted by the analytical model for that same test truck. The predicted value of stress is computed using BRASS. No load factors or impact factors are used so that the results are consistent with the test results. For example, the predicted peak bending stress for Bridge 1-704 due to the test truck was 5.35 ksi, while the peak bending stress measured was 2.96 ksi. This immediately indicates that the bridge is 1.80 times stiffer than the model currently being used for rating.

Step 3) If the current model is not accurately predicting the true response, the data collected is used to evaluate a few significant bridge parameters. These parameters include (1) the lateral load distribution as defined in many cases by a distribution factor (DF), (2) the amount of unintended support restraint, and (3) the flexural stiffness of the superstructure elements including the existence or non-existence of composite action. In addition, in some cases it may be possible to assess the dynamic effects that are typically approximated using the live load impact factor (I). Another factor that can caused the measured strain to be significantly lower than expected is the effect of longitudinal load distribution caused by fill or concrete slabs between the wearing surface and the superstructure. This effect can be hard to evalaute exactly, but can possibly be incorporated by applying an approporiate uniform live load (as suggested by AASHTO) in place of wheel loads.

Step 4) Using the bridge parameters determined from the field test, the analytical model is refined. This involves incorporating the parameters directly into the BRASS data file. The refined BRASS model is then used to re-evaluate the predicted response due to the test truck. Since only a few of the most important bridge parameters are evaluated, it is likely that the refined model will not exactly predict the measured response (for example, the effects of the parapet or fill may be hard to explicitly

quantify). In any event, the new model should be more accurate than the existing model. In the case of Bridge 1-704, the refined model predicted a peak stress of 3.46 ksi, meaning it accounted for 1.55 of the 1.80 increase in stiffness (i.e. 25% of the measured increase in stiffness remained unexplained).

Step 5) Of the explained portion of the stiffness increase, one must decide how much to count on in the final rating. This is done by considering each of the identified parameter seperately, and making rational decisions. For example, one can generally count on the entire amount of added stiffness due to better than assumed transverse load distribution, while one may not want to count on any of the added stiffness caused by unintended support restraint (possibly caused by frozen bearings).

Step 6) Like the explained stiffness increase, one must decide how much if any of the unexplained stiffness increase to count upon. The most conservative assumption would be to not count on any of the unexplained stiffness increase. However, if a large amount of unexplained stiffness exists, there is one existing method that can be adapted to suggest how to handle this. This method is presented by A.G. Lichtenstein in the "Manual for Bridge Rating Through Load Testing" (NCHRP 12-38(13)A Final Report). In the end it may be wise to have an upper bound on how much of the entire increase in stiffness should be allowed in the final rating.

Step 7) The bridge is rated using the updated BRASS model. In the case of Bridge 1-704, the load ratings will increase by a factor of 1.55 if only the explained portion of the increase in stiffness is counted upon. It should be noted that whatever refined BRASS model is used, it should be checked to make sure that is conservative compared to the actual bridge response (i.e. the refined model must always predict more stress than the amount measured).

Please note that while a method for accounting for the unexplained stiffness increase is presented in the body of the report, in the final ratings that follow, only the explained portion of the improved response was included. This was done to give a

conservative rating. Should DelDOT choose to include some of the unexplained benefit, that would certainly be justifiable. Thsi can simply be done by scaling the distribution factor accordingly.

Summary of Bridge 1-704 Field Test Results

On October 30, 1995, the University of Delaware load tested the center span of the Christina Creek bridge (1-704). The bridge is located on I-95 near the Maryland border and just north of Route 896. The bridge is a three-span, simply-supported, slab-on-steel-girder bridge with a 13 degree skew. It was designed compositely with shear connectors between the steel girders and concrete deck. The bridge crosses over the Christina Creek, which is a nearly stagnant body of water with a width of 40 ft and depth of 3 ft to 4 ft under the span.

The southbound span consists of four traffic lanes, two breakdown lanes, and one exit lane and is responsible for carrying large amounts of commuter traffic between Wilmington, DE and Maryland. Since its original completion date, three construction changes have been made to the bridge to support the growing amount of traffic. All three changes entailed adding two girders to the existing span to increase the width. The first and third added two to the southern-most side, and the second added two to the northern-most side, increasing the span width from 41'8" to 57' 4" for the first addition, 57' 4" to 67' 10" for the second addition, and 67' 10" to 80' 10" for the third. As a result of the new construction, there is non-symmetrical spacing between the different girders ranging from 5' 3" to 8' 4". At its present state, it is 80'-10" wide from centerline to centerline of the outside girders. The approach spans are each 24'-7" while the main span is 63'-2".

DelDOT identified this bridge for testing due to limited capacity for overload (permit) vehicles. Only the center span of the southbound bridge was evaluated.

The instrumentation of this bridge consisted of 32 strain transducers to measure the strains in the top and bottom flanges of the girders. In the test, a total of

eight passes were made by one three-axle dump truck weighing a total of 34 tons. Six of the passes were semi-static. Four different paths were used. Two of those passes were duplicated to check data redundancy. The last two passes were dynamic, meaning the truck's speed was approximately 55 mph as it crossed the bridge.

The predicted peak bending stress for Bridge 1-704 due to the test truck was 4.87 ksi, while the peak bending stress measured was 2.96 ksi (peak strain of 102 με). This immediately indicates that the bridge is 1.65 times stiffer than the model currently being used for rating.

Based on the field test data, it was determined that the actual multiple lane DF was 0.98 as compared to the AASHTO value of 1.318. No support fixity was found, and the flexural stiffness of the girders was found to be consistent with design values.

The refined BRASS model (DF=0.98) predicted a peak field test stress of 3.46 ksi, meaning it accounts for 1.41 of the 1.65 increase in stiffness (i.e. 24% of the measured increase in stiffness remained unexplained).

Finally, rating of the bridge using the refined BRASS model and including only the explained increase in stiffness due to better than expected load distribution (see existing and refined data files below, changes in **bold**) leads to the revised load ratings shown in Table 1. The revised load ratings are 1.55 higher than the original ratings. If one wanted to include the entire measured increase in stiffness, one would use a DF=0.84.

Since the approach span has the same girder spacing (although smaller girders), it can be assumed that the distribution benefits will be similar, and the same measured distribution factor for the center span can be used for the approach span. In this case, it would be wise to not count on any of the unexplained portion of the stiffness increase. Furthermore, the sister bridge (1-705, northbound) has a similar design and can be assumed to behave similar to this structure. These recommendations is further discussed in the reports Conclusions.

Table 1. Bridge 1-704 Load Ratings

Rating Vehicle	Original Rating Factors From BRASS			Revised Rating Factors From BRASS		
	Inv.	Oper.	Post.	Inv.	Oper.	Post.
HS20T	1.17	2.70		1.65	3.81	2.37
S220	1.99	4.60		2.81	6.48	4.03
S335	1.07	2.45		1.50	3.46	2.15
S437	1.03	2.37		1.45	3.35	2.08
T330	1.63	3.75		2.29	5.29	3.29
T435	1.48	3.40		2.08	4.80	2.99
T540	1.30	2.99		1.83	4.22	2.63

Pre-Load Test BRASS Data File (1-704)

```
 TLE BRIDGE NO. 1-704, TURNPIKE BRIDGE OVER CHRISTINA (WESTBOUND)
 TLE SPAN # 2 OF 3 SPAN CSC BRIDGE, CONTRACT # 7002 (S4)
 COM *NOTE*: This File was modified on 08/08/95. Refer to Further comments
COM *NOTE*: This is DelDOT's existing data file before the load test
ANL 1,0,4
XST 1, WN36X150
XSA 1,32
XSC 90.0,7.5,0.55,0,0,0
XST 2,WN36X150
XSA 2,32
XSC 90.0,7.5,0.55,14.0,0.875,0
SPA 1,63.14,5
SPC 1,7.07,1,2
SPD 56.07,2,1,63.14,1
FIX 1,1,0,0,1,0
PS1  , ,3
PS2 10, ,33
COM WIDENING CONTRACT 7058 DOESN'T CONTROL.
COM DEAD LOADS STAGE 1: SLAB = 782 LB/FT, HAUNCH = 32 LB/FT
COM DEAD LOADS STAGE 2: P.PET= 191 #/', 2 " H.MIX = 167 LB/FT
DLD 1,0.814,0.358
LDE 1, , ,DIAPHRAGM DEAD LOAD
PTD  ,0.355,1,18.0
PTD  ,0.355,1,42.0
COM  *NOTE*: Live Load Dist. Factor Changed to 1.381 from 1.515
COM as per 1994 AASHTO Specs.
LLD 2, 1.381, ,50.0
TR1    HS20T,S220,S335,S437,T330,T435
TR2    T540
DES 3, 1
COM WS Parameters were Replaced with LF on 08/08/95
INV 1.3, 1.0, 1.67, 1.0, 1.0, 1.0
OPG 1.0, 1.0, 1.67, 1.0, 1.0, 1.0
COM POSTING LEVEL 3
PST 1.3, 1.0, 1.00, 1.0, 1.0, 1.0
SLD 1.0, 1.0, 1.0, 1.0, 1.0, 1.0
SL1 100,4
SL1 104,4
SL1 105,4
```

Post-Load Test BRASS Data File (1-704)

```
 TLE BRIDGE NO. 1-704, TURNPIKE BRIDGE OVER CHRISTINA (WESTBOUND)
TLE SPAN # 2 OF 3 SPAN CSC BRIDGE, CONTRACT # 7002 (S4)
COM *NOTE*: This file was modified based on the 10/30/95 load test.
ANL 1,0,4
XST 1, WN36X150
XSA 1,32
XSC 90.0,7.5,0.55,0,0,0
XST 2,WN36X150
XSA 2,32
XSC 90.0,7.5,0.55,14.0,0.875,0
SPA 1,63.14,5
SPC 1,7.07,1,2
SPD 56.07,2,1,63.14,1
FIX 1,1,0,0,1,0
PS1  , ,3
PS2 10, ,33
COM WIDENING CONTRACT 7058 DOESN'T CONTROL.
COM DEAD LOADS STAGE 1: SLAB = 782 LB/FT, HAUNCH = 32 LB/FT
COM DEAD LOADS STAGE 2: P.PET= 191 #/', 2 " H.MIX = 167 LB/FT
DLD 1,0.814,0.358
LDE 1, , ,DIAPHRAGM DEAD LOAD
PTD  ,0.355,1,18.0
PTD  ,0.355,1,42.0
COM *NOTE*: Based on analysis of the load test results,
COM *NOTE*: the DF was changed from 1.381 to 0.98.
LLD 2, 0.98, ,50.0
TR1    HS20T,S220,S335,S437,T330,T435
TR2    T540
DES 3, 1
COM WS Parameters were Replaced with LF on 08/08/95
INV 1.3, 1.0, 1.67, 1.0, 1.0, 1.0
OPG 1.0, 1.0, 1.67, 1.0, 1.0, 1.0
COM POSTING LEVEL 3
PST 1.3, 1.0, 1.00, 1.0, 1.0, 1.0
SLD 1.0, 1.0, 1.0, 1.0, 1.0, 1.0
SL1 100,4
SL1 104,4
SL1 105,4
```

Summary of Bridge 1-791 Field Test Results

On October 31, 1995, the University of Delaware load tested the southern most and central span of Bridge 1-791 (northbound bridge), located north of Wilmington on I-95, and crossing Darley Road. The bridge is a three-span continuous slab-on-steel-girder structure with a composite main span and non-composite approach spans. The northbound span consists of 2 traffic lanes and one breakdown lane and carries a large amount of traffic between Philadelphia, PA and Wilmington, DE. The approach spans each measure 35'-0", and the main span measures 58'-0". The overall width from centerline to centerline of the exterior girders is 35'-10".

DelDOT identified this bridge for testing due to limited capacity for overload (permit) vehicles. For rating, only the center span of the northbound bridge was evaluated, since moment in this span governs the current loading.

The instrumentation of this bridge consisted of 32 strain transducers to measure the strains in the top and bottom flanges of the girders. In the test, a total of eight passes were made by the same testing vehicle used to test the Christina Creek bridge the previous day (34 ton three-axle dump truck). Six of the eight passes were semi-static. Three load paths were chosen with each path being tested twice for the test of data redundancy. The last two passes on this bridge were dynamic as well with the truck maintaining a speed of approximately 55 mph.

The predicted peak bending stress for Bridge 1-791 due to the test truck was 7.96 ksi, while the peak bending stress that was measured was 3.86 ksi (peak strain of 134 $\mu\varepsilon$). This immediately indicates that the bridge is 2.06 times stiffer than the model currently being used for rating.

Based on the field test data, it was determined that the actual multiple lane DF was 0.94 as compared to the AASHTO value of 1.30. No support fixity was found, and the flexural stiffness of the girders was found to be consistent with design values.

The refined BRASS model (DF=0.94) predicted a peak field test stress of 5.78 ksi, meaning it accounted for 1.38 of the 2.06 increase in stiffness (i.e. 68% of the measured increase in stiffness remained unexplained). If one wanted to include the entire measured increase in stiffness, one would use a DF=0.63.

Finally, rating of the bridge using the refined BRASS model and including only the explained increase in stiffness due to better than expected load distribution (see existing and refined data files below, changes in **bold**) leads to the revised load ratings shown in Table 2. The revised load ratings are 1.38 times higher than the original ratings.

Since the sister bridge (1-790, southbound) is of an identical design, it can be assumed to behave similar to this structure and the same DF=0.94 can be used. This recommendation is further discussed in the reports Conclusions.

Table 2. Bridge 1-791 Load Ratings

Rating Vehicle	Original Rating Factors From BRASS			Revised Rating Factors From BRASS		
	Inv.	Oper.	Post.	Inv.	Oper.	Post.
HS20T	0.95	2.12	1.34	1.32	2.93	1.86
S220	1.55	3.43	2.18	2.14	4.75	3.01
S335	0.82	1.82	1.15	1.14	2.52	1.60
S437	0.82	1.81	1.15	1.13	2.50	1.59
T330	1.38	3.07	1.94	1.92	4.25	2.70
T435	1.18	2.62	1.66	1.63	3.62	2.29
T540	1.09	2.42	1.53	1.51	3.34	2.12

Pre-Load Test BRASS Data File (1-791)

```
 TLE BRIDGE # 1-791, I-95 NB OVER DARLEY ROAD
TLE 3 SPAN CONTINUOUS STEEL BEAM BRIDGE, FATIGUE SENSITIVE
COM *NOTE*: This File was modified on 08/08/95. Refer to Further comments
COM *NOTE*: This is DelDOT's existing data file before the load test
ANL 1,0,4
XST 1,WN30X99
XSA 1,36
XST 2,WN30X99
XSA 2,36,,,1
XSC 8.0,0.5,0.0,8.0,0.5,0.0
XST 3,WN30X99
XSA 3,36
XSC 86.0,7.50,1.0,0,0,0
SPA 1,35.0,5
SPC 1,25.5,1,2
SPD 35.0,2,2
FIX 0,1,0,1,1,0
SPA 2,58,5
SPC 2,5.5,2,1
SPD 11.75,1,3,46.25,3,1
SPD 52.5,1,2,58.0,2
FIX 1,1,0,0,1,0
SPA 3,35.0,5
SPC 2,9.5,2,1
SPD 35.0,1,1
FIX 0,1,0,0,1,0
PS1  , ,3
PS2 10, ,40
COM DEAD LOADS STAGE 1: SLAB = 672 LB/FT, HAUNCH = 18 LB/FT
COM DEAD LOADS STAGE 2: PARAPET = 185 LB/FT, WEAR. SURF. = 173 lb/ft
DLD 1,0.690,0.358
LDE 1, , ,DIAPHRAGM DEAD LOAD
PTD  ,0.240,1,17.5
PTD  ,0.240,2,14.5
PTD  ,0.240,2,29.0
PTD  ,0.240,2,43.5
PTD  ,0.240,3,17.5
COM  *NOTE*: Live Load Dist. Factor WAS NOT Changed to 1.378 from 1.303
COM   As per 1994 AASHTO Specs. It would have been 1.378
LLD 2, 1.30, ,50.0
TR1  HS20T,S220,S335,S437,T330,T435
TR2  T540
DES 3, 1
COM WS Parameters were Replaced with LF on 08/08/95
INV 1.3, 1.0, 1.67, 1.0, 1.0, 1.0
OPG 1.0, 1.0, 1.67, 1.0, 1.0, 1.0
```

COM POSTING LEVEL 3
PST 1.3, 1.0, 1.00, 1.0, 1.0, 1.0
SLD 1.0, 1.0, 1.0, 1.0, 1.0, 1.0
SL1 100,2
SL4 ,,1
SL1 104,2
SL4 ,,1
SL1 105,2
SL4 ,,1
SL1 200,2
SL4 ,,1
SL1 205,4
SL4 ,,1

Post-Load Test BRASS Data File (1-791)

```
 TLE BRIDGE # 1-791, I-95 NB OVER DARLEY ROAD
TLE 3 SPAN CONTINUOUS STEEL BEAM BRIDGE, FATIGUE SENSITIVE
COM *NOTE*: This file was modified based on the 10/31/95 load test.
ANL 1,0,4
XST 1,WN30X99
XSA 1,36
XST 2,WN30X99
XSA 2,36,,,1
XSC 8.0,0.5,0.0,8.0,0.5,0.0
XST 3,WN30X99
XSA 3,36
XSC 86.0,7.50,1.0,0,0,0
SPA 1,35.0,5
SPC 1,25.5,1,2
SPD 35.0,2,2
FIX 0,1,0,1,1,0
SPA 2,58,5
SPC 2,5.5,2,1
SPD 11.75,1,3,46.25,3,1
SPD 52.5,1,2,58.0,2
FIX 1,1,0,0,1,0
SPA 3,35.0,5
SPC 2,9.5,2,1
SPD 35.0,1,1
FIX 0,1,0,0,1,0
PS1  , ,3
PS2 10, ,40
COM DEAD LOADS STAGE 1: SLAB = 672 LB/FT, HAUNCH = 18 LB/FT
COM DEAD LOADS STAGE 2: PARAPET = 185 LB/FT, WEAR. SURF. = 173 lb/ft
DLD 1,0.690,0.358
LDE 1, , ,DIAPHRAGM DEAD LOAD
PTD  ,0.240,1,17.5
PTD  ,0.240,2,14.5
PTD  ,0.240,2,29.0
PTD  ,0.240,2,43.5
PTD  ,0.240,3,17.5
COM *NOTE*: Based on analysis of the load test results,
COM *NOTE*: the DF was changed from 1.378 to 0.94.
LLD 2, 0.94, ,50.0
TR1  HS20T,S220,S335,S437,T330,T435
TR2  T540
DES 3, 1
COM WS Parameters were Replaced with LF on 08/08/95
INV 1.3, 1.0, 1.67, 1.0, 1.0, 1.0
OPG 1.0, 1.0, 1.67, 1.0, 1.0, 1.0
COM POSTING LEVEL 3
```

```
PST 1.3, 1.0, 1.00, 1.0, 1.0, 1.0
SLD 1.0, 1.0, 1.0, 1.0, 1.0, 1.0
SL1 100,2
SL4 ,,1
SL1 104,2
SL4 ,,1
SL1 105,2
SL4 ,,1
SL1 200,2
SL4 ,,1
SL1 205,4
SL4 ,,1
```

Summary of Bridge 1-788 Field Test Results

On May 21, 1997, the University of Delaware load tested Bridge 1-788. The bridge, a reinforced concrete box culvert that allows water to pass beneath I-95 has three rectangular openings measuring 14' in width and is located just north of Harvey Road. The culvert supports 20' of fill and carries four lanes of I-95 traffic (two lanes in each direction). The total length of the culvert is 195 feet.

The interesting aspect of this box culvert is that based on the 20 feet of fill between the wearing surface and the top of thew culvert, one can assume that live load effects are negligible. It is generally assumed that for every two units of depth, load distributes laterally by a single unit. Over a 20 foot depth, an axle load would be expected to be distributed 10 feet in either direction (or over a 20 foot width). It is for this reason that live loads should have no impact on this particular box culvert (i.e., they should cause very little strain). The existing rating reflects this (see Table 3) as the rating values are very high. By conducting a load test, this assumption of no live load effect could be checked. If the load test indeed suggests that live load effects are negligible, as long as the culvert is structurally sound under the action of the dead load, it need not be restricted in terms of live load capacity (i.e., superload permit vehicles will have little impact on the bridge).

A total of ten strain transducers where attached to the soffit and walls of the box culvert. Because it is important to get concrete strains over a long gage length, aluminum gage extensions where used. This allows strain measurements to be taken over gage lengths up to 24 inches. This will help to minimize eliminate erroneous readings reflecting large local strains caused by concrete cracking.

Unlike the load tests of the Bridges 1-704 and 1-791, this bridge was tested using ambient traffic. The reason for this is that it was strongly suspected that live loads would have little to no effect on the culvert. If this could be proven under ambient traffic, the disruptions to I-95 traffic caused by conducting controlled load tests (i.e., the need for

traffic control on I-95) could be avoided. Therefore, as a first step, strain monitoring due to ambient traffic was conducted.

Data was recorded for ten second intervals at 100 Hz every time a large truck crossed the bridge. This was done 32 times since it was not know which of the trucks might be fully loaded or which might be empty. By collecting multiple data sets, it was felt that some would reflect heavily loaded vehicles. In a few instances, several trucks passed over the culvert during the 10 second recording period.

The maximum flexural tensile strain in the soffit measured during any of the passes was 11.4 με, and the maximum compression strain in the walls was 8.8 με.

The test results indicate that as long as the box culvert is safely carrying the dead loads imposed on it, it should be considered to have the very large live load capacity currently indicated by the BRASS analysis (see Table 3). The tests have shown that in no case did ambient live loads cause strains to exceed 1% of the capacity of the material.

Table 3. Bridge 1-788 Load Rating

Rating Vehicle	Original Rating Factors From BRASS		
	Inv.	Oper.	Post.
HS20T	7.39	12.35	12.35

Pre-Load Test BRASS Data File (1-788)

```
 TITLE BRIDGE NO. 1-788,I-95 OVER SO. BR. NAAMANS CREEK
TITLE 3 CELL BOX CULVERT, BUILT IN 1966 - CONTRACT NO. 65-07-019
COM *NOTE*: This is DelDOT's existing data file before the load test
ANL 1,0,2
XSA 1
XSB 12
XSG 1,2,7,2.4375
XSG 4,2,6,2.375
XSA 2
XSB 12
XSG 1,2,7,2.4375
XSG 4,2,9,2.564
SPA 1,14.0,1,18.,18.
SPC 1,10.,1,2
SPD 14.0,2
FIX 1,0,0,0,0,0
SPA 2,14.0,1,18.,18.
SPC 2,14.0,2
FIX 0,0,0,0,0,0
SPA 3,14.,1,18.,18.
SPC 2,4.0,2,1
SPD 14.0,1
FIX 0,0,0,1,0,0
SPA 7,7.54,1,12.,12.
SPC 1,7.54,1
FIX 0,0,0,1,1,1
SPA 8,7.54,1,12.,12.
SPC 1,7.54,1
FIX 0,0,0,1,1,1
SPA 9,7.54,1,12.,12.
SPC 1,7.54
FIX 0,0,0,1,1,1
SPA 10,7.54,1,12.,12.
SPC 1,7.54
FIX 0,0,0,1,1,1
PRC 150, , ,3.0,40
COM ASSUME 20 FT COVER & NO IMPACT
DLD 1,2.4
LDE 1,1,,EARTH PRESSURE
UL1 7,0,-0.41,7.54,-0.56
UL1 10,0,0.41,7.54,0.56
LLD 3,1.0,0.0,50
COM HS20T = SPECIAL LANE 1
SLN 1,.0578,0.,0.,36.
DES 3,1
COM POSTING LEVEL 4
```

```
OPG 1.3,1.0,1.0
PST 1.3,1.0,1.0
CR1 100.
CR2 1
CR1 104.
CR2 1
CR1 200.
CR2 1
CR1 205.
CR2 1
```

Summary of Bridge 1-138 Field Test Results

The University of Delaware performed a semi-static diagnostic load test on Bridge 1-138 in July of 1994. The bridge carries traffic from the much traveled Lancaster Pike over the Red Clay Creek. This bridge, built in 1939, has no skew and has a non-composite slab-on-steel-girder superstructure. Its three spans are simply-supported and non-composite. The center span contains nine girders with the two W36X194 facia girders being fully encased in concrete. The seven interior girders are W36X170. All girders were imbedded into the deck (underside of flange flush with the deck).

Inspection reports on the bridge indicated that corrosion (and associated loss in section) has played a major role in causing the bridge to be posted. Cover plates were welded onto the flanges of some of the diaphragms due to extensive corrosion. One of the main span girders showed corrosion around one of its supports. Another repair was also made in which the ends of the main span girders were welded to their supports, thus restricting longitudinal movement. As a result of the longitudinal movement restriction, the piers below the two support locations showed several cracks. Other concrete deterioration included spalling of the parapet wall tops until the reinforcing steel became visible. The bridge had recently been repainted to help prevent further corrosion. Inspection reports also indicated that nearly 11 inches of asphalt overlay had been applied and accumulated over the life of the bridge.

DelDOT identified this bridge for testing because it was recently posted. Only the center span was instrumented, since moment in this span governs the current loading.

The instrumentation of this bridge consisted of 32 strain transducers to measure the strains in the top and bottom flanges of the girders. The test vehicle used was a three-axle, single unit truck with a total weight of 25 tons. This weight was chosen because of the bridge's posting rating of 26 tons for this type of vehicle. In the test, a total of six passes were made on three different load paths (each path was duplicated).

The predicted peak bending stress for Bridge 1-138 due to the test truck was 3.60 ksi, while the peak bending stress that was measured was 2.10 ksi (peak strain of 73 με). This immediately indicates that the bridge is 1.72 times stiffer than the model currently being used for rating.

Based on the field test data, it was determined that the actual multiple lane DF was 0.66 as compared to the AASHTO value of 0.91. While some unintended support fixity was found, it was determined that it should not be counted on in the rating process. In terms of flexural stiffness of the girders, two important observations were made. First, the girders were acting compositely even though they were designed non-compositely (the existing BRASS model was already assuming composite action). Second, the large asphalt overlay created by repeated resurfacing without removal of the old asphalt has led to a stiffer section (the composite section acts as if it has an 11 inch concrete deck even though the concrete deck itself is 8.5 inches thick).

The refined BRASS model (DF=0.66, Composite Deck Thickness=11 in.) predicted a peak field test stress of 2.46 ksi, meaning it accounted for 1.47 of the 1.72 increase in stiffness (i.e. 25% of the measured increase in stiffness remained unexplained).

Finally, rating of the bridge using the refined BRASS model (see existing and refined data files below, changes in **bold**) leads to the revised load ratings shown in Table 4. The revised load ratings are roughly 1.50 times higher than the original ratings.

It should be noted that the depth of the web in the original BRASS data file was found to be in error and was corrected to be d_W=33.96 inches.

Table 4. Bridge 1-138 Load Ratings

Rating Vehicle	Original Rating Factors From BRASS			Revised Rating Factors From BRASS		
	Inv.	Oper.	Post.	Inv.	Oper.	Post.
HS20T	0.76	1.27	0.93	1.18	1.97	1.44
S220	1.29	2.16	1.58	2.01	3.35	2.46
S335	0.69	1.14	0.84	1.06	1.78	1.30
S437	0.68	1.13	0.83	1.05	1.75	1.28
T330	1.06	1.76	1.29	1.64	2.74	2.01
T435	0.96	1.60	1.17	1.49	2.48	1.82
T540	0.85	1.42	1.04	1.32	2.2	1.61

Pre-Load Test BRASS Data File (1-138)

TITLE BRIDGE 1-138, RD.237(SR48), S. OF WOODDALE, OVER RED CLAY CRK
TITLE STEEL BEAM CONC. COMPOSITE, BUILT IN 1940, CT#673
COM 3-SPAN BR.,MIDDLE BEAM ON MIDDLE SPAN ANALYZED
COM *NOTE*: This is DelDOT's existing data file before the load test
COM *NOTE*: Depth of web was corrected to be 33.96 inches
COM *NOTE*: 750 lbs/ft for asphalt overlay which has accumulated over the years
ANALYSIS 1,0,4
XSECT-A 1,33
XSECT-B 0.68,,12.027, ,1.10,1.10
XSECT-C 60.0,8.5,-1.0,0.0,0.0,0.0
SPAN-A 1,62.5,1,**33.96,33.96**
SPAN-C 1,62.5,1
FIXITY 0,1,0,1,1,0
PROPERTIES-ST1 , ,2.5
PROPERTIES-ST2 10.2, ,33
COMMENT SLAB=531 LBS/FT W.S.=750 LBS/FT PARAPET=190 LBS/FT
COMMENT SIDEWALK=0.0 LBS/FT HAUNCH=31.25 LBS/FT
DEAD-LOAD 1,0.562,0.940
LDE 1, , ,DIAPHRAM DEAD LOADS
POINT-DL 0,.274,1,0.0
POINT-DL 0,.274,1,20.83
POINT-DL 0,.274,1,41.66
POINT-DL 0,.274,1,62.5
LIVE-LOAD 3,0.91, ,50
TRUCK-CODE1 HS20T,S220,S335,S437,T330,T435
TRUCK-CODE2 T540
DESIGN 3,1
INVENTORY 1.3,1.0,1.67,1.0,1.0,1.0
OPERATING 1.0,1.0,1.67,1.0,1.0,1.0
COMMENT POSTING LEVEL 2
POSTING 1.3,1.0,1.0,1.0,1.0,1.0
SLD 1.0,1.0,1.0,1.0,1.0,1.0
STEEL-1 104,4
STEEL-1 105,4

Post-Load Test BRASS Data File (1-138)

TITLE BRIDGE 1-138, RD.237(SR48), S. OF WOODDALE, OVER RED CLAY CRK
TITLE STEEL BEAM CONC. COMPSITE, BUILT IN 1940, CT#673
COM 3-SPAN BR.,MIDDLE BEAM ON MIDDLE SPAN ANALYZED
COM *NOTE*: This file was modified based on the 7/94 load test.
ANALYSIS 1,0,4
XSECT-A 1,33
XSECT-B 0.68,,12.027, ,1.10,1.10
COM *NOTE*: Concrete deck thickness was changed from 8.5 to 11 in.
XSECT-C 60.0,**11.00**,-1.0,0.0,0.0,0.0
SPAN-A 1,62.5,1,**33.96,33.96**
SPAN-C 1,62.5,1
FIXITY 0,1,0,1,1,0
PROPERTIES-ST1 , ,2.5
PROPERTIES-ST2 10.2, ,33
COMMENT SLAB=531 LBS/FT W.S.=750 LBS/FT PARAPET=190 LBS/FT
COMMENT SIDEWALK=0.0 LBS/FT HAUNCH=31.25 LBS/FT
DEAD-LOAD 1,0.562,0.940
LDE 1, , ,DIAPHRAM DEAD LOADS
POINT-DL 0,.274,1,0.0
POINT-DL 0,.274,1,20.83
POINT-DL 0,.274,1,41.66
POINT-DL 0,.274,1,62.5
COM *NOTE*: Based on analysis of the load test results,
COM *NOTE*: the DF was changed from 0.91 to 0.66.
LIVE-LOAD 3,0.66, ,50
TRUCK-CODE1 HS20T,S220,S335,S437,T330,T435
TRUCK-CODE2 T540
DESIGN 3,1
INVENTORY 1.3,1.0,1.67,1.0,1.0,1.0
OPERATING 1.0,1.0,1.67,1.0,1.0,1.0
COMMENT POSTING LEVEL 2
POSTING 1.3,1.0,1.0,1.0,1.0,1.0
SLD 1.0,1.0,1.0,1.0,1.0,1.0
STEEL-1 104,4
STEEL-1 105,4

APPENDIX A.

EXPERIMENTAL LOAD RATING OF A POSTED BRIDGE

By Michael J. Chajes,[1] Associate Member, ASCE, Dennis R. Mertz,[2] Member, ASCE, and Brett Commander[3]

ABSTRACT: Results of an experimental load test of a posted, three-span, steel-girder-and-slab bridge are presented. The bridge was designed to have three simple supported spans, each consisting of a cross section with nine noncomposite steel girders. Through diagnostic load testing, it was determined that the girders were acting compositely with the concrete deck and that significant restraint was being developed at the bearing supports. A finite-element model of the main span was generated using the measured response of the bridge. Results of analyses conducted using the numerical model were compared to the measured response and found to be quite similar. Using this model, along with models that account for the loss of composite action and/or support restraint, a variety of load ratings for the bridge was determined. By comparing the various load ratings, and by considering the nature of the unintended composite action and support restraint, decisions regarding the determination of a safe bridge rating are discussed. Final conclusions suggest that the current posting levels may be unnecessary.

INTRODUCTION

As the condition of our nation's bridges continues to deteriorate, and the weight of trucks on our highways continues to increase, an ever-growing number of bridges require posted load limits. It has been estimated that 100,000 bridges in the United States are currently posted, and another 50,000 bridges should be posted (Pinjarkar et al. 1990). While these load limits are meant to ensure the public safety, the time consumed in detouring around a posted bridge imposes an inconvenience to the traveling public and a significant financial cost to society. Furthermore, posted bridges are among those most likely to receive costly repairs or to be replaced. Because of the associated safety issues and costs, it is important that the load-carrying capacity of a posted bridge be determined accurately.

Currently, most bridges are evaluated using simplified models that rely on structural dimensions and properties determined from original design plans and/or observations made during on-site inspections. In most cases, the person who inspects a bridge is not directly involved in either the analysis or rating of the bridge. As a result, ratings determined in this manner may not always accurately reflect a bridge's actual safe load-carrying capacity. This means that the factor of safety for a given bridge may be different than expected, and will vary from bridge to bridge. In fact, researchers typically find that traditional load-rating methods are quite conservative (Aktan et al. 1993; Bakht and Jaeger 1990; Commander 1989; Lichtenstein 1995).

One method for more accurately determining a bridge's load-carrying capacity is to conduct an experimental load test (Schulz 1993). A state-of-the-art survey of experimental load rating of bridges by Edberg (1995) indicates that many researchers are actively working on this area including Aktan and Raghavendrachar (1990), Bakht and Jaeger (1990, 1992), Burdette and Goodpasture (1988), Fu and Tang (1992), Goble et al. (1992), Moses et al. (1994), and Pinjarkar et al. (1990). Work on developing appropriate, nondestructive test methodologies for bridge testing by these researchers and others, combined with the increasing capacity and affordability of testing equipment (Schulz 1989), has made the prospect of conducting routine bridge load tests a reality. In recognition of this, a report titled "*Bridge Rating through Nondestructive Load Testing*" has recently been written (Lichtenstein 1995a). In fact, the Florida Department of Transportation (El Shahawy and Garcia 1989), the New York Department of Transportation (Fu et al. 1992), the Ontario Ministry of Transportation (Bakht and Csagoly 1979; Bakht and Jaeger 1990), and Switzerland (Markey 1991) are already making extensive use of experimental load testing to rate bridges.

While much of the prior work involves testing of new bridges, old bridges scheduled for demolition, or bridges with specific problems, this paper focuses on the evaluation and subsequent load rating of posted bridges. The paper will concentrate on how nondestructive experimental load tests can be used to develop relatively simple, yet accurate, numerical bridge models, and how these models can in turn be used to rate a posted bridge.

BRIDGE DESCRIPTION

The steel-girder-and-slab bridge tested in this study was built in 1940. The bridge was designed for H15 loading, using steel with a yield strength of 227 MPa, and concrete having a compressive strength of 17.2 MPa. It is located on the heavily traveled Lancaster Pike, carrying traffic across the Red Clay Creek in Wilmington, Delaware. The average daily traffic (ADT) and average daily truck traffic (ADTT) for the bridge are 17,600 and 900, respectively. The bridge is 128.8 m wide and carries two lanes of traffic. The superstructure consists of three skewless, simply supported spans measuring 6.9 m, 19.5 m, and 6.9 m, respectively. The cross section consists of nine noncomposite steel girders, with the outer girders spaced 1.37 m apart and the interior girders spaced 1.52 m on center. On the approach spans, the fascia girders consist of W24 × 74 sections encased in concrete, and the interior girders are W21 × 63 sections. The end diaphragms are made of I10 × 25.4 sections. For the center span, the fascia girders consist of W36 × 194 sections encased in concrete, while the interior girders are W36 × 170 sections. On the center span, four equally spaced beams (I18 × 54.7) act as end and intermediate diaphragms. The original roadway consisted of a 216-mm-thick concrete deck with a 50.8-mm-thick asphalt overlay. Plan and section views of the bridge are shown in Fig. 1.

Over the history of the bridge, a variety of repairs have been made. Corrosion of diaphragms has been repaired with field-welded plates. One of the steel girders has experienced corrosion in the region below an expansion joint and was repaired with a field-welded plate. To prevent further corrosion damage

[1]Assoc. Prof., Dept. of Civ. Engrg., Univ. of Delaware, 137 Dupont Hall, Newark, DE 19716.

[2]Assoc. Prof., Dept. of Civ. Engrg., Univ. of Delaware, 137 Dupont Hall, Newark, DE.

[3]Testing Engr., Bridge Diagnostics Inc., 5398 Manhattan Circle, Ste. 280, Boulder, CO 80303.

Note. Discussion open until October 1, 1997. To extend the closing date one month, a written request must be filed with the ASCE Manager of Journals. The manuscript for this paper was submitted for review and possible publication on June 7, 1995. This paper is part of the ***Journal of Bridge Engineering***, Vol. 2, No. 1, February, 1997. ©ASCE, ISSN 1084-0702/97/0002-0001–0010/$4.00 + $.50 per page. Paper No. 10920.

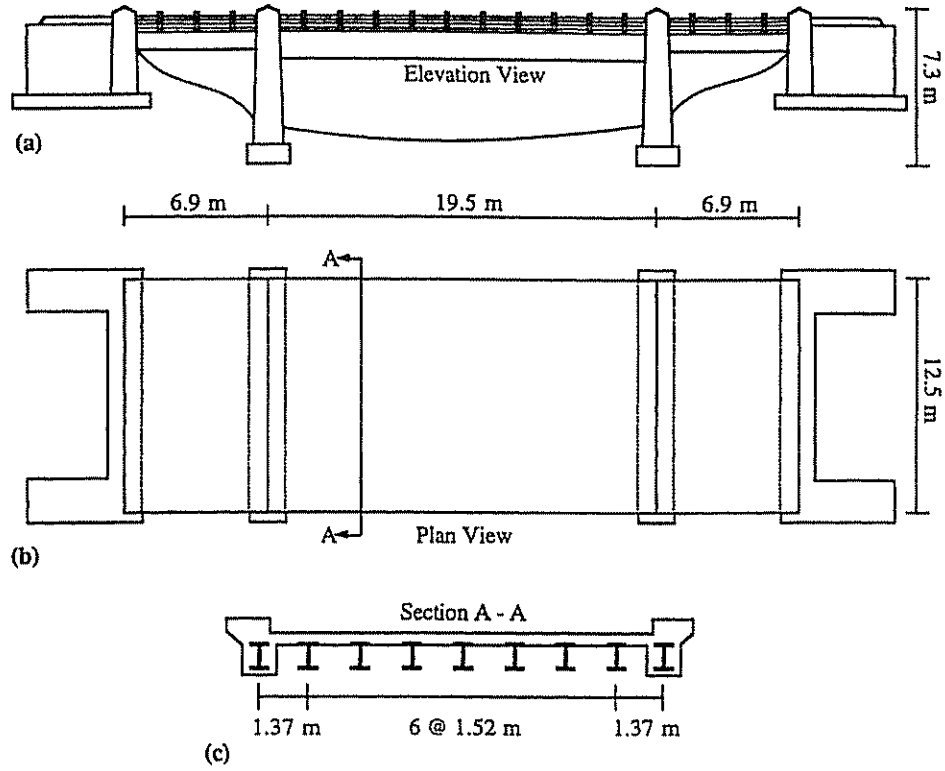

FIG. 1. Plan and Section Views of Test Bridge

TABLE 1. Current Rating Factors

Rating vehicle (GVW kN/tons) (1)	Inventory rating factor (2)	Operating rating factor (3)	Posting rating factor (4)
HS20T-AASHTO HS20-44 (320/36)	0.51	1.43	0.82
S220-Delaware two-axle single unit (178/20)	0.86	2.43	1.39
S335-Delaware three-axle single unit (312/35)	0.46	1.29	0.74
S437-Delaware four-axle single unit (325/36.5)	0.45	1.27	0.72
T330-Delaware three-axle semi (267/30)	0.70	1.98	1.13
T435-Delaware four-axle semi (312/35)	0.64	1.80	1.03
T540-Delaware five-axle semi (356/40)	0.57	1.59	0.91

to the girders, they have recently been repainted. In another repair, for unknown reasons, the ends of the beams of the center span were welded to their bearing plates, thereby restraining relative movement. This condition has led to cracking of the pier caps just below the support locations. The parapets have experienced a considerable amount of concrete spalling, exposing much of the top reinforcing steel. Finally, additional asphalt overlays have been added to the bridge, covering the expansion joints, and bringing the thickness of the current wearing surface to approximately 280 mm.

In March of 1994, the bridge was analyzed and rated by the Delaware Department of Transportation using the Bridge Rating and Analysis of Structural Systems (BRASS) program (*Brass 4.2 User Manual* 1987). The analysis, which incorporated an estimate of the corrosion damage to the girders, indicated that load restrictions were needed. The computed inventory, operating, and posting rating factors for Delaware's seven rating vehicles are shown in Table 1. Based on the strength limit state, the rating factors for posting range from 0.72 to 1.39 (allowable stress approach, noncomposite behavior). In Delaware, rating factors for posting are taken to be equal to two-thirds of the inventory rating plus one-third of the operating rating. All ratings were governed by insufficient midspan moment capacity of the center span. As a result of the analysis, the bridge was posted for several vehicle types, partially restricting truck traffic.

BRIDGE TESTING

To better evaluate the load-carrying capacity of the bridge, a nondestructive field test was conducted. Experimental load testing on a bridge can be categorized as either a diagnostic or proof test. In a diagnostic test, a predetermined load, typically near the bridge's rated capacity, is placed at several different locations along the bridge and the bridge response is measured. The measured response is then used to develop a numerical model of the bridge. The bridge model can then be used to estimate the maximum allowable load. In a proof test, incremental loads are applied to the bridge until either a target load is reached or a predetermined limited state is exceeded. Using the maximum load reached, the capacity of the bridge can be determined. While diagnostic tests provide only an estimate of a bridge's capacity, they have several practical advantages including a lower cost, a shorter testing time, and less disruption to traffic. Because of these advantages, diagnostic testing was used in this case.

Instrumentation

Based on the fact that the center span controls the current posting, only this span was instrumented. To gather data, reusable strain transducers with a gauge length of 76.2 mm were attached to all girders at midspan and to selected girders at locations halfway between the end of the girder and the first internal diaphragm. In all but one case, transducers were attached to the top and bottom flanges of the beams at each location. For one of the concrete-encased fascia beams, four transducers were attached along the depth. To improve their accuracy, the transducers placed on the bottom face of the

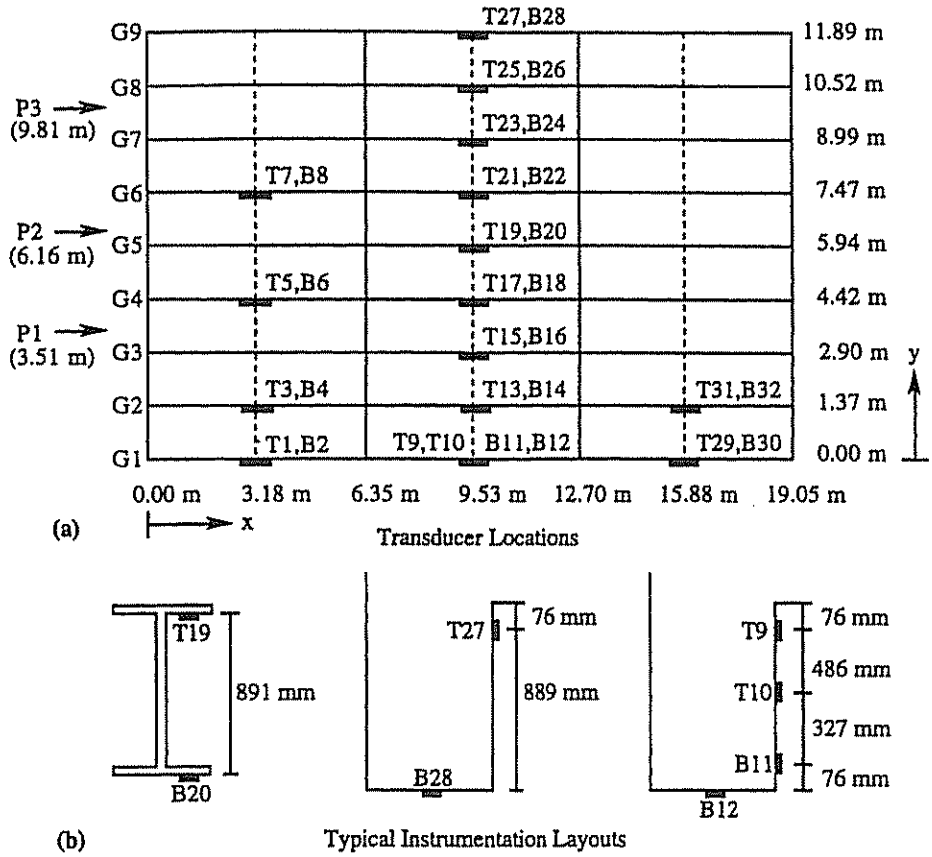

FIG. 2. Instrumentation Plan and Paths for Loading Vehicle

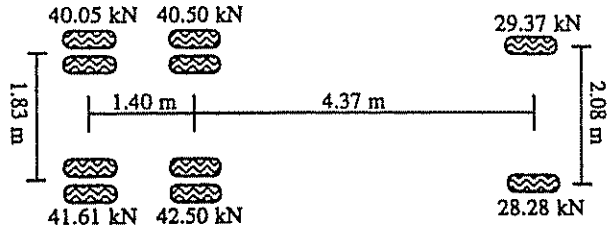

FIG. 3. Wheel Configuration of Loading Vehicle

concrete-encased beams utilized a 305-mm extension. Shorter gauge lengths are suitable for measuring strains on the steel girders and for measuring compressive strains in concrete. However, cracks that occur when concrete is in tension lead to high localized strains. Using an average strain value computed over a longer gauge length can lead to more accurate strain measurements.

The transducers were connected to a digital data acquisition system, which recorded strain histories caused by a loading vehicle (discussed in the following section). All transducers were mounted using either c-clamps or a quick-setting adhesive applied to special mounting tabs. In all, 32 strain transducers were used. The location and number assigned to each transducer are shown in Fig. 2. For the numbering, *T* signifies that the transducer is attached to the top of the girder and *B* to the bottom.

Loading

With the bridge temporarily closed to traffic, a loading vehicle of known weight was slowly driven across the deck at approximately 8 km/h, and strain data was recorded for each channel at 32 Hz. The loading vehicle was a three-axle, single-unit truck weighing 223 kN (25 tons). The measured wheel load distribution is shown in Fig. 3. This weight was slightly less than the rated posting (231 kN) for the three-axle configuration and, therefore, was not expected to cause the bridge response to exceed the linear-elastic range. To verify this, after each truck pass, strains were monitored to ensure that they did, in fact, go back to zero. To obtain meaningful data regarding both transverse and longitudinal load distribution, the truck's driver-side wheels were driven along three marked paths, each having a different transverse position (approximately 3 m apart) on the deck. These three paths (P1–P3) are shown in Fig. 2. To ensure consistent results, measurements were taken as the truck made two passes along each path.

Recorded Data

Six passes of the truck were needed to collect all of the data. During each pass, traffic was stopped for approximately 1 min. This allowed the driver of the truck time to position the vehicle and to cross the bridge at a crawl speed. As the loading vehicle moved across the bridge, a position indicator was used to correlate strain readings with the longitudinal position of the truck's front axle. It took a crew of eight only 5 h to completely instrument and test the bridge.

During the testing, the maximum strain recorded was 73 mm/mm. This occurred at transducer 16, when the loading vehicle passed along path P1. This value of strain corresponds to a tensile stress of 14.5 MPa (2.1 ksi). Typical strain history plots measured by transducers on a girder's top and bottom flanges at midspan (transducers 15 and 16, and truck path P1) are shown in Fig. 4. Positive strains indicate tension.

BRIDGE ANALYSIS

Test results were used to develop a numerical model of the bridge's center span. Results computed using the model were compared to the measured results to verify the accuracy of the model.

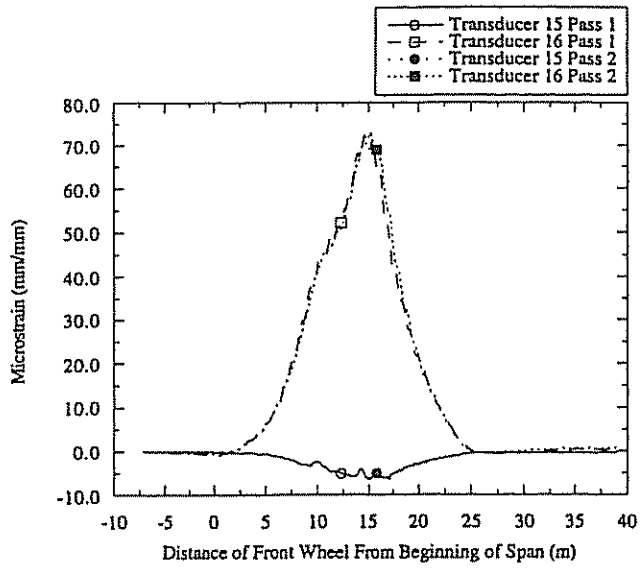

FIG. 4. Recorded Strains at Midspan of Girder 3 due to Loading Vehicle on Path P1

Development of a Numerical Model

In order to estimate a safe load rating for the bridge, a finite-element model (FEM) was created based upon the data from the diagnostic test. This numerical model could then be used to approximate the bridge's behavior to limiting loads. In creating a model, the objective was to keep the model as simple as possible, while still capturing the nature of the bridge response. With this simplicity in mind, a two-dimensional grid model of the main structural elements, combined with a plate element representing the deck, was used. The grid model consisted of one-dimensional beam elements representing the discrete girders and diaphragms. The diaphragms were modeled with moment releases at their ends. The spacing between the girders and the diaphragms was the same as the spacing on the actual bridge. The girder supports allowed for partially rigid connections. A fine mesh of plate elements was created and added to the top of the grid model. For a truck placed anywhere on the deck, the mesh allowed accurate transverse distribution of wheel loads to the girders. A depiction of the finite-element mesh is shown in Fig. 5.

From the measured data, two important characteristics of the bridge were identified. First, under the loads applied, it was evident that unintended composite action between the girders and the deck was occurring (see Fig. 4). Second, the longitudinal strain distribution observed along the second girder indicated that some degree of support restraint, referred to by Bakht and Jaeger (1990, 1992) as bearing restraint forces, was developed. To generate an accurate numerical model, these conditions needed to be accounted for. To account for the composite action, girder properties that accurately represented the composite section needed to be developed. To account for the support restraint, rotational springs with appropriate stiffness were incorporated into the standard pin-and-roller boundary conditions.

The development of appropriate modeling parameters is described in the following sections. All of these properties were determined directly from the measured girder strains. It is important to note that the procedure followed herein is only valid if there are no "significant" axial forces and related strains in the girders (as was the case for the tested bridge). While strains due to axial forces can be induced as a result of end restraint, with the exception of very short spans, their magnitude is usually much less than the strains due to flexure. When axial strains are significant, measured curvatures can be used to find some of the needed parameters, and some form of optimization process can be used to determine other needed values (Goble et al. 1992).

Composite Section Properties

The determination of composite section properties for the girders involved a series of steps including: (1) the identification of the neutral axis location from the measured strain data; (2) the determination of an effective deck thickness; and (3) the final calculation of section properties including the composite moment of inertia.

Because strains due to axial forces in the girders were small compared to flexural strains, the actual location of the neutral axis was found directly from the measured strain data. Since transducers were placed on the top and bottom flanges of the girders, the depth of the neutral axis could be computed assuming plane strain. Plots of the location of a section's neutral axis as the truck passed over the bridge were made for each set of transducer locations. By averaging results from all plots, it was determined that the neutral axis location of the interior girders was approximately 813 mm above the bottom flange. For the exterior, concrete-encased girders, the neutral axis was found to be approximately 793 mm above the beam soffit. For the loads applied and the range of girder strains induced (maximum measured strain of 73 m/mm), in no instance was loss of composite action observed.

Once the actual neutral axis location was determined, the next step was to find an effective depth of concrete deck. Assuming a ratio of the elastic modulus of the steel to that of the concrete equal to nine, and using a composite beam section (for the interior beam) with an effective slab width equal to the girder spacing of 1.52 m, it was determined from equilibrium of internal forces that the effective concrete deck is roughly 280-mm thick. This value seems reasonable in that the actual deck consists of 216 mm of concrete with approximately 280 mm of asphalt overlay.

By assuming that the girders acted compositely with the 280-mm-thick concrete deck, and by transforming the concrete curb and reinforced concrete encasement (for the exterior girders), and deck (for both interior and exterior girders) to equivalent amounts of steel, section properties for the composite girders were established. Values for the computed moments of inertia are given in Table 2. It should be noted that the combined grid-and-plate model used did not possess an interface

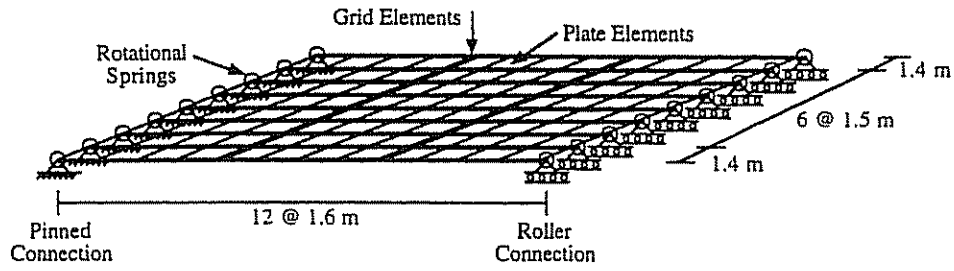

FIG. 5. Finite-Element Mesh of Middle Span

TABLE 2. Summary of Properties Used in Finite-Element Model

Element (1)	Parameter (2)	Value used (3)
Effective concrete deck	Thickness	0.279 m (11 in.)
Exterior girders (non-composite)	Moment of inertia	0.00504 m^4 (12,100 $in.^4$)
Exterior girders (composite)	Moment of inertia	0.0195 m^4 (46,923 $in.^4$)
Interior girders (non-composite)	Moment of inertia	0.00437 m^4 (10,500 $in.^4$)
Interior girders (composite)	Moment of inertia	0.0115 m^4 (27,658 $in.^4$)
Exterior supports	Rotational stiffness	1.96×10^5 kN·m/rad (1.73×10^6 k-in./rad)
Interior supports	Rotational stiffness	1.19×10^5 kN·m/rad (1.05×10^6 k-in./rad)

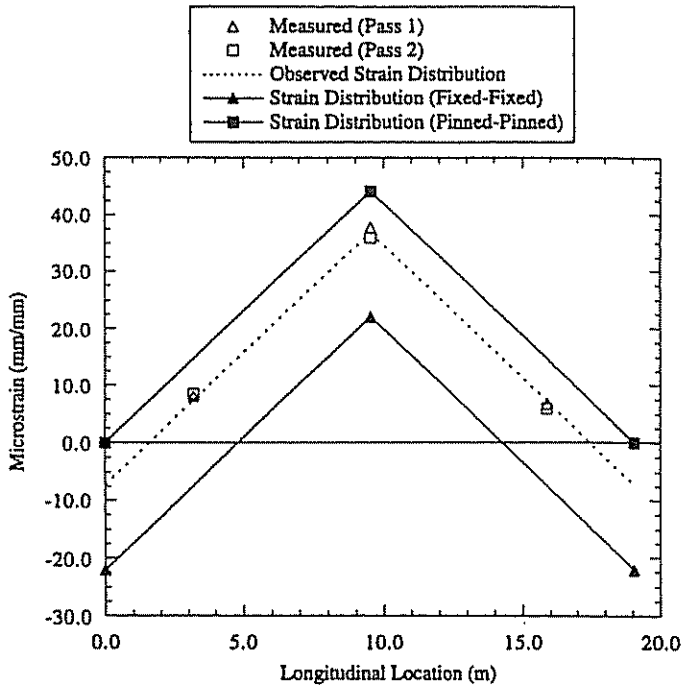

FIG. 6. Measured Strains along Girder 2 due to Loading Vehicle on Path P1 with Its Centroid at Midspan

element that could ensure continuous strain compatibility along the length of the girder-deck interface. As a result, another method of representing the composite action was used. The method chosen involved ensuring that the sum of the moments of inertia of the girder and plate was equal to the composite section moment of inertia. This was accomplished by assigning a moment of inertia to each girder that equaled the desired moment of inertia of the composite section minus the moment of inertia of the plate.

Support Restraint

The degree of restraint at the supports was found using the measured longitudinal strain distribution. Even though the bridge was designed to have pin-and-roller joints, modifications to the supports by maintenance forces (which involved field-welding of the bearing plates to the ends of the girders) introduced a measurable amount of restraint. Bakht and Jaeger (1990, 1992) have observed unintended end restraint in load tests conducted by the Ontario Ministry of Transportation. They suggest that one cause for these bearing restraint forces is friction that develops between the bottom flange of the girder and the abutment. Another cause of restraint can be frozen bearings. The result of this unintended bearing restraint is that a bridge will be stiffer than it is calculated to be if no restraint is assumed. In a test of a slab-on-girder bridge, Bakht and Jaeger (1992) found that the end restraint forces caused reduction in midspan moments ranging from 11 to 18% of that expected if ideal pin-and-roller connections were present.

One way to model bearing-restraint forces is to have a horizontal force acting at the bottom flange of the girder. The eccentricity of this force with the girder's effective neutral axis (neutral axis of composite section) produces rotational restraint at the support. While the horizontal force can be modeled using a linear spring, there is no direct way to determine the appropriate spring stiffness. Furthermore, the spring must be offset vertically from the grid that is modeling the structural elements. Another method of accounting for the end restraint is to incorporate a rotational spring into the model at the supports. This produces the same effect, and the moment generated in the spring can be used to find the resulting bearing-restraint forces. This procedure has several advantages, including: (1) that it is relatively easy to assess the degree of rotational fixity from measured strains along a girder's length and translate the degree of fixity measured to an appropriate rotational spring constant; and (2) the rotational spring does not need to be offset from the plane of the grid.

To determine an appropriate rotational spring constant, one can begin by looking at strain measurements along the length of a girder when the centroid of the loading vehicle is at midspan. A plot of the strains measured along the second girder (at the bottom flange) when the centroid of the loading vehicle was at midspan on path P1 is shown in Fig. 6. By assuming the loading on the girder to be a point load, a linear strain distribution (shown by the dashed line in Fig. 6) will result. If there were no end restraint (ideal pin-roller boundary conditions), the strains would go to zero at the reaction. In this case the absolute value of the end-to-midspan strain ratio would be equal to zero ($|M_{end}/M_{midspan}| = 0.0$). If the ends of the girder were completely restrained (fixed boundary condition), the absolute value of the end-to-midspan strain ratio would be equal to one ($|M_{end}/M_{midspan}| = 0.0$). By computing the measured end-to-midspan strain ratio, the degree of restraint or percent of fixity can be determined. In this case, using plots such as Fig. 6, the actual end-to-midspan strain ratio was estimated to be 0.20 (20% fixity) for both interior and exterior girders.

Once the equivalent percentage of fixity is determined, the appropriate rotational spring stiffness, k_s, can be found. In their study of building frames having flexible connections, Gerstle and Ackroyd (1990) showed that for a simply supported beam having a flexible connections (for instance, rotational springs at the ends), the spring stiffness can be conveniently related to the beam's moment of inertia I, length L, and modulus of elasticity E, via the ratio of the fixed-end moment to the fixed-end moment of a fixed-fixed beam. Based on this work, a general relationship between the parameters E, L, I, k_s, and the ratio $|M_{end}/M_{midspan}|$ for a beam having a point load at midspan can be established by considering a simply supported beam with equal rotation spring at its ends. By analyzing such a beam with various values of the dimensionless quantity EI/Lk_s, a relationship between EI/Lk_s and the ratio $|M_{end}/M_{midspan}|$ can be established. This relationship is plotted in Fig. 7. For the bridge tested, using a percent fixity of 0.20 ($|M_{end}/M_{midspan}|$) for both exterior and interior girders, and the composite girder properties, the equivalent spring constants for the reactions were found to be 1.96×10^5 kN·m/rad and 1.19×10^5 kN·m/rad for the exterior and interior girders, respectively. In the FEM, to model the support restraint, rotational springs having the computed stiffness were incorporated into the standard pin-and-roller boundary conditions at all supports.

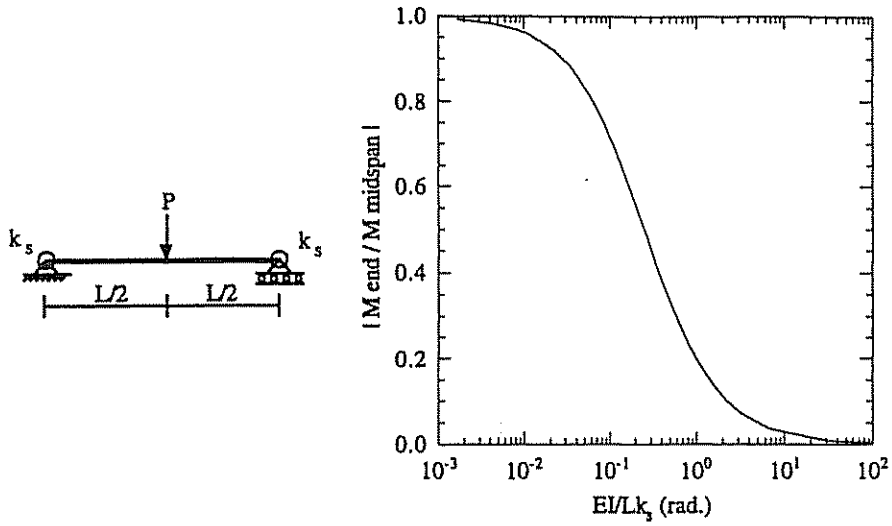

FIG. 7. Relationship between End-to-Midspan Moment Ratio and Rotational Spring Stiffness

As long as the loading vehicle is short compared to the length of the bridge, the approximation of the truck as a point load will yield reasonable results. For the bridge considered, the ratio of the span-to-vehicle length is 3.38. For cases where the ratio is small (for instance, ratios less than 2), the actual wheel loads and spacing should be used to determine expected strain distributions due to actual and idealized boundary conditions. A summary of important parameters used in the analysis are given in Table 2.

Applied Loading

Loads were applied to the model in a manner consistent with the actual load test. A two-dimensional model of the loading vehicle, which had the same wheel configurations and loads, was established. The test truck was then placed on the structure at 11 discrete locations along each of the three loading paths (a total of 33 truck positions).

Computed Results

An analysis was performed for each of the 33 loading cases. In order to compare the computed results to those measured in the field, computed moments were used to find strains at each of the gauge locations. The conversion of moments to strains involved using composite section properties, the assumptions that plane sections remain plane, and that all stresses were in the linear-elastic region.

To illustrate the accuracy of the model in predicting the longitudinal load distribution, a series of plots comparing measured and computed strains along the bottom flange of girders 1, 2, 4, and 6 (caused by the loading vehicle with its centroid at midspan along path P2) are presented in Fig. 8. To see how well transverse load distribution is predicted, Fig. 9 presents a series of plots comparing measured and computed strains on the bottom flange of each girder at midspan caused by the loading vehicle with its centroid at midspan along paths P1, P2, and P3. In both cases, the FEM does a good job of capturing the recorded bridge response.

In addition to the visual data composition, the accuracy of the model was also evaluated statistically. By utilizing 1,056 comparisons between measured strains ε_m and computed strains ε_c (33 truck locations × 32 strain transducers), absolute error, percent error, scale error, and a correlation coefficient were computed. The absolute error ($\Sigma|\varepsilon_m - \varepsilon_c|$) was 1,850 mm/mm. On average, this represents an error of less than 2 microstrain per reading. The percent error $[\Sigma(\varepsilon_m - \varepsilon_c)^2/\Sigma(\varepsilon_m)^2]$ and scale error ($\max|\varepsilon_m - \varepsilon_c|/\max|\varepsilon_m|$) were 7.9 and 10.0%, respectively, and the correlation coefficient $\{\Sigma(\varepsilon_m - \bar{\varepsilon}_m)(\varepsilon_c - \bar{\varepsilon}_c)/\Sigma[(\varepsilon_m - \bar{\varepsilon}_m)(\varepsilon_c - \bar{\varepsilon}_c)^2]^{0.5}\}$ was 0.97. These values, like the visual comparisons, indicate the high degree of accuracy of the numerical model.

Transverse Load Distribution

One very useful piece of information provided by experimental load testing is the actual transverse distribution of live loads. To some extent, the transverse distribution is illustrated by Fig. 9(a,b,c). In traditional bridge design and analysis, this transverse distribution is accounted for by use of a distribution factor (DF). Therefore, another way of examining this phenomena is to compare distribution factors computed using the calibrated FEM to the standard distribution factors used in bridge design, analysis, and rating.

According to the American Association of State Highway and Transportation Officials (AASHTO) (*Standard* 1989), the distribution factor for multiple lane design is defined as DF = *S*/5.5 where *S* is the transverse girder spacing in feet. This DF allows one to get the maximum girder moment by taking a moment computed for a wheel line of the vehicle and multiplying that moment by the DF. To get the corresponding distribution factor for the bridge tested, the calibrated FEM developed from the test data is used. One begins by finding the maximum possible moment on the interior and exterior girders due to multiple-lane loading using the FEM (M_{max}). After this has been done, the maximum beam moment on an idealized beam caused by the same truck load is computed (M_{beam}). The measured DF is then defined as DF = M_{max}/M_{beam}. For the bridge tested, the distribution factors for the interior and exterior beams based on AASHTO (*Standard* 1989) are 0.91 and 0.82, respectively, while the distribution factors computed using the FEM are 0.71 and 0.87 for the interior and exterior beams, respectively. In the case of the interior beams, which governed the posting, the AASHTO distribution factor is conservative by 28%.

Optimization

In the present study, no attempt to optimize the numerical model was made. Approximate parameters for the model were determined based on rational interpretation of the data and simplifying assumptions. Of course, optimization may be useful, or even needed, in some cases. Procedures that allow one to compare measured and computed bridge response and to optimize parameter determination systematically already exist

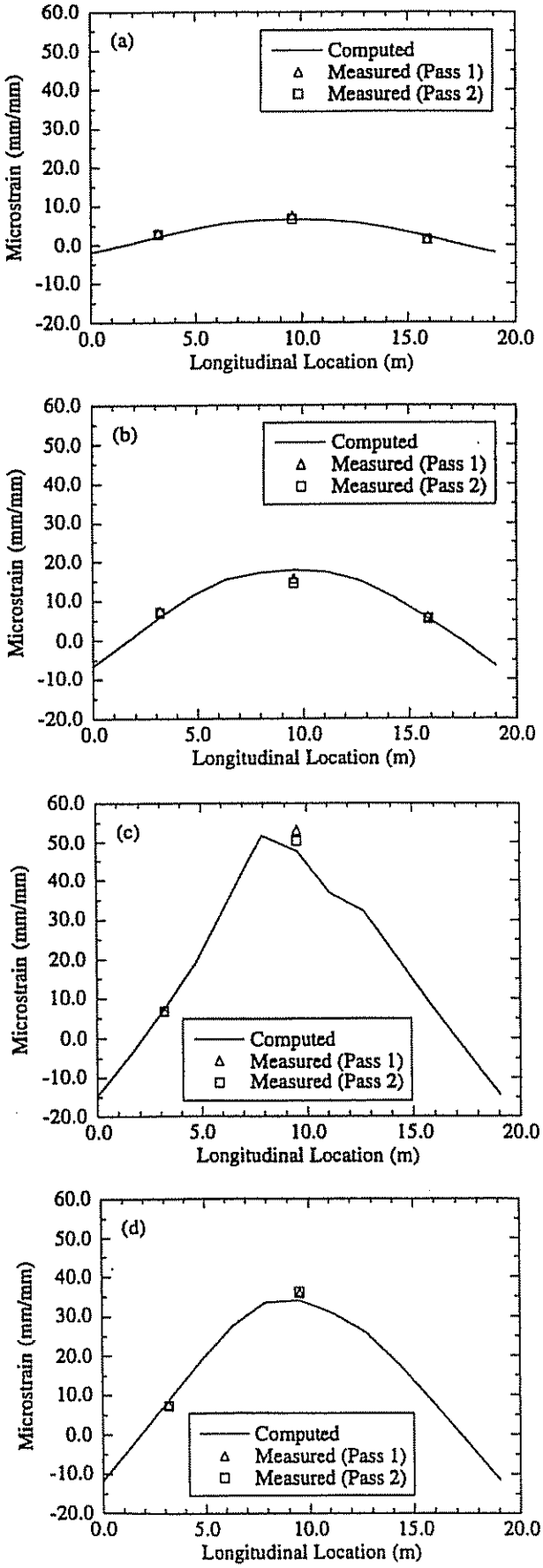

FIG. 8. Comparison of Measured versus Computed Strains along Girder's Bottom Flange due to Loading Vehicle on Path P2 with Its Centroid at Midspan: (a) Girder 1; (b) Girder 2; (c) Girder 4; (d) Girder 6

(Goble et al. 1992). These procedures can be used to fine-tune initial parameters found through the methodology described herein, or they can be used when determination of initial parameters becomes too complicated.

BRIDGE RATING

Since an FEM of the center span that accurately simulates the measured response has been established, the bridge can now be load-rated. However, because the applied load was limited to a 223 kN truck, two important decisions regarding modeling assumptions need to be made to extrapolate results to higher loads. These decisions are: (1) whether unintended composite action should be counted on at the higher loads; and (2) whether support restraint should be maintained at the higher loads. However, before a final decision is made, it is useful to see how various answers to these questions affect the computed load-carrying capacity of the bridge.

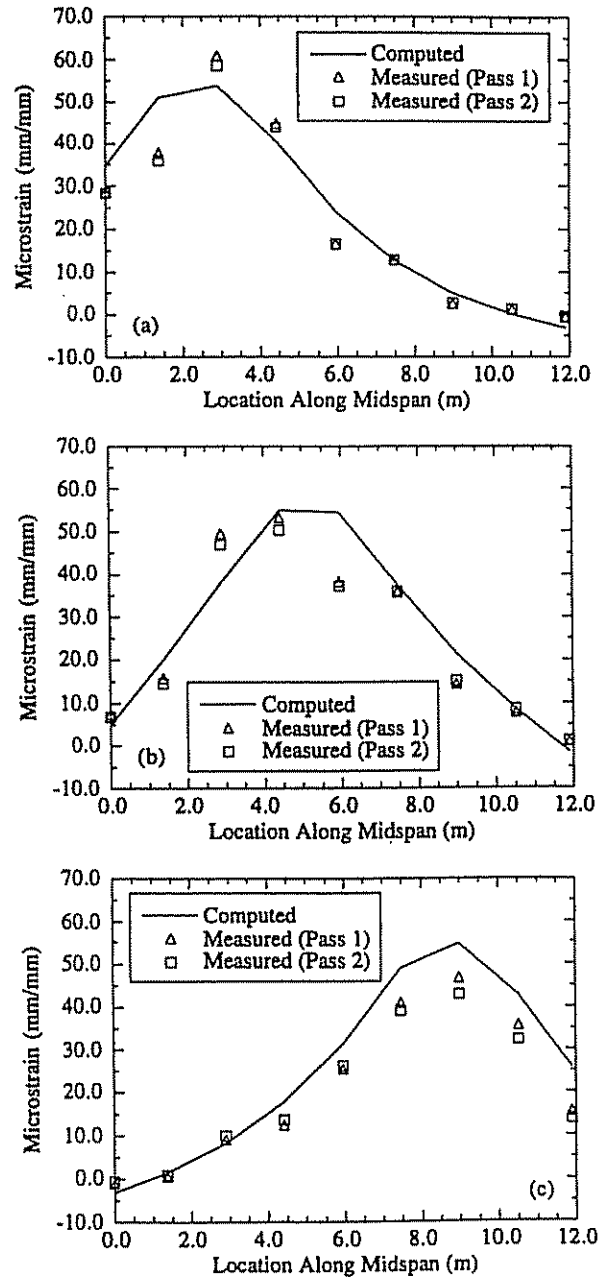

FIG. 9. Comparison of Measured versus Computed Strains on Bottom Flange of Girders across Midspan due to Loading Vehicle with Its Centroid at Midspan: (a) on Path P1; (b) on Path P2; (c) on Path P3

To evaluate the effects of unintended composite action and partial support restraint, three FEMs were used to get three sets of load ratings. Model 1, the stiffest model, was the one established based on the diagnostic test. This model incorporated the measured support restraint and composite section properties. Model 2, having intermediate stiffness, incorporated composite section properties and simply supported ends (no support restraint). Model 3, the most flexible of the three, was based on the assumption of noncomposite behavior and simply supported ends. While a fourth model incorporating noncomposite behavior and partial support restraint could also have been investigated, it was felt that the poor condition of the piers beneath the bearing plates would result in a loss of support restraint under elevated loads prior to a loss of composite behavior.

Based on these three FEMs, load ratings were established. Rating factors (RF) for each element were computed based on the equation.

$$\text{RF} = \frac{C - A_1 D}{A_2 L(1 + I)} \tag{1}$$

where C = member capacity based on a specified stress limit; D = maximum stress developed due to dead loads; L = maximum stress developed due to live loads; I = impact factor; and A_1 and A_2 (equal to 1.0 in the allowable stress method) = dead-load and live-load factors for load factor design (LFD) rating, respectively.

Results from the load-test and the finite-element analyses were used to determine the terms in (1). Member capacities were defined based on the measured neutral axis location and the inventory and operating stress levels. In this case, limiting values for inventory and operating stresses for the steel girders were taken to be 124 MPa (18 ksi) and 172 MPa (25 ksi), respectively. These values were based on an assumed steel yield strength of 227 MPa (33 ksi), which was chosen because of the age of the structure. Because of inclement weather at the end of the test, no impact data could be acquired. As such, an impact factor of 27%, as suggested by AASHTO (1989), was used. Live-load and dead-load effects were computed using the FEM. First, stresses due to self-weight of the beams and deck were computed using a noncomposite structure. Next, the additional dead load of the asphalt overlay was applied to the structure, and the effects were combined with those from the self-weight to get the entire dead-load effect. Finally, all live-load effects were computed by applying appropriate loadings caused by standard rating vehicles. In the case of models 1 and 2, the additional dead load of the asphalt and the live load were applied to a structure with composite behavior. The one significant difference between this rating procedure and the more traditional technique is the use of a two-dimensional numerical model of the bridge. Since the entire bridge is modeled as a system, the use of a distribution factor to determine load effects on a particular beam was not necessary. Instead, to account for multiple-lane loadings, several truck paths were defined for the rating vehicles, and stresses computed for each path were superimposed to obtain the maximum live-load response. While the current bridge is marked for only two lanes of traffic, it is wide enough to carry three lanes, according to AASHTO (*Standard* 1989). As a result, the bridge was rated based on the worst case arising from one, two, or three lanes being loaded. In general, the number of traffic lanes used to rate the bridge should be decided upon through consultation with the bridge owner and will likely depend on site-specific conditions.

Critical inventory and operating rating factors were computed for each of Delaware's seven rating vehicles. Based on the analysis, rating of the exterior girders was controlled by two lanes being loaded, while three-lane loads combined with the 10% reduction (*Standard* 1989) controlled the rating of the interior girders. In all cases, the final load ratings were governed by flexural stresses in the interior girders. The final rating factors for all three models, referred to as rating factors based on flexure, are given in Table 3.

TABLE 3. Computed Rating Factors

Rating vehicle (GVW kN/t) (1)	Rating Factor Based on Flexure			Rating factor based on interface shear (5)
	Inventory (2)	Operating (3)	Posting (4)	
	(*a*) Model 1			
HS20T (320/36)	1.52	3.09	2.04	1.02
S220 (178/20)	2.50	5.07	3.36	1.71
S335 (312/35)	1.37	2.78	1.84	0.97
S437 (325/36.5)	1.35	2.74	1.81	0.98
T330 (267/30)	2.18	4.43	2.93	1.50
T435 (312/35)	1.83	3.72	2.46	1.23
T540 (356/40)	1.65	3.35	2.21	1.09
	(*b*) Model 2			
HS20T (320/36)	1.11	2.42	1.55	1.07
S220 (178/20)	1.83	4.00	2.55	1.80
S335 (312/35)	1.01	2.20	1.41	1.02
S437 (325/36.5)	0.99	2.16	1.38	1.03
T330 (267/30)	1.57	3.43	2.19	1.57
T435 (312/35)	1.33	2.91	1.86	1.29
T540 (356/40)	1.20	2.61	1.67	1.14
	(*c*) Model 3			
HS20T (320/36)	0.62	1.59	0.94	NA*
S220 (178/20)	1.02	2.62	1.55	NA*
S335 (312/35)	0.57	1.45	0.86	NA*
S437 (325/36.5)	0.56	1.43	0.85	NA*
T330 (267/30)	0.89	2.28	1.35	NA*
T435 (312/35)	0.76	1.94	1.15	NA*
T540 (356/40)	0.68	1.74	1.03	NA*

*Not applicable.

Since unintended composite action was utilized in models 1 and 2, additional rating factors were computed that indicate the load at which composite action should no longer be counted upon. These limits were based on the horizontal shear stresses developed at the concrete slab/steel flange interface. Lichtenstein (1995b) suggests that composite action is primarily achieved because of the chemical bond between the deck slab and the steel girder. Based partially on experimental findings of Agarwal and Selvadurai (1991), Lichtenstein suggests that limiting bond strengths of 70 psi for nonimbedded flanges, and 100 psi for partially or fully embedded flanges, can be conservatively used. Since the flanges of the bridge studied here were partially imbedded into the concrete deck, a limiting value for shear stress of 100 psi was assumed. Rating factors were generated for Delaware's seven rating vehicles using this limiting value of shear stress, and taking the shear stress at the concrete slab/steel flange interface τ to be given by

$$\tau = \frac{VQ}{It} \tag{2}$$

where V = section shear force; Q = first moment of the area above the slab-girder interface; I = composite sections moment of inertia; and t = flange width. In these calculations, only load applied to the composite section was considered (for instance, asphalt overlay and truck load). These rating factors, referred to as rating factors based on interface shear, are also given in Table 3. The presence of bearing restraint has no significant effect on shear distribution. As such, models 1 and 2 have very similar shear rating factors.

SUMMARY AND CONCLUSIONS

Results of an experimental load test and numerical analysis of a posted, three-span, steel-girder-and-slab bridge have been presented. The bridge, whose cross section consists of nine steel girders, was originally designed to act as three, noncomposite, simply supported spans. Test results indicated that the girders were acting compositely with the concrete deck and that significant restraint was present at the bearing supports.

Based on the measured bridge response, an FEM of the structure's main span was generated. The model consisted of thin plate elements superimposed on a two-dimensional grid made up of line elements. The model utilized composite section properties and support restraint. Straightforward methods for determining appropriate composite section properties, as well as linear rotational springs to model the support restraint, were presented. Results of analyses conducted using the numerical model were compared to the measured response and found to be quite similar.

Based on the findings, three potential models to be used for rating the bridge were established. To decide which of the three models is the most appropriate for the final load-rating, a judgement regarding the reliability of the unintended composite action and support restraint must be made.

Unintended Composite Action

Several factors should be considered in deciding whether or not to use the benefits of unintended composite action in a load rating. These factors include the current condition of the bridge, its past traffic history (has the bridge experienced heavy truck loads in the past?), future traffic (will it be similar to the past?), structural redundancy, and the potential for future nondestructive structural evaluation. In this case, the condition of the deck and girders was relatively good. Neglecting the three months immediately prior to the load test during which the bridge had been posted, there is no reason to expect a change in traffic patterns from earlier years if the bridge were unposted (a weigh-in-motion study would provide useful data in this regard). Since the bridge has maintained composite action to date, there is nothing to suggest that it would abruptly lose composite action in the future. Furthermore, since nine longitudinal girders carry two lanes of traffic, the bridge has a high degree of redundancy, and a loss of composite action would be likely to occur gradually and not result in a sudden failure. Finally, ratings based on shear stresses at the slab/girder interface also indicate that normal traffic is not likely to cause a loss of composite action (all shear rating factors are ≥ 0.97).

Based on this evidence, the bridge engineer may want to include the effects of composite action in the final load rating of this particular bridge. If the bridge rating is to be based on unintended composite action, a relatively frequent inspection program is recommended. Future inspections should include examination of the deck-girder interface. If integrity of the composite action is ever in question, additional load tests using ambient traffic should be performed to determine neutral axis locations.

Support Restraint

With regard to the supports, it may not be as reasonable to rely on this unintended restraint at higher load levels. The restraint is a result of repair work done to the bridge, which involved welding the ends of the beams to their bearing plates. This restraint has led to cracking of the piers just below the support locations. Because of the poor condition of the piers, which implies that significant bearing forces may not be able to be developed, it seems reasonable to base the final load rating of this bridge on a model that neglects support restraint (has simply supported boundary conditions). In fact, by repairing the supports and restoring simply supported conditions, further damage to the piers may be prevented.

Final Rating

As earlier comments make clear, Model 2 appears to be the most appropriate for determining the final load-ratings for the bridge. Based on Model 2, inventory and operating load ratings for Delaware's seven load vehicles range from 0.99 to 1.83 and 2.16 to 4.00, respectively. Using these ratings, the posted rating factors for this Delaware bridge would range from 1.38 to 2.55. These results indicate that the bridge's load-carrying capacity may be substantially higher than the current load levels indicate (recall that the current posted rating factors range from 0.72 to 1.39) and suggest that the posting levels on the bridge may be unnecessary. This illustrates the benefits which can be derived from the experimental load rating of some of our posted bridges.

ACKNOWLEDGMENTS

The writers are grateful for support of this work provided by the Delaware Department of Transportation through the Delaware Transportation Institute (Grant No. TRA/DTI-4222312018). The writers would also like to acknowledge the help of the Delaware Department of Transportation with special thanks being extended to Chao Hu, Muhammad Chaudhri, Dennis O'Shea, Chuck Lightfoot, and Steve Bunting for their contributions. We would also like to thank graduate students William Edberg, William Finch Jr., Scott Holsinger, Ted Januszka, and Ted Thomson Jr., who helped during the instrumentation and field-testing of the bridge. Finally, we would like to recognize the efforts of undergraduate students Cortney Dula and Cory Farschman, who not only helped with the bridge testing, but also spent many hours analyzing data and developing preliminary computer models. The findings reported herein are those of the writers and do not necessarily reflect the view of the sponsors.

APPENDIX. REFERENCES

Agarwal, A. C., and Selvadurai, A. P. S. (1991). "Behavior of shear connection between steel girder and concrete deck slab." *Proc., CSCE Annu. Conf., Vol. 3*, Can. Soc. Civ. Engrg., Toronto, Canada.

Aktan, A. E., and Raghavendrachar, M. (1990). "Nondestructive testing and identification for bridge rating: pilot project." *FHWA/OH-90/005 Final Rep.*, Fed. Hwy. Admin. (FHWA), Washington, D.C.

Aktan, A. E., Chuntavan, C., Lee, K. L., and Toksoy, T. (1993). "Structural identification of a steel-stringer bridge." *Preprint, TRB Paper 930560*, Transp. Res. Board, Washington, D.C.

Bakht, B., and Csagoly, P. F. (1979). *Bridge testing*. Ministry of Transp. and Communication, Ont., Canada.

Bakht, B., and Jaeger, L. G. (1990). "Bridge testing—a surprise every time." *J. Struct. Engrg.*, ASCE, 116(6), 1370–1383.

Bakht, B., and Jaeger, L. G. (1992). "Ultimate load test of slab-on-girder bridge." *J. Struct. Engrg.*, ASCE, 118(6), 1608–1624.

BRASS 4.2 User Manual. (1987). Wyoming State Hwy. Dept., Cheyenne, Wyo.

Burdette, E. G., and Goodpasture, D. W. (1988). "Correlation of bridge load capacity estimates with test data." *NCHRP Rep. 306*, Transp. Res. Board, Washington, D.C.

Commander, B. C. (1989). "An improved method of bridge evaluation: comparison of field test results with computer analysis," MS thesis, Univ. of Colorado, Boulder, Colo.

Edberg, W. M. (1995). "State-of-the-art survey in experimental load rating of bridges," MS thesis, Univ. of Delaware, Newark, Del.

El Shahawy, M., and Garcia, A. M. (1989). "Structural research and testing in Florida." *Struct. Res. Rep. No. SRR-01-89*, Fla. Dept. of Transp., Tallahassee, Fla.

Fu, G., Sardis, P., and Tang, J. (1992). "Proof testing of highway bridges." *Res. Rep. 153*, Engrg. Res. and Devel. Bureau, N.Y. State Dept. of Transp., Albany, N.Y.

Fu, G., and Tang, J. (1992). "Proof load formula for highway bridge rating." *Transp. Res. Rec. 1371*, Transp. Res. Board, Washington, D.C., 129–141.

Gerstle, K. H., and Ackroyd, M. H. (1990). "Behavior and design of flexibly-connected building frames." *Engrg. J.*, 27(1), 22–29.

Goble, G., Schulz, J., and Commander, B. (1992). "Load prediction and structural response." *Final Rep. FHWA DTFH61-88-C-00053*, Univ. of Colorado, Boulder, Colo.
Lichtenstein, A. G. (1995a). "Bridge rating through nondestructive load testing." *Final Rep. NCHRP Proj. 12-28(13)A*, Transp. Res. Board, Washington, D.C.
Lichtenstein, A. G. (1995b). "Bridge rating through nondestructive load testing." *Tech. Rep. NCHRP Proj. 12-28(13)A*, Transp. Res. Board, Washington, D.C.
Markey, I. (1991). "Load testing of Swiss bridges." *Steel Constr. Today*, 5(1), 15–20.
Moses, F., Lebet, J. P., and Bez, R. (1994). "Applications of field testing to bridge evaluation." *J. Struct. Engrg.*, ASCE, 120(6), 1745–1762.
Pinjarkar, S. G., Guedelhoefer, O. C., Smith, B. J., and Kritzler, R. W. (1990). "Nondestructive load testing for evaluation and rating." *Final Rep., NCHRP Proj. 12-28(13)*, Transp. Res. Board, Washington, D.C.
Schulz, J. L. (1989). "Development of a digital strain measurement system for highway bridge testing," MS thesis, Univ. of Colorado, Boulder, Colo.
Schulz, J. L. (1993). "In search of better load ratings." *Civ. Engrg.*, ASCE, 63(9), 62–65.
Standard specification for highway bridges. (1989). American Association of State Highway and Transportation Officials (AASHTO), Washington, D.C.

APPENDIX B.

BRIDGE EVALUATION

AND

LONG-TERM MONITORING

by

Jonathan S. Reid

A thesis submitted to the Faculty of the University of Delaware in partial fulfillment of the requirements for the degree of Master of Civil Engineering

Summer 1996

BRIDGE EVALUATION

AND

LONG-TERM MONITORING

by

Jonathan S. Reid

Approved: _____

Michael J. Chajes, Ph.D.
Professor in charge of thesis on behalf of the Advisory Committee

Approved: _____

C.P. Huang, Ph.D.
Chair of the Department of Civil Engineering

Approved: _____

Stuart L. Cooper, Ph.D.
Dean of the College of Engineering

Approved: _____

John Cavanaugh, Ph.D.
Interim Associate Provost for Graduate Studies

ACKNOWLEDGMENTS

The author would like express sincere gratitude to Dr. Michael Chajes for his support, guidance, and friendship throughout the course of study and development of this thesis. Acknowledgment is also due to Dennis O'Shea and the Delaware Department of Transportation for the funding that allowed this study to take place and to Jeff Schultz and Bridge Diagnostics, Inc. for providing equipment and direction for the field testing of the bridges.

Appreciation is given to the bridge rating crew, Geoff Reichelt, Bill Finch, Al Meyer, Jack Demitz, and Ed Schluter, for all the hard work they did to get the job done. Thanks are also due to the undergraduate students, Wendy Neal, Dana Heffernan, and Mark Parker for helping out with the tedious calculations involved in this analysis. To the structural engineering graduate students, thanks for making this an enjoyable experience and for all the fun.

Finally, special thanks go to MSgt Dennis Stiff of the Delaware Air National Guard for his friendship and for giving me the extra work days whenever I needed them.

TABLE OF CONTENTS

LIST OF TABLES

LIST OF FIGURES

ABSTRACT

A method for diagnostic field testing of bridges has been presented in this thesis. Through the use of strain transducers, data retrieval and storage devices, and the application of known truck loads, an engineer can analyze field data to find bridge characteristics. These characteristics include, neutral axis location, composite action, concrete strength, effective slab width, impact factors, distribution factors, end restraints, and axial forces. By utilizing these values in bridge rating methods provided by AASHTO, a more accurate load carrying capacity for the bridge can be determined. The bridge testing and data analysis are discussed in detail in this thesis, while details of the actual rating process are to be described in a separate thesis.

Having already determined the current bridge characteristics, advantages of the long-term monitoring of these same properties are discussed, as well as some of the equipment available to perform this type of evaluation.

Chapter 1

INTRODUCTION TO BRIDGE EVALUATION AND LONG-TERM MONITORING

1.1 INTRODUCTION

Attaining a long service life is an important goal when structures are being designed. However, it is not safe to assume that an initially well-designed structure will exhibit desired long-term performance characteristics. As our infrastructure grows older; age, maintenance neglect, and exposure to severe weather conditions are contributing to its deterioration. Due to these problems, the need for initial, non-destructive evaluation and continued long-term monitoring has grown and has become a valuable method for evaluating a structures useful service life. Techniques for this evaluation and monitoring have varied in the past and only recently, thanks to the introduction of advanced field instrumentation, high-speed computers, and data retrieval equipment, has field testing and long-term monitoring been considered a feasible and cost effective task. With the benefit of this technology, we can tell what loads and strains are present on a bridge over short or long periods of time, we can evaluate the existing bridge conditions, and we can continue to monitor these bridge conditions throughout its life.

1.2 BRIDGE EVALUATION

The bridge evaluation utilized herein (diagnostic testing) involves the placement of strain transducers at various strategic locations on a bridge. Once this is

accomplished, trucks of known weight are driven across the bridge at both semi-static and dynamic speeds. The strains imposed on the bridge are measured and recorded. These strains are then evaluated to determine parameters such as load distribution factors, neutral axis locations and their implication regarding composite action of the deck, impact factors, axial forces, percent fixity at the reactions, and other section properties. Load distribution factors allow us to analyze a single beam at a time by predicting how many truck loads a given girder will support when the bridge is loaded with trucks, side-by-side, across the width of the roadway. Impact factors show the additional forces carried by the bridge due to trucks at normal (dynamic) crossing speeds, versus static loading. Axial forces, if present, will cause strains that will be superimposed on the strains caused by flexure and will affect the location of the neutral axis of a section. Percent fixity defines the behavior at the supports. The section properties that can be evaluated include concrete strength, effective slab width, deck thickness, moment of inertia, and section modulus. The neutral axis location is used to evaluate section properties and can also be used to determine whether or not composite action between a steel girder and the slab above is taking place. If the neutral axis of the section is above the mid-point of the girder, then composite action is taking place. If it occurs at the mid-point of the girder, then non-composite behavior is present. For many older bridges, while shear connectors were not used, composite behavior is often present. The existence of unintended composite behavior increases the capacity of the bridge. Using all of the parameters listed above, the current load carrying capacity of the bridge can be estimated.

1.3 LONG-TERM MONITORING

Resistive gages tend to drift with time and are often not suitable for long-term monitoring. Other gages, such as vibrating wire gages can be used for long-term monitoring of strains imposed due to temperature fluctuations and applied loads. Along with these gages are remote data acquisitioning systems that are normally mounted on the bridge to retrieve strain measurements as they occur. When these strains occur, the time and date is recorded along with the magnitude of strain. The information is stored in the acquisitioning system and can be retrieved periodically. Using such a system, strain readings can be taken at predetermined intervals and used to indicate any changes in the bridge's behavior or "health", between more in-depth evaluations.

1.4 OBJECTIVE

There are two objectives to this study. The first objective is to evaluate two of Delaware's bridges located on I-95. These bridges were chosen from a list of bridges in Delaware that were thought to be capable of carrying normal traffic loads, but were believed to be unable to carry heavy permit vehicle loads. Permit loads are those loads that exceed HS-20 type loading and require special permits to travel on our highways. The two bridge evaluations were accomplished using typical strain transducers to measure strains present along the girders as trucks of known weight cross. The second objective is to evaluate the potential benefits of long-term monitoring and some of the equipment currently available.

Chapter 2

DETERMINATION OF BRIDGE RATING PARAMETERS

2.1 Rating Techniques

Another thesis following this one will use the results of the data analysis presented here to rate the two bridges under consideration. The two rating techniques being considered helped to guide the data analysis procedure. One rating technique being considered is the use of a computer program developed by the Wyoming Department of Transportation called Bridge Rating and Analysis of Structural Systems (BRASS).[1] This program is used by the Delaware Department of Transportation (DelDOT) to evaluate all of Delaware's bridges. The second method under consideration is the one presented in the final report for NCHRP (National Cooperative Highway Research Program), Project 12-28(13)A titled "Bridge Rating Through Nondestructive Load Testing."[2] This particular approach was developed by A.G. Lichtenstein and Associates and was used to evaluate two bridges located on I-84 of the New York State Thruway.[3] Results from the two methods will be compared. To incorporate the results of the field test into the rating procedures, particularly for BRASS, specific parameters need to be determined from the test data. BRASS uses common design parameters as defined in the American Association of State Highway and Transportation Officials (AASHTO) Standard Specifications for Highway Bridges.[4] The evaluation is based on the bridge rating formula given in the

AASHTO Guide Specifications for Strength Evaluation of Existing Steel and Concrete Bridges[5] and is expresses as:

$$R.F. = \frac{\phi R_n - \gamma_D D}{\gamma_L L(1 + I)} \qquad (2.1)$$

Where:

R.F. = rating factor

R_n = nominal strength or resistance

γ_D = dead load factor

γ_L = live load factor

D = dead load

L = live load

I = impact factor

ϕ = resistance factor

The factors needed to evaluate Equation 2.1 dictated what parameters were concentrated on during this project. The determination of those parameters from field test data is the primary focus of this thesis.

2.2 Equipment Used and Test Procedure

The equipment that was used to measure and store the strains produced by the truck loads was provided by Bridge Diagnostics, Inc. and the tests were performed by a team of students. Team members installed strain transducers at various locations

on the bridge girders. While the exact locations of the transducers used in the field tests is detailed in later sections, a typical layout is shown in Figure 2.1.

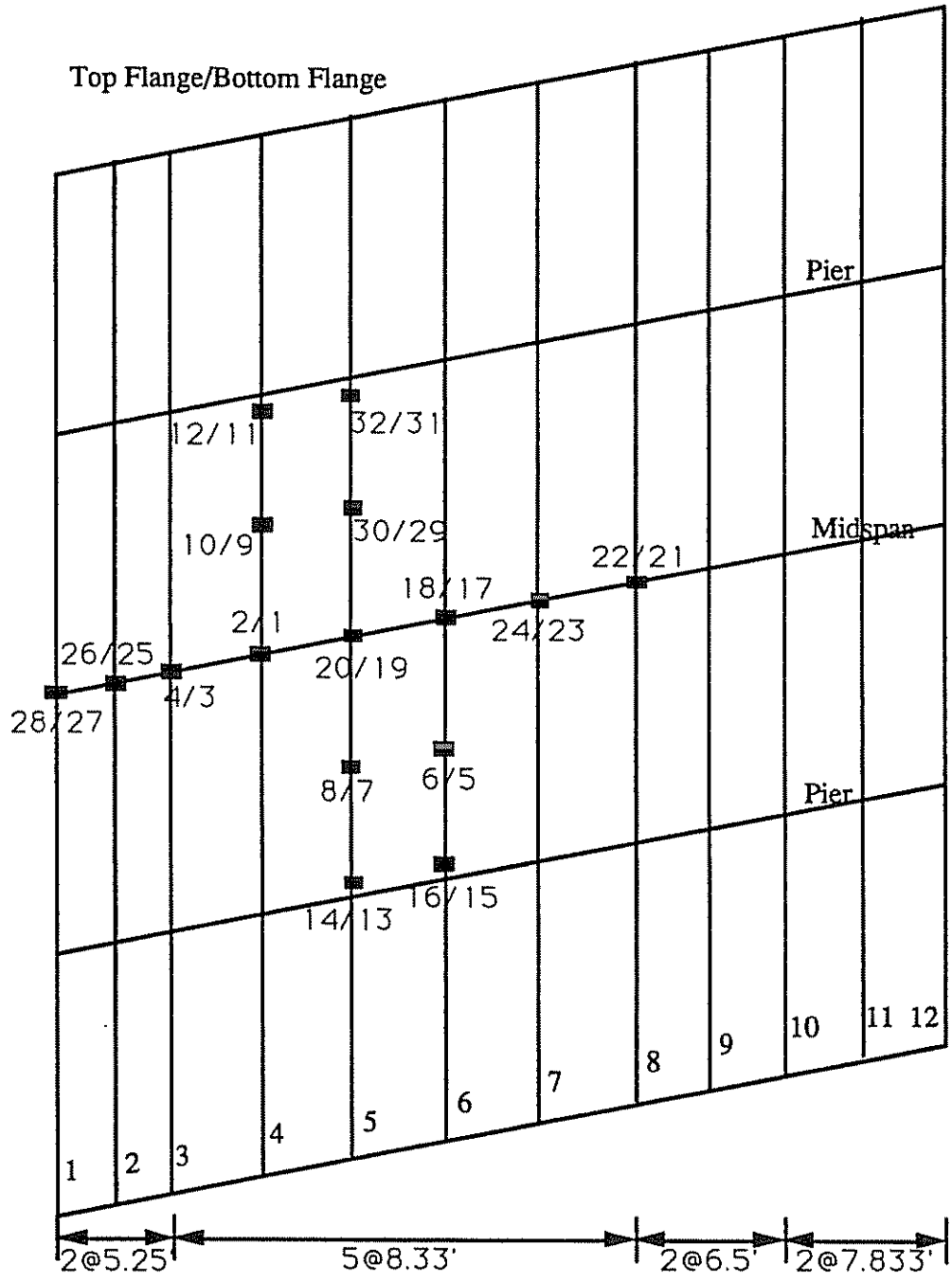

Figure 2.1. Typical Gage Layout

In selecting the layout, it is important to have gages near the top and bottom faces of the bridge beams to help identify section properties, to locate gages along the length of some beams to evaluate end restraints and axial forces, and to locate gages on all beams at selected cross-sections of the bridge deck to evaluate load distribution effects. Both bridges tested were steel-girder-and-slab structures and the transducers were fixed to the girders using C-clamps or by using an adhesive to glue the gages directly to the member. The member surface was cleaned of debris and paint using a grinder to ensure good contact and an accurate reading of steel strain. A laptop computer with the appropriate data acquisition software was connected to a strain conditioner box for the 32 channels, which in turn was connected to the 32 strain transducers. The entire instrumentation was completed in a safe and timely (matter of hours) manner with few problems. Although 32 gages were used, there were less than 32 locations monitored. In most cases, gages were placed on the top and bottom flanges at a single location. Figure 2.2 details a strain transducer, which has a 3 inch gage length.

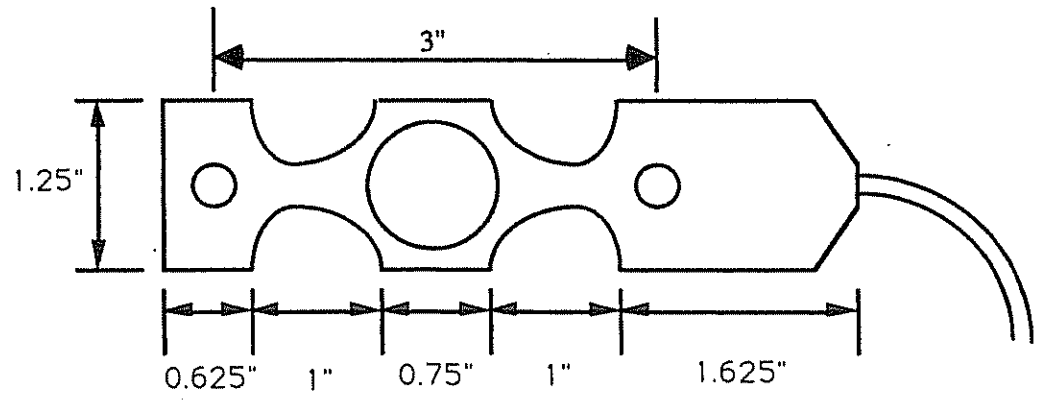

Figure 2.2. Strain Transducer

The laptop was connected to a conditioning box in order to condition and normalize initial strain readings. Eight junction boxes with cables were connected to the conditioning box and run to the transducers. Each of these cables was responsible for linking four transducers to the main system. Before each test, various longitudinal paths were selected for the truck to pass along. By having different paths across the bridge width, valuable information regarding load distribution can be gained. For a given pass, the truck drove over the deck at approximately 5 mph and strains were recorded at a frequency of 30 Hz. A remote location indicator was used to put a marker in the data record to indicate truck location. The remote location indicator was activated according to 10 foot intervals that were laid out along the bridge length. Overall, this system proved to be a worthy means of measuring the strains produced on the bridge.

2.3 Parameters

There are five areas of the rating process for which load test results can be used to provide site-specific data for an existing bridge. These five areas are (1) section properties and flexural behavior of the slab-and-girder system (or other longitudinal load carrying system) including the presence of unintended composite action, (2) the effect of dynamic traffic loads (impact), (3) transverse load distribution behavior, (4) the presence of any unintended end restraint (support fixity), and (5) the presence of axial forces in the main flexural members.

Without data from a load test to quantify actual behavior of the aged structure, parameters related to the five areas listed are computed based on the original bridge design plans and by using conservative, non-site-specific formulas provided by AASHTO.[4,5] However, others have shown that when field tested, existing bridges

tend to have a significantly different capacity than predicted based on plans and the associated simplified analysis procedures used.[6] In fact, actual bridge capacities computed using parameters established through field testing have proven to be higher than initially computed.[6]

The following sections will detail how parameters related to the five areas are commonly computed, how site-specific values can be computed based on field test data, and why the actual values may differ from the code prescribed values.

2.3.1 Section Properties

The section properties considered to be important for rating are the moment of inertia, the section modulus, and whether or not the deck and girder are acting compositely. These section properties are dependent on (1) concrete strength, (2) the deck thickness, (3) the effective width of the compression flange (deck), and (4) the neutral axis location of the section. Since the neutral axis location is known from the test data (details will follow), two of the remaining three parameters must be chosen and then the remaining term can be evaluated. The choice as to which term to evaluate will depend on the specific bridge being considered. Deck thickness can typically be taken from the bridge plans, unless asphalt buildup has occurred. Effective widths can be approximated using theories developed for composite design. In many cases, the value for concrete strength will be left as the unknown, since it may have a significantly different strength than called for on the original design plans. If an accurate value is desired, a core sample can be taken, or a Schmidt Hammer or Windsor Probe can be used. The effect of approximating particular values rather than others will be addressed later.

Another point of interest that should be considered when evaluating the effective deck width, is the effect of the magnitude of strain present at the section. This will be discussed later in this section.

2.3.1.1 Neutral Axis Location

The neutral axis location of a section is found by making use of the assumption that plane sections remain plane. At a given instant, the neutral axis can be determined by plotting the strain at the top and bottom flanges and using similar triangles (i.e. assuming a linear strain distribution). Figure 2.3 demonstrates this technique.

The following equation simplifies the approach:

$$Y = \frac{\varepsilon_b d_g}{\Delta\varepsilon} \tag{2.2}$$

Where:

Y = location of neutral axis from bottom flange

ε_b = strain present at bottom flange of beam

d_g = distance between strain gages

$\Delta\varepsilon$ = change in strain between gages

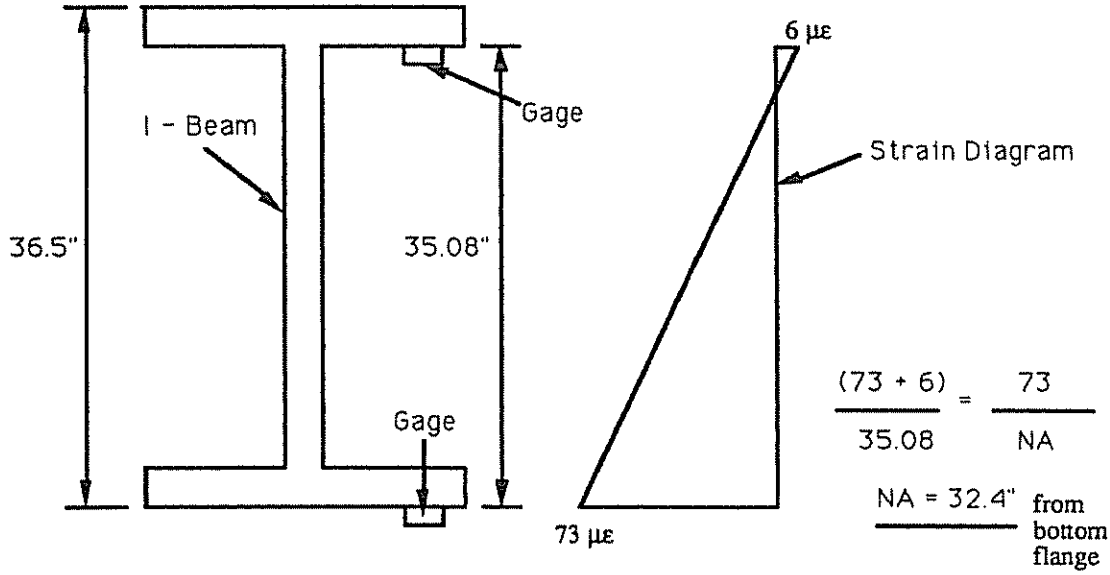

Figure 2.3. Neutral Axis Location Determination

The neutral axis for each girder across a given width of the bridge due to a single truck location (preferably at midspan) can then be graphed. Next, the location of the actual truck load path is drawn on the graph as in Figure 2.4. The point where the truck path crosses the neutral axis plot corresponds to the representative value of the neutral axis for that pass. Some consistency between passes should be found when this is complete, depending on the girder spacing. Neutral axis graphs for the various pairs of gages attached to the bridges in this thesis are located in the Appendices.

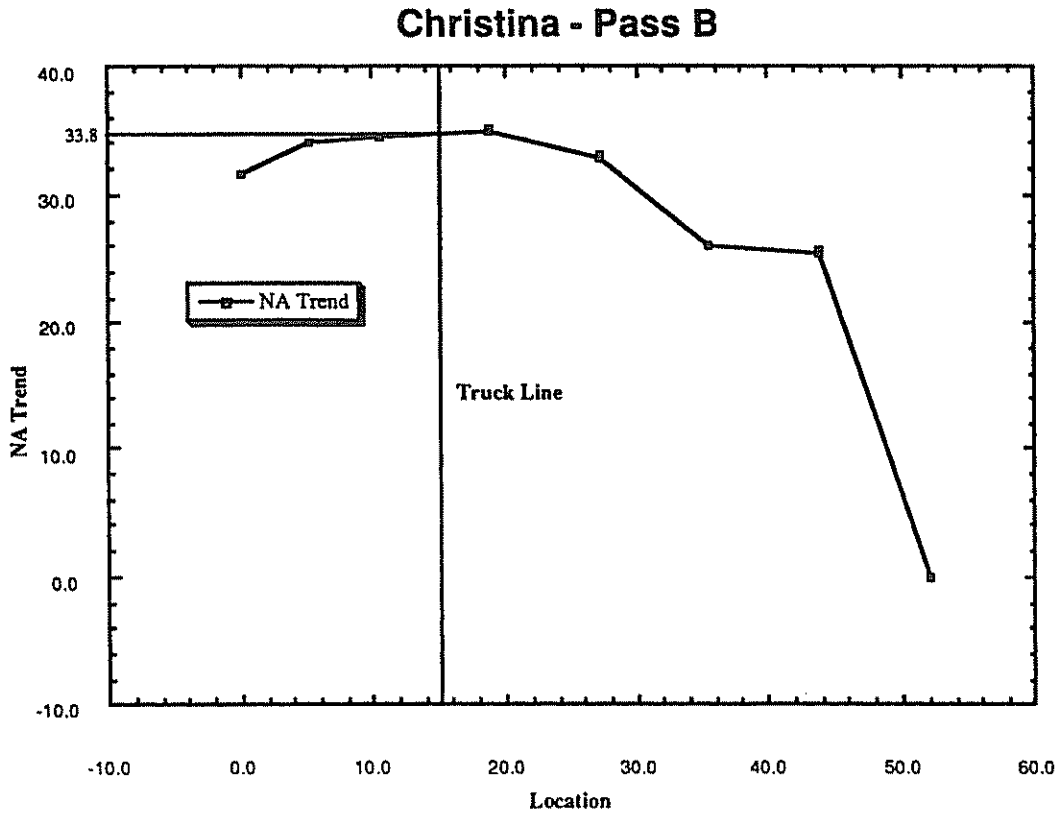

Figure 2.4. Neutral Axis - Truck Pass Location and Strain Intensity.

During a bridge test, each pair of gages (top and bottom flange) will record vast amounts of data. The magnitude of strains recorded will vary from very small readings when the truck is far from the gage locations, to some maximum readings when the truck is in close proximity to the gages. It is important to note that the magnitude of strain (level of applied stress) can affect the location of the neutral axis. The primary reason for this is that as the level of stress decreases, the effective width will decrease. This change in effective width will cause the neutral axis to move closer to the bottom flange. This trend can be seen in Figure's 2.4 and 2.5. In Figure 2.5, the transducers (25 and 26) are located at the midspan location of girder 2.

The time-history of the neutral axis shows the value approaching a maximum (closest to the top flange) at the point where the truck reaches midspan (higher stresses) and shows the value dropping off (moving away from the flange) before and after the midspan (lower stresses).

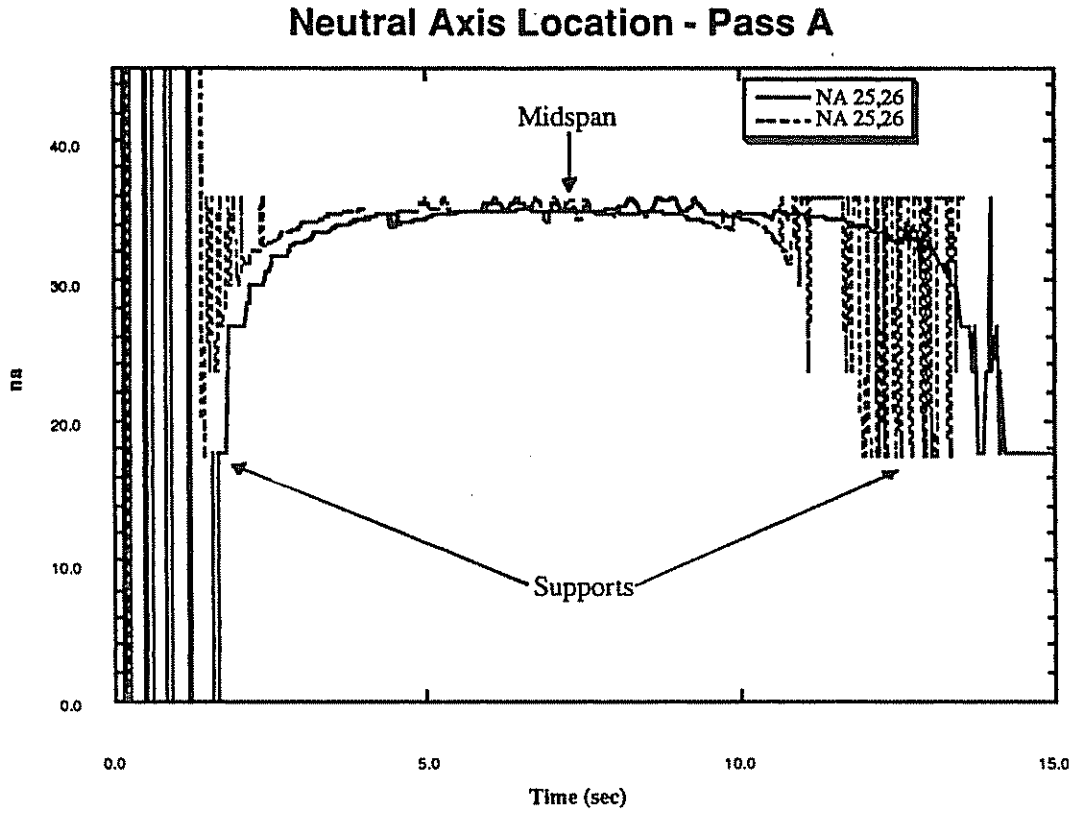

Figure 2.5. Neutral Axis - Time history.

Since ratings are based on limiting stress cases, neutral axis locations should be selected based on data resulting from truck loads close to the gage being used to compute the neutral axis value. One should also be aware that as strain values get very small, such as when the truck is at either end of the bridge or far from the gage in question, inaccuracies caused by dividing by very small strains will lead to erroneous neutral axis locations (see Figure 2.5).

In order to use the tributary area of the deck as the effective width for each girder, the strains used to calculate the neutral axis location must be within a certain percentage of the maximum strain felt on the bridge at any point. Analysis of site-specific data must be performed to find this required tolerance. Finally, the neutral axis location can also be influenced by the presence of axial force. This will be discussed later.

2.3.1.2 Concrete Strength

The concrete strength of the deck is a property that can be estimated or evaluated using non-destructive techniques. For older structures, a reasonable estimate may be to use twice the specified initial concrete strength. Using the assumed strength f'c, a value for the modular ratio N can be computed using the following formula:

$$N = \frac{E_s}{E_c} \qquad (2.3)^7$$

Where :

N = modular ratio

$E_s = 29{,}000{,}000$ psi

$E_c = 57{,}000\sqrt{f'c}$ psi $\qquad (2.4)^7$

If the deck thickness and effective width are assumed, then estimating the concrete strength is not necessary. In that case, the value of the concrete strength can be determined using a formula developed for this project and detailed in Section 2.3.1.3.

2.3.1.3 Deck Thickness

The deck thickness can be determined using any of several methods. Two methods are considered in this project. The first is to use the deck thickness specified in the original design plans. This is by far the easiest method, but is dependent on the presence of accurate plans. This also neglects any contribution of a wearing surface. In some cases, accumulation of overlays can add a measurable amount to the deck. The second method is to take field measurements. Once the correct deck thickness is found, an equation developed for this thesis may be used to find effective width or concrete strength. Recognizing the lengthy requirements of determining the deck thickness through the use of diagrams and sketches, the following formula was developed to aid in this calculation:

$$D = \frac{b_{eff}(Y - db) \pm \sqrt{[b_{eff}(Y - db)]^2 - 4[\frac{b_{eff}}{2}(Ab)(y_b - Y)]}}{b_{eff}} \qquad (2.5)$$

Where:

D = deck thickness

Y = distance to neutral axis of section from bottom flange, found by strain measured

db = depth of beam

y_b = neutral axis of beam alone

A_b = area of beam

$$b_{eff} = \frac{\text{Width of Concrete Applied}}{N} \qquad (2.6)$$

Note - Width of concrete applied is defined in the ACI Code[7] as the smallest of the following:

1. b_E = L/4 (2.7)[7]
2. b_E = center-to-center spacing of beams (2.8)[7]

Where:

L = span length of beam

It should be noted that Equation 2.5, combined with a known neutral axis location from testing, can be used to find any one of the three parameters (concrete strength, effective width, deck thickness) once the other two are assumed. If the deck thickness and effective width are assumed, the concrete strength can be found by varying its value until the correct deck thickness is achieved. If the deck thickness and concrete strength are assumed, the effective width can be found by varying its value until the correct deck thickness is achieved. If the concrete strength and effective width are assumed, then the deck thickness can be directly solved for using Equation 2.5.

Since the main purpose of determining the neutral axis of the system is to calculate the actual moment of inertia (I), a study was performed to see what affect various assumptions would have on its value. Using dimensions of one of the tested bridges, the effect on I of changing the concrete strength and deck thickness, while maintaining a constant effective width equal to the girder spacing and a fixed neutral axis location, was studied. The following behavior was observed:

Table 2.1. Deck Thickness vs. Concrete Strength Effects on Moment of Inertia

f'c (psi)	Thickness (in)	I_X (in^4)
4000(plan)	8.52(plan)	22460
5000	7.98	22236
6000	7.56	22061
7000	7.22	21920
8000	6.94	21807

The findings of this study indicated that as the concrete strength and the deck thickness varied by as much as 100% and 23% respectively, the corresponding moments of inertia varied by 3%. This indicates that an error in the assumed value of f'c or deck thickness should cause only a relatively small change in the related moment of inertia, which is the value needed for rating the bridge.

2.3.1.4 Moment of Inertia

The moment of inertia can be determined once the neutral axis location and the deck thickness have been determined. Using simple formulas from engineering mechanics, the following formula was developed:

$$I = [I_d + A_d d^2_d] + [I_b + A_b d^2_b] \qquad (2.9)$$

Where:

I = moment of inertia of composite section

I_d = moment of inertia of the transformed deck

A_d = area of transformed deck

d_d = distance (neutral axis of transformed deck to neutral axis of section)

I_b = moment of inertia of the beam alone

A_b = area of beam alone

d_b = distance (neutral axis of beam to neutral axis of section)

2.3.1.5 Section Modulus

The section modulus can be determined for the steel girder and the deck separately using the following formulas:

$$S_b = \frac{I}{c_b} \tag{2.10}$$

$$S_d = \frac{I}{c_d} \tag{2.11}$$

Where:

S_b = section modulus of beam

S_d = section modulus of deck

I = moment of inertia of total section

c_b = distance from section neutral axis to bottom flange

c_d = distance from section neutral axis to top of deck

By dividing the maximum applied moment by the section modulus, the maximum applied stress can be found.

2.3.2 Impact Factors

Impact factors indicate the amplification of loads due to dynamic loading (i.e. trucks moving at full speed). AASHTO[4] currently dictates that impact factors will be determined by the following formula:

$$I = \frac{50}{L + 125} \tag{2.12}$$

Where:

I = impact fraction (maximum of 30%)

L = length in feet of the portion of the span that is loaded to produce the maximum stress in the member

Through field testing, impact factors (I+1) are determined by comparing the magnitude of strain produced at a specific location due to semi-static loading with that produced by dynamic loading. Semi-static loading is defined as a fully loaded truck passing over the bridge at slow speeds to ensure little or no dynamic effects. In our tests, dynamic loads were produced by fully loaded trucks passing across the bridges at approximately 55 mph on several different paths. Impact factors for all gages are computed by comparing peak strains measured at a given gage location due to dynamic and semi-static loading. All of the values are then plotted on an impact factor (due to peak strain) vs. magnitude of peak strain plot. This plot is used to select the most appropriate value for I+1. The implementation of this factor into the load rating technique allows for a rating to be computed that accurately reflects the effects

of dynamic traffic loads, since, for the most part, the impact factors found are greater than 1. According to AASHTO[4], impact factors of 30% or more (1+ 0.3) need not be accounted for, however, field tested impact factors may prove to be greater than 1.3.

Impact factors are useful since the affect that a moving vehicle has can be much different than that of static conditions and must be considered to ensure bridge safety. It is important to note that impact factors are very dependent on the condition of the wearing surface and joints and, therefore, are site specific. As a result, determination of actual impact factors through field testing is very useful.

2.3.3 Distribution Factors

The distribution factor allows one to compute the equivalent number of trucks carried by a single girder for a bridge loaded by vehicles in all available lanes at a cross-section. AASHTO[4] dictates that distribution factors, in terms of the number of wheel lines, for concrete decks supported by 4 or more steel girders will be determined using the following formulas:

$$DF = \frac{S}{5.5} \qquad (\text{for } S = 6 \text{ ft or less}) \qquad (2.13)$$

$$DF = \frac{S}{4.0 + 0.25S} \qquad (\text{for } 6 \text{ ft} < S < 14 \text{ ft}) \qquad (2.14)$$

Where:

DF = distribution factor

S = spacing of girders in feet

In order to determine distribution factors experimentally, it is necessary to place strain transducers on the bottom flanges of girders across the width of the bridge at one or more locations. It is also necessary to load the bridge on several paths across the bridge width. The distribution factors are determined by utilizing influence line graphs created from field test data from gages at a particular cross-section. Once influence lines have been drawn, the span width is divided by 12 feet, according to the AASHTO Bridge Design Specifications[4]. The number calculated is the maximum number of vehicle lane widths allowed. Within each of these 12 ft. lanes, a 6 ft. vehicle width is placed. This vehicle is placed anywhere within the 12 ft. in order to get the highest strain reading on the influence line graph. Each subsequent vehicle is placed in the adjacent lanes according to this directive, with caution given to allow for a 2 ft. clearance from the edge of any lane. After this has been accomplished, the corresponding strain readings at the vehicle center lines are added and compared to the total strain of one wheel line on the bridge. This total strain value can be found by taking the sum of the strains in the bottom flanges across a cross-section caused by a truck located at mid-span, and then dividing by two wheel lines. In order to get the value of the distribution factor, the influence line strain sum must be divided by the total strain that would be experienced due to a single truck (or wheel line).

Distribution factors determine how effective the deck system is at distributing loads transversely. In other words, a deck that has fewer girders may require each of its girders to carry more that 100% of one truck load. In the same sense, a deck system with many girders may require each girder to carry less than 100% of one truck load. Since the distribution factors provided by AASHTO[4] must be conservative to be safe for all bridges, combined with the fact that all bridges act differently, the ability to experimentally determine these factors is valuable.

2.3.4 End Restraints

The end restraints indicate the amount of fixity present at the supports. Theoretically, pinned or hinged deck supports are modeled as frictionless. Some fixity may be found due to weathering deterioration causing bearings to freeze in place, or due to friction in the supports. Through field testing, actual restraint at the bearing is determined by comparing actual strains at the supports with those expected for cases of 100% fixity and 0% fixity. In order to do this, it is necessary to have several strain gage locations along the length of a single beam. For a simply supported beam with a point load at midspan and having 0% fixity, the strain reading on the tension flange at the bearing is zero, which indicates no moment present. For the same beam having 100% fixity, the strain readings on the tension flanges at the bearings should be equal in magnitude to strain in the tension flange at the midspan of the beam. Using the absolute value of the ratio of end strain to midspan strain, a percentage of fixity can be determined. Figure 2.6 illustrates this relationship.

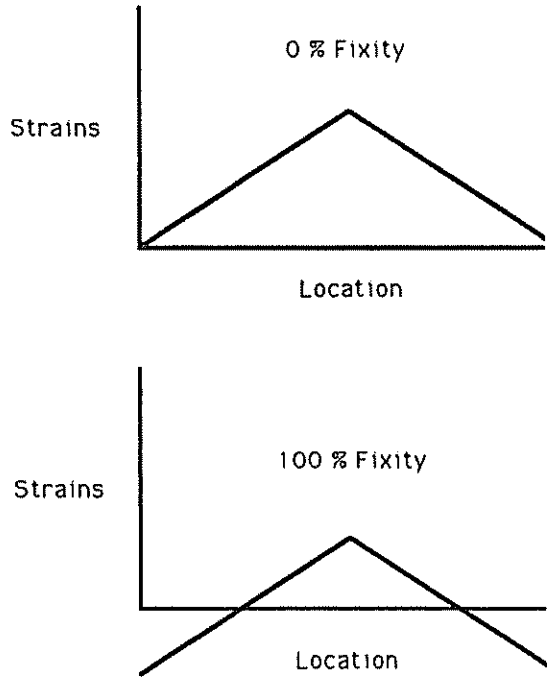

Figure 2.6. End Restraint Theory

In general, measured strain diagrams will fall somewhere between these two cases and the percent fixity can be found through a linear interpolation. While simple-span and continuous-span systems will have different moment distributions and, therefore, strain distributions, the same principle can be used.

2.3.5 Axial Forces

Bridges are typically designed with bearings and expansion joints (continuous bridges) so that axial forces will not occur due to thermal expansion and contraction. If these design features are functioning properly, axial forces due to vehicular live loads will only occur due to arching action. However, if the bridge bearings have become frozen or have been altered as part of a rehabilitation, or if the expansion joints are not working properly or have been paved over by a wearing

surface, it is possible that vehicular live loads will cause axial forces to develop in the bridge girders. While identifying the magnitude of axial forces from the field test data is not straight forward, two methods for easily identifying its presence have been developed. In most cases, only insignificant amounts of axial force will be present and their affect on the strain data can be neglected. If, however, axial force is thought to be present and producing significant axial strains, their affect on the computation of parameters discussed earlier must be considered.

One method of identifying the presence of axial forces in a particular girder is to look at the variation of neutral axis location along the length of the girder. From Figures 2.7 and 2.8, one can see that both simply-supported and fixed-supported beams exhibit a constant neutral axis location along the beam length when loaded transversely (flexure). However, when the beams are loaded with transverse and axial loads (flexure and axial), the location of the neutral axis varies along the length of the beam. As a result, if one finds a constant neutral axis location along the length of a girder for a fixed location of load, it can be safely assumed that the axial force is negligible.

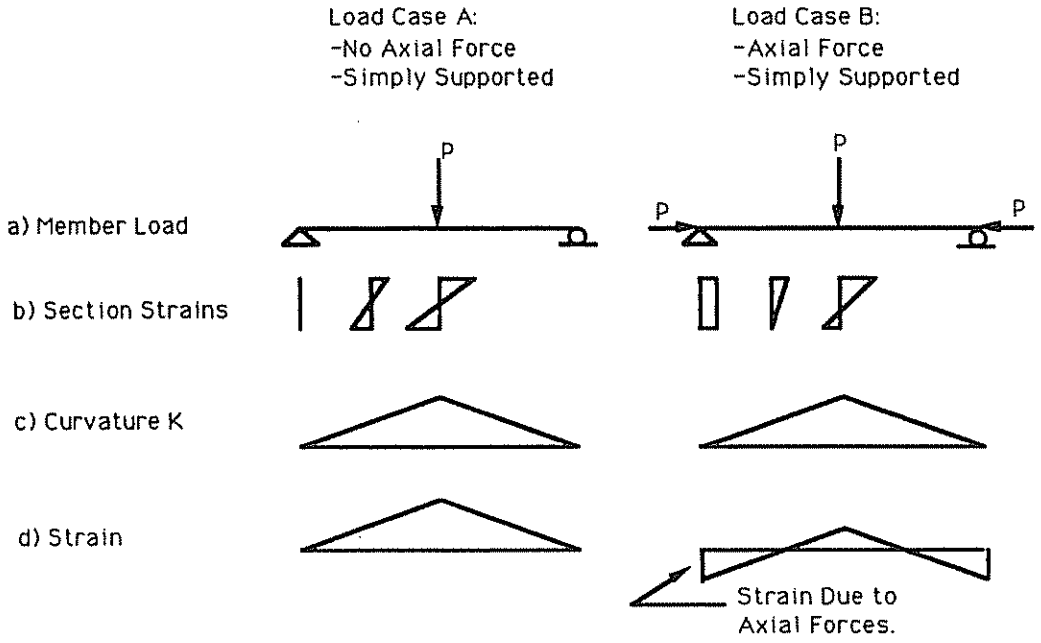

Figure 2.7. Axial Load Theory - Simple Supports

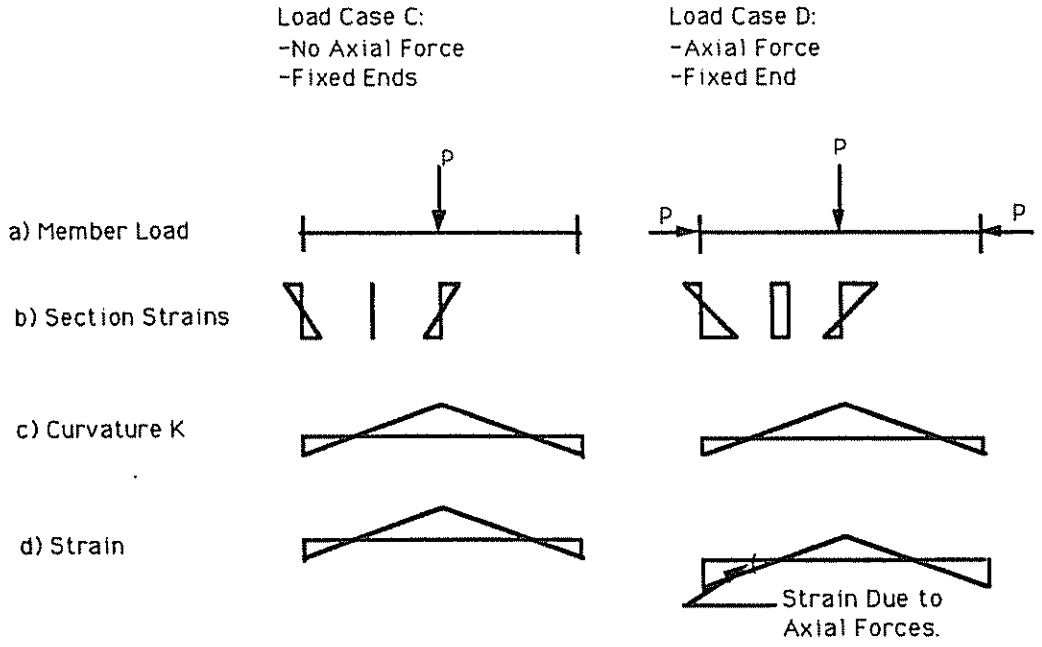

Figure 2.8. Axial Load Theory - Fixed Supports

A second check for the presence of axial force is to look at the strain distribution through the depth of the girder at, or near, the support locations. Since a properly functioning bearing will lead to very small strains due to flexure, the identification of a superimposed constant strain distribution caused by axial force is easy to distinguish (Figure 2.9). In this case, the magnitude of axial force can be found by multiplying the uniform axial stress by the cross-sectional area of the girder. It should be noted that if the end supports are providing partial fixity, one must locate a point of inflection (i.e. zero moment) to be able to easily evaluate the axial strain component.

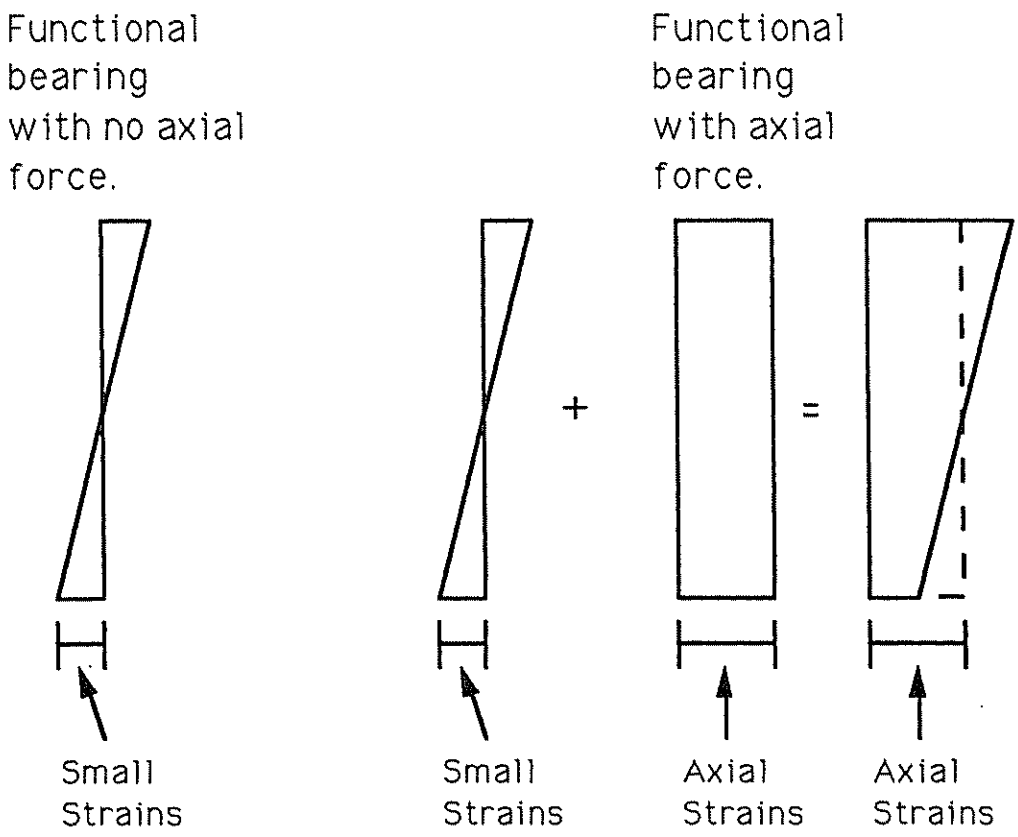

Figure 2.9. Axial Force Based on Strains at Bearings.

2.4 Summary

As stated earlier, there are several parameters required to complete a successful bridge evaluation. Considering the examples that will be used for this project, the parameters that will be determined are the impact factors, distribution factors, axial loads, end restraints, and several section properties including, section modulus, moment of inertia, deck thickness, concrete strength, effective width, and neutral axis location; which indicates the presence of composite or non-composite action in the system.

Chapter 3

THE CHRISTINA CREEK BRIDGE ON I-95

3.1 Background of the Christina Creek Bridge

The Christina Creek Bridge is located on I-95 near the Maryland border. This bridge consists of three simply supported spans in both the northbound and southbound directions. Only the center span of the southbound bridge was evaluated, since that span was believed to have a low overload capacity (i.e. permit loads). The southbound bridge is a compositely designed, slab-and-steel-girder system consisting of four traffic lanes, two breakdown lanes, and one exit lane. It is responsible for carrying large amounts of commuter traffic between Wilmington, DE and Maryland. Figure 3.1 shows the bridge in plan view. Since its original completion date, three additions have been made to the bridge to support the growing amount of traffic. Each of the three additions entailed adding two girders to the existing span to increase the width. The first and third additions added two girders each to the southern-most side, and the second addition added two girders to the northern-most side, increasing the bridge width from 41' 8" to 57' 4" for the first addition, 57' 4" to 67' 10" for the second addition, and 67' 10" to 80' 10" for the third. As a result of these additions, there is non-symmetrical spacing between the different girders ranging from 5' 3" to 8' 4". Figure 3.2 shows this girder spacing. The center span is 62' 6" in length and 80' 10" in width between outside girders. As its title indicates, this bridge crosses over the Christina Creek, which is a nearly stagnant body of water that has a width of 40' and a maximum depth of 3' to 4' under the span.

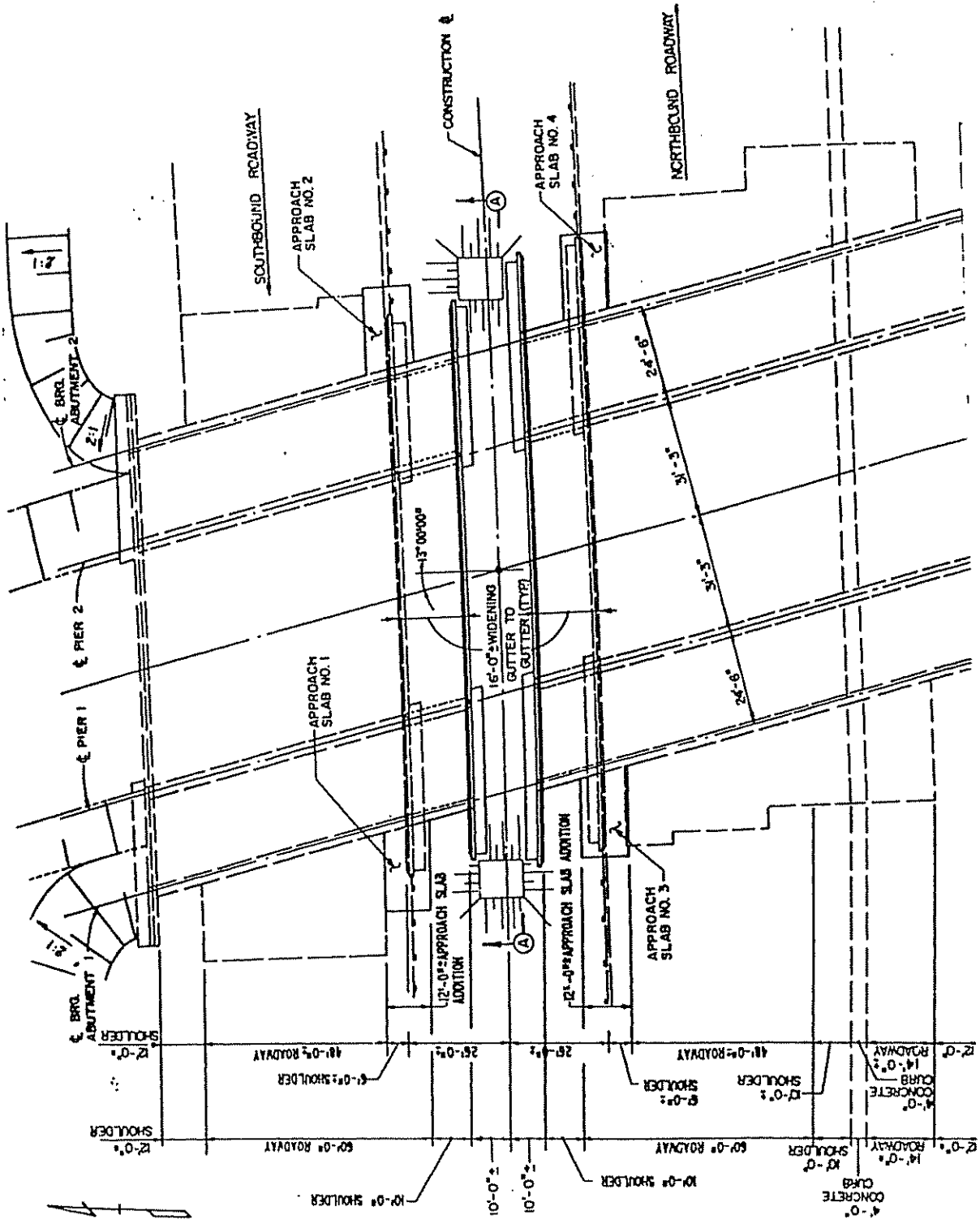

Figure 3.1. Christina Creek Bridge Plan View.

3.2 Preparation and Instrumentation of Bridge

A site survey was conducted in July of 1995 to determine what obstacles and site specifics would be encountered during the test setup and test itself. As would be expected, the creek posed a considerable obstacle to the instrumentation of the bridge at the center and quarter points of the span. In order to overcome this, a series of cables and scaffolding was used. This provided adequate accessibility to all of the girders, while maintaining a safe working platform for the bridge testing team.

In November of 1995, the instrumentation of this bridge was performed using 32 strain transducers to measure the strains in the top and bottom flanges of the girders at 16 locations. The span itself was at a 13 degree skew, as detailed in Figure 3.2. Since load paths were assumed to be relatively symmetric about the lateral midspan location, the bridge was gaged accordingly. Emphasis was placed on the midspan of the bridge, gaging all of the first eight girders from the north side at this point. This was done in order to have sufficient data across the bridge to determine the distribution factors. Girders 4 and 5 were gaged at the quarter and end points on the eastern-most side and girders 5 and 6 were similarly gaged on the western-most side. These locations were chosen in order to have measurements for the determination of the longitudinal load distribution behavior of the bridge, thereby allowing information regarding end restraint to be determined. Figure 3.2 details the gage layout on the span. This approach was taken and assumed to be adequate to measure the important points on the span. The whole gaging process took approximately 6 hours to complete.

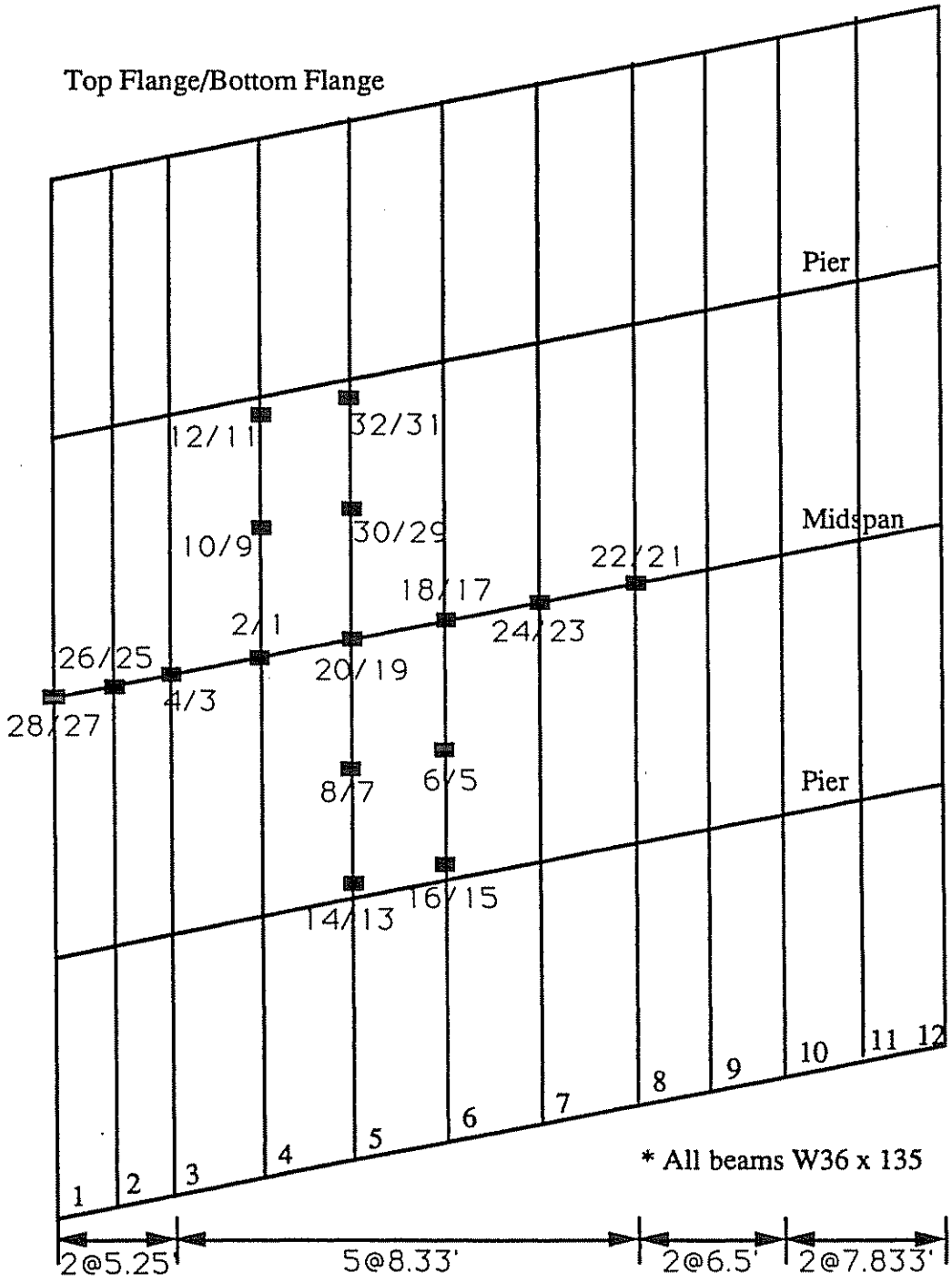

Figure 3.2. Gage Location and Girder Spacing.

3.3 Load Test of the Christina Creek Bridge

The load test for this bridge was conducted immediately following the gaging of the span. Typically, one would use a vehicle loaded to the legal limit if the bridge being tested had no load restrictions. In this case, a dump truck weighing 67.75 kips was used to load the bridge along various longitudinal paths, enabling substantial strain data to be collected. The truck load used was limited by the amount of sand that could fit in the back of the truck. Figure 3.3 details the wheel spacing and weight distribution.

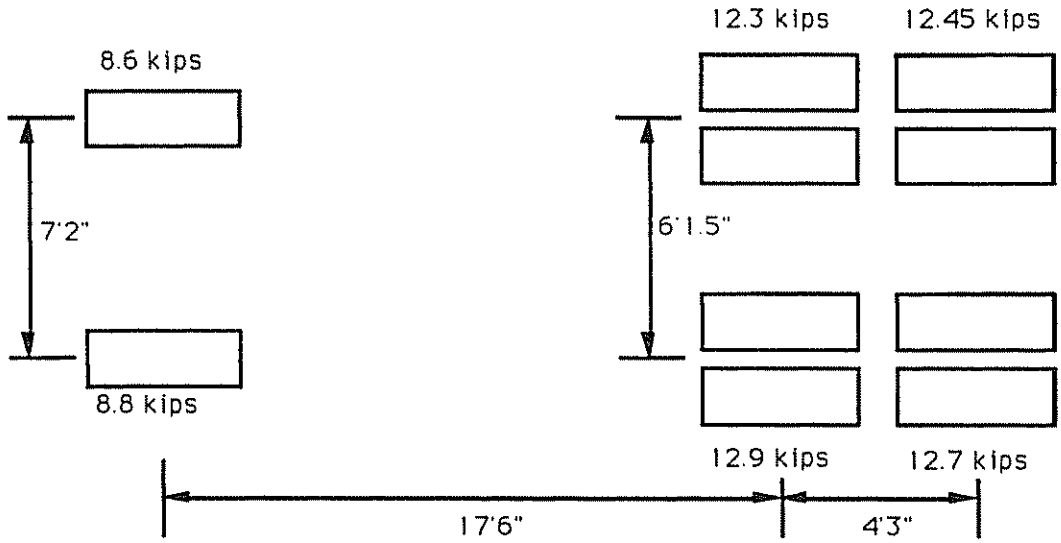

Figure 3.3. Truck Weight Distribution Detail.

Four longitudinal load paths were established using existing traffic lanes. Two were located on either side of a painted lane line 11.2 feet from the northern edge of the bridge and the other two were located on either side of a painted line located 32 feet from the northern edge. Path A corresponded to the truck moving with the driver-side wheels on the 11.2 foot painted line, while Path B corresponded to the truck having its passenger-side wheels on the 11.2 foot line. Similarly, Path C corresponded

to the truck moving along with its driver-side wheels on the 32 foot line and Path D had the passenger-side wheels on the 32 foot line. The load paths are detailed in Figure 3.4. These paths were chosen since they provide easy paths to follow and were where the actual lanes were painted on the bridge. Since the purpose of this evaluation was to determine the operating capacity, the actual lanes represented some of the critical load paths.

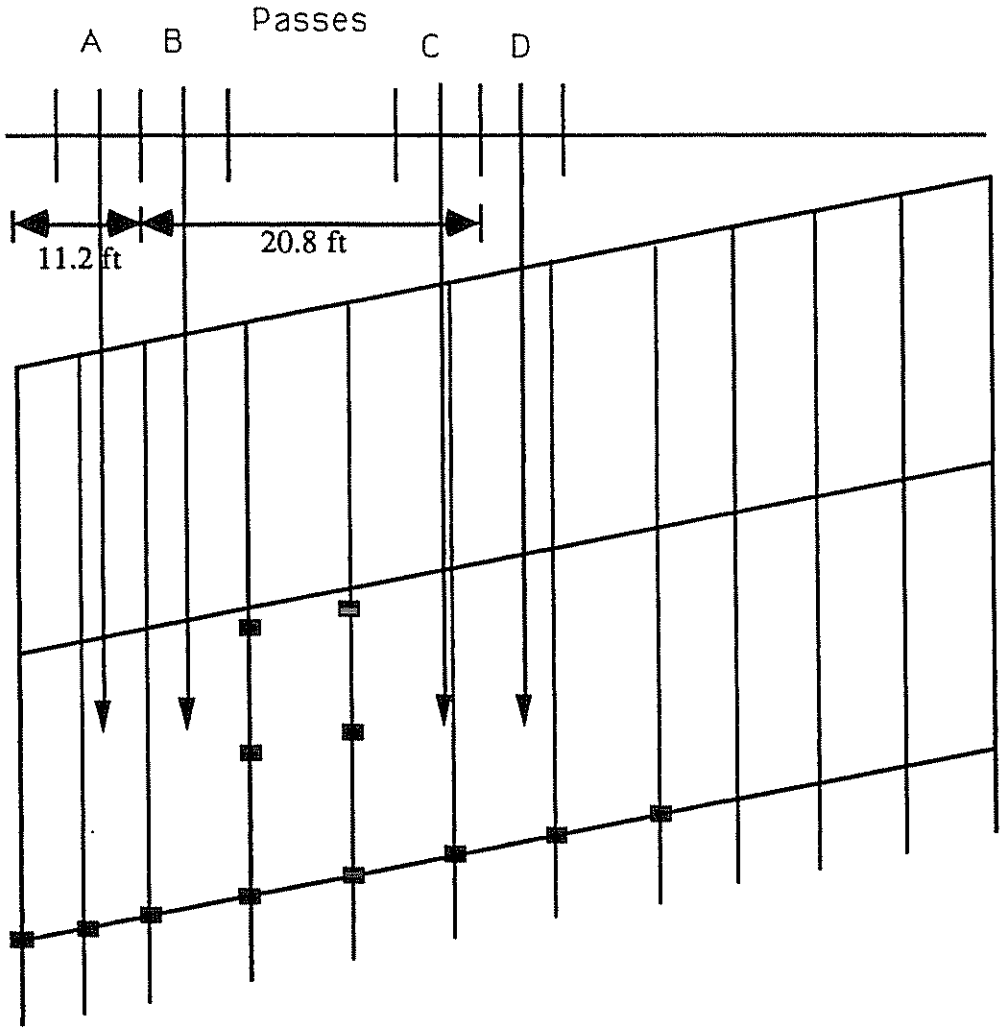

Figure 3.4. Truck Load Paths.

Starting at a datum that was roughly 10 feet before the beginning of the center span, chalk lines were marked every 10 feet along the two painted lane lines. These marks were used to identify the longitudinal location of the truck in the strain-data, time-history record. Since the truck moved at a relatively constant speed of 5 mph, these location indicators allow the data to be converted from strain vs. time to strain vs. distance. As the truck passed along the span, a remote hand sensor was pressed at each 10 foot marking. A total of nine passes were made, seven of which were semi-static tests with the truck speed at 5 mph and 2 at 55 mph for dynamic tests. Table 3.1 details the pass number, location, and speed. The reason for identical passes under the semi-static condition was to ensure accurate readings were being measured. During the run of these tests, I-95 traffic was controlled by DelDOT through the use of a rolling road block. The entire test took approximately 2 hours.

Table 3.1. Truck Pass, Location, and Speed.

Pass	Location	Speed
1	A	Semi-static
2	A	Semi-static
3	B	Semi-static
4	C	Semi-static
5	D	Semi-static
6	C	Dynamic
7	A	Semi-static
8	C	Semi-static
9	D	Dynamic

3.4 Analysis of Data

There are several areas that were considered to be most important during the data analysis phase of this project. These areas included impact factors, distribution factors, axial forces, end restraints, and section properties; such as neutral axis location, moment of inertia, deck thickness, and effective width of the concrete slab. Through finding these, the presence of composite action was also determined. Since the load rating techniques that are being considered require this type of information, these parameters were deemed critical for this project. All strain-time histories are located in Appendix A.1.

3.4.1 Section Properties

Figure 3.5 illustrates the typical cross-section and its dimensions. When analyzing the strain data from the tests, a neutral axis value was found for each girder in the system. Figure 3.6 illustrates a typical graph of neutral axis location vs. time found from the strain data of gages 25 and 26. Similar graphs for each pass and the various gage pairs are located in Appendix A.2.

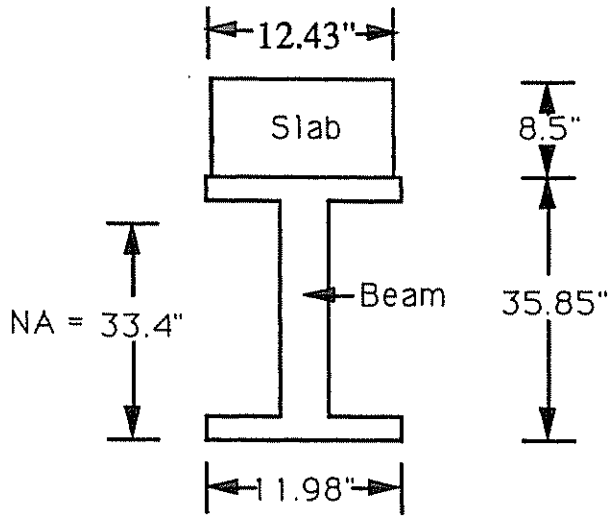

Figure 3.5. Typical Transformed Cross-Section - 8.33' Spaced Girders.

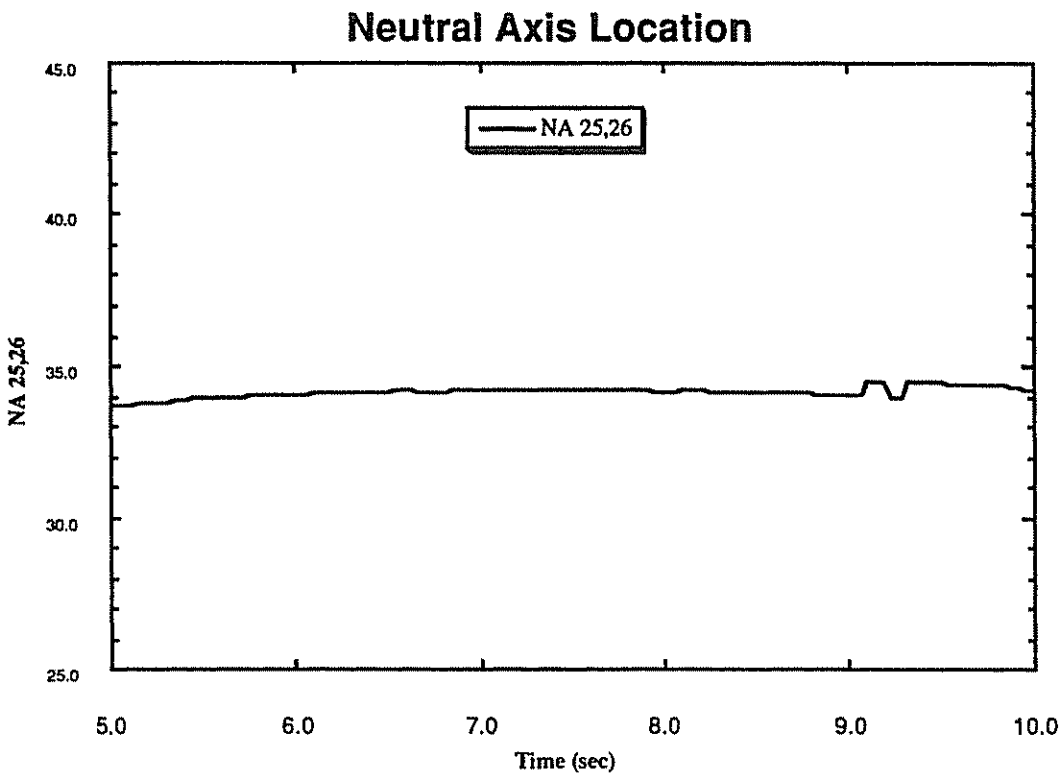

Figure 3.6. Neutral Axis Location - Christina Creek

Once graphs were made for each gage due to each pass, the neutral axis values were plotted. On this new plot, the truck path was drawn and the value at the point where the truck crossed the neutral axis line seemed to be an average value and was taken as the neutral axis location, as detailed in Figure 3.7.

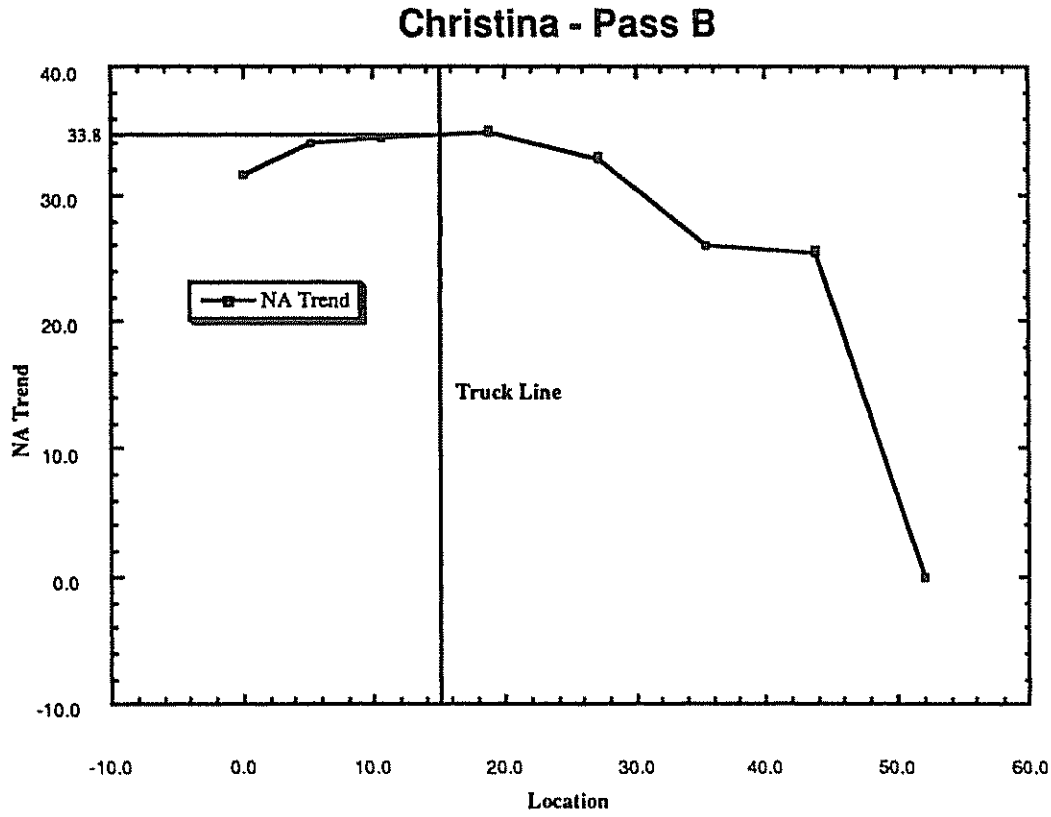

Figure 3.7. Neutral Axis Distribution.

Since there was no overlay and the concrete deck was the wearing surface, the deck thickness was taken from the plans to be 8.5". With the values of the neutral axis and deck thickness known and the effective concrete width assumed to be the tributary area of the girder, the concrete strength was taken as the unknown value. By plugging in different concrete strengths into Equation 2.5, the computed deck thicknesses were compared to 8.5". Through trial and error, the concrete strength that yielded the prescribed deck thickness was 4 ksi. (This value yielded a deck thickness of 8.52" for the girders at 8.33' spacing.) As stated earlier, the plan deck thickness was 8.5", which indicates that the current concrete strength appears to be similar to the initially specified concrete strength. However, as indicated in Chapter 2, a small

change in deck thickness can cause a significant change in the resulting concrete strength. Therefore, if some decrease in deck thickness due to wear has occurred, the concrete strength needed to maintain the neutral axis location found would increase. Table 3.2 lists the effects of choosing different known and unknown values.

Table 3.2. Effects of Different Assumptions

Known		Unknown	I
f'c	Effective Width	Deck Thickness	24272 in^4
8000 psi	8.33'	6.94"	
f'c	Deck Thickness	Effective Width	22441 in^4
8000 psi	8.5"	5.9'	
Eff. Width	Deck Thickness	f'c	22433 in^4
8.33'	8.5"	4000 psi	

Notice in Table 3.2 that if the concrete strength had been twice the initial value, either the deck thickness or effective widths would have to be smaller than assumed. The neutral axes, moments of inertia, and section moduli were calculated for each girder based on an assumed deck thickness of 8.5" and an assumed effective width of 8.33'. The computed values are listed in Table 3.3. Since the neutral axis was found to be near the top flange, it is obvious that the deck and girder are acting compositely, as designed.

Table 3.3. Neutral Axes, Moments of Inertia, and Section Moduli.

Girder #'s	NA (in) Actual	Moment of Inertia (in^4)	Section Modulus (in^3) Deck	Beam
1	34.8	22, 695	2454	652
2	34.8	22, 214	2402	638
3	34.8	23, 061	2493	663
4	33.8	24, 227	2364	717
5	33.8	24, 227	2364	717
6	33.8	24,227	2364	717
7	33.8	24,227	2364	717
8	34.8	23,404	2530	673

3.4.2 Impact Factors

Figure 3.8 details the approach used to find the impact factors using the strain-time histories produced by semi-static and dynamic passes at a single gage location. In this case, the strains are from gage 1 and the truck passes are along Path C. Notice that the length of time for the semi-static pass (5 mph) is roughly 10 times the length of time for the dynamic pass (55 mph). By comparing the strain responses, it is evident that the faster vehicle had a different effect on the system than the semi-static one. By selecting the peak strains from the two time-histories, the following equation can be used to determine an impact factor:

$$I+1 = \frac{\varepsilon_d}{\varepsilon_s} \qquad (3.1)$$

Where:

I = impact factor

ε_d = maximum strain for dynamic pass

ε_s = maximum strain for semi-static pass

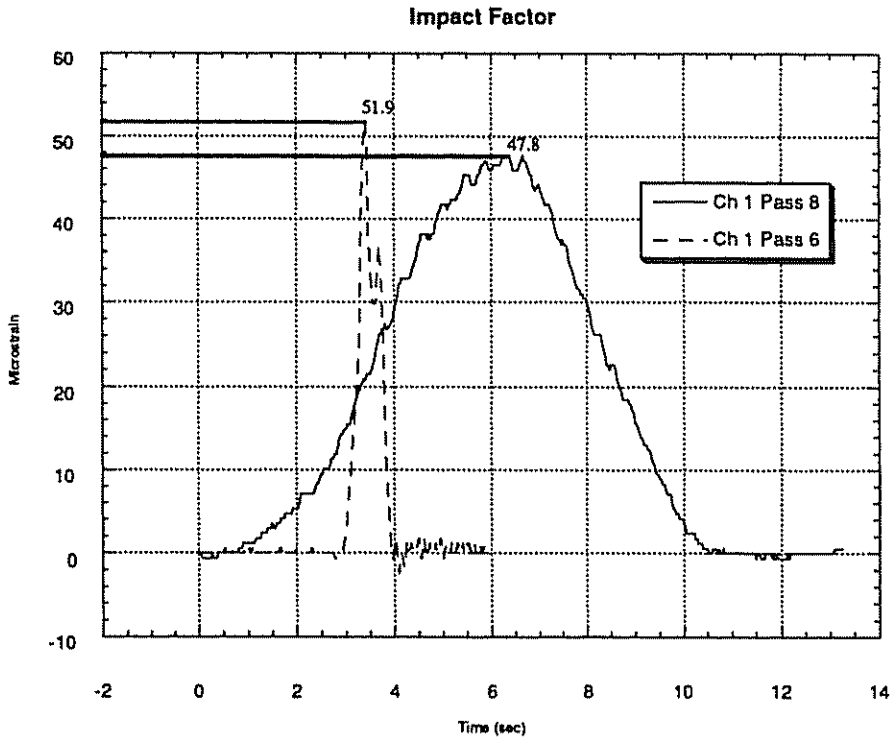

Figure 3.8. Impact Factor Strain Graph.

Similar graphs for other passes and gages are located in Appendix A.3. This same procedure was used for all bottom flange (tension) gages and applicable passes. Because it was believed that the magnitude of peak strain recorded at a gage

may affect the amount of dynamic amplification, a plot of impact factors vs. magnitude of peak strain was made (see Figure 3.9). The graph indicates that as the peak strain magnitude increases, the impact factors become more consistent. All of the impact factors for this bridge are listed in Table 3.4. This table lists values for all of the gages due to the pass locations where static and dynamic loads were applied. The final impact factor for this bridge was determined to be 1.3, as compared to an AASHTO value of 1.27. This seems to be a conservative upper bound on all of the points computed for strains greater than 40 microstrain. The fact that a location that experiences a low level of strain may have a higher impact factor than 1.3 is not critical in the load rating procedure.

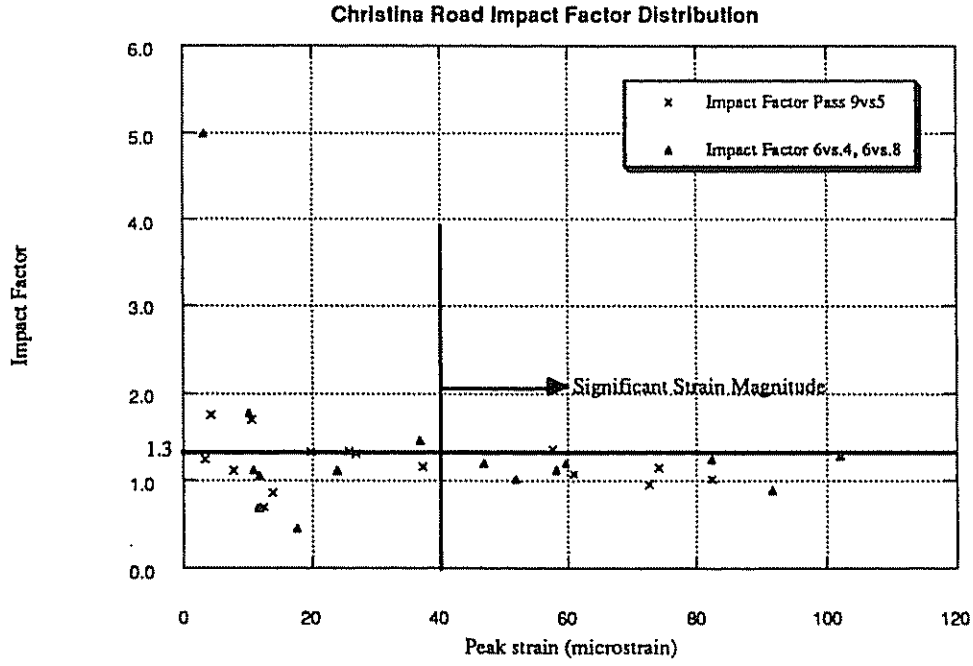

Figure 3.9. Impact Factor Value Distribution.

Table 3.4. Christina Creek Impact Factors

	Pass 6-Lane C (Dyn) Vs. Pass 4-Lane C (Static)	Pass 6-Lane C (Dyn)Vs. Pass 8-Lane C (Static)	Strain Range	Pass 9-Lane D (Dyn) Vs. Pass 5-Lane D (Static)	Strain Range
Ch. 27	5	Infinity	0 to 5	Infinity	0 to 5
Ch. 25	1.125	1.2	5 to 15	1.751	0 to 5
Ch. 3	1.118	1.188	15 to 25	1.7	5 to 15
Ch. 1	1.024	1.088	45 to 55	1.344	15 to 30
Ch. 19	0.898	0.898	90 to 105	1.076	55 to 65
Ch. 17	1.198	1.141	45 to 60	0.959	70 to 80
Ch. 23	1.462	1.39	25 to 40	1.15	60 to 75
Ch. 21	1.778	1.454	5 to 15	1.313	20 to 30
Average	1.23	1.19	****	1.33	****
Highest	1.778	1.454	****	1.751	****
Ch.11	0.692	0.783	10 to 20	1.25	0 to 5
Ch. 31	0.458	0.458	15 to 40	0.704	10 to 20
Average	0.575	0.621	****	0.977	****
Highest	0.692	0.783	****	1.25	****
Ch. 9	1.206	1.169	35 to 50	1.333	10 to 20
Ch. 29	1.289	1.279	75 to 105	1.354	40 to 60
Average	1.248	1.224	****	1.344	****
Highest	1.289	1.279	****	1.354	****
Ch. 7	1.253	1.24	65 to 85	1.167	30 to 40
Ch. 5	1.127	1.328	40 to 60	1.024	80 to 85
Average	1.19	1.284	****	1.096	****
Highest	1.253	1.328	****	1.167	****
Ch. 13	0.692	0.692	10 to 20	1.12	5 to 10
Ch. 15	1.063	1	10 to 15	0.87	10 to 20
Average	0.878	0.846	****	0.995	****
Highest	1.063	1	****	1.12	****
Pass AVG	1.024	1.033		1.148	
Pass High	1.778	1.454		1.751	

3.4.3 Distribution Factors

The first step in determining the distribution factors for this bridge was to add all of the tensile strains at midspan due to the truck being located at midspan, for each pass. Figure 3.10 graphs the strains felt at each gage at midspan vs. the transverse location with the sum of the strains for a given pass listed above each line. It should be noted that the girders on the southern edge of the bridge were not gaged. The graph indicates that gages at these girders would have had readings near zero since none of the load paths were close to the southern-most edge. In general, all beams should be gaged if equipment is available. The total values of strain across the midspan ranged from 245 με to 310 με. Once all of these strains were added, they were averaged to get a normalized total strain value of 290 με. This value was assumed to be the maximum amount of strain caused by a truck in a single girder. To get the value for one wheel line, the total was divided by two to get 145 με. Figure 3.10 also shows that the amount of strain experienced by a girder depends on the location of the truck passes. Since none of the passes are on the southern-most side, the strain values on the right portion of the graph are all approaching zero.

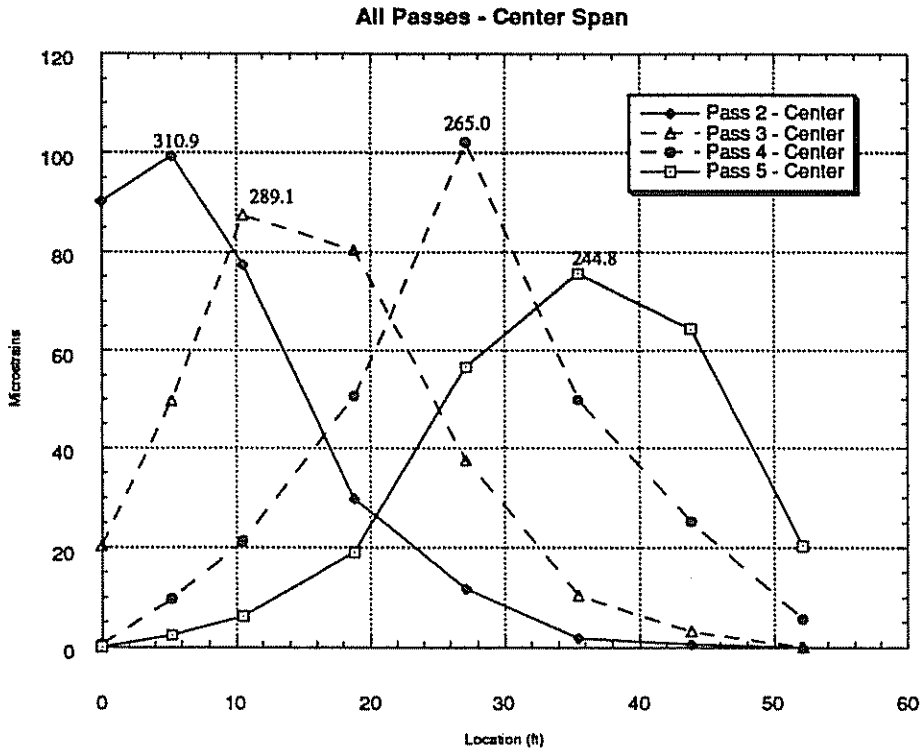

Figure 3.10. Total Strain Due to All Passes.

Influence lines for bottom flange gages across the midspan were drawn for each gage due to all of the passes for the situation when the truck was located at midspan. Because of the limited number of truck paths (four), each influence line consists of only four actual data points. Since the location of truck paths does not necessarily lead to a loading that would cause a maximum strain, an assumed value was selected. A value of 120 με was chosen as the maximum strain after looking at strain values recorded where the truck did pass close to directly over a girder. A more complete influence line was generated by assigning this value of strain on the influence line at a location corresponding to a hypothetical truck pass, directly over

the gage that the influence line was being plotted for. Next, according to the AASHTO Guide on Bridge Design,[4] lanes were measured every 12 feet from the edge of the bridge to the center, resulting in a total of 3 lanes for the width measured. Within these 12 ft lanes, 6 ft vehicle widths were placed, keeping a 2 ft clearance from each of the 12 ft lane ends, so the vehicle would produce the most strain on the girder for which the influence line was drawn (values based on center line of truck were used). Figure 3.11 details an influence line graph and the lane spacing. All of the resulting influence lines exhibited consistent behavior suggesting that a reasonable value for maximum strain was used.

For each vehicle center line, the corresponding value on the influence line graph was taken. These strain values for the three lane locations dictated by AASHTO[4] were added together and divided by the maximum strains due to one wheel line, as shown previously and found to be 145 με. The following exercise exhibits this step for the outer girder on which gage 27 was placed:

$$\text{E.D.F.} = \frac{I_\varepsilon}{W_\varepsilon} \qquad (3.2)$$

$$\text{E.D.F.} = \frac{120\mu\varepsilon + 17.5\mu\varepsilon + 0.5\mu\varepsilon}{145\mu\varepsilon}$$

$$\text{E.D.F.} = 0.952$$

Where:

E.D.F. = Experimental Distribution Factor

I_ε = influence line total strain

W_ε = wheel-line strain

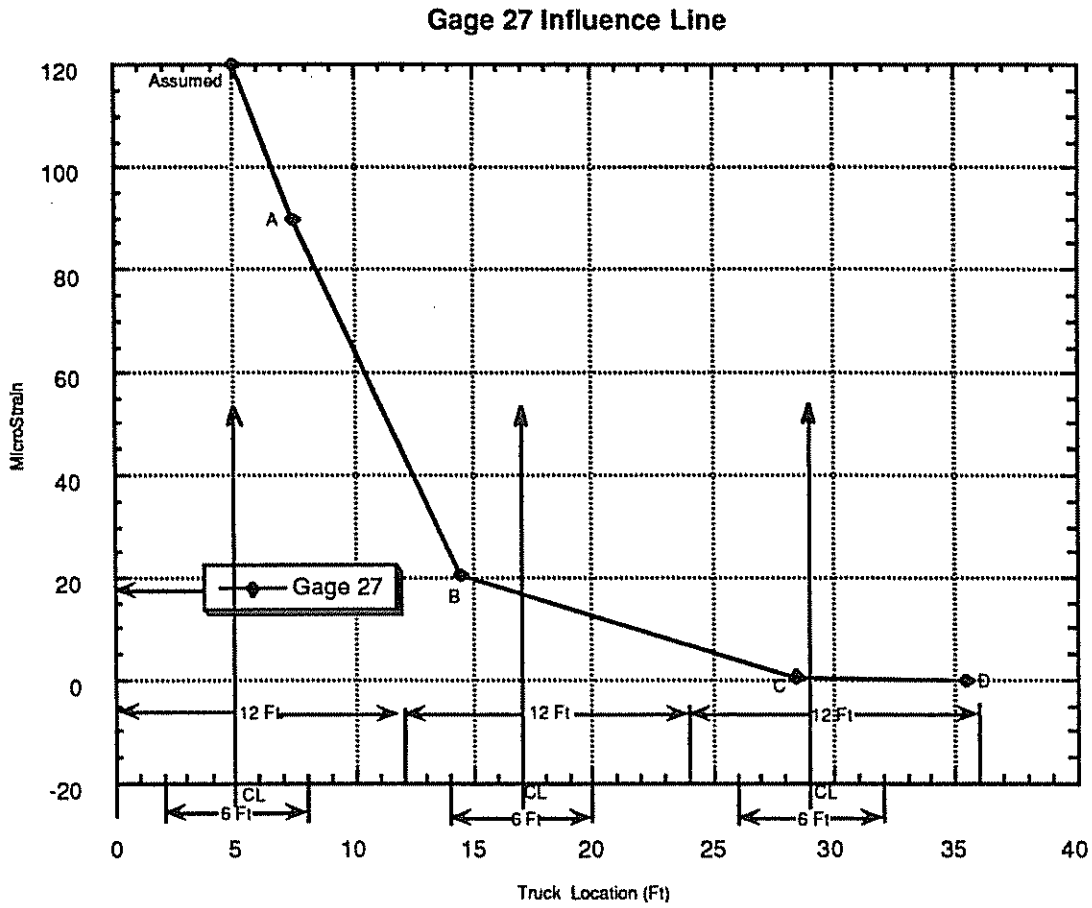

Figure 3.11. Influence Line for Gage 27.

This experimental distribution factor was then compared to the value computed based on the AASHTO design code[4]. Typically, a multiple-presence factor would then be multiplied by the EDF, based on the number of load lanes available. To be conservative, multiple-presence factors will be neglected for this rating. The following exercise details the AASHTO[4] method of determining distribution factors, using the outer girder as an example:

$$A.D.F. = \frac{S}{5.5} \qquad (2.13)$$

$$A.D.F. = \frac{5.25'}{5.5'}$$

$$A.D.F. = 0.955$$

Where:

A.D.F. = AASHTO Distribution Factor

S = girder spacing

Table 3.5 lists the distribution factors for all of the girders calculated and all of the ADF's for those same girders. These girders have different values since there is variable spacing between them. Also note that the edge girder (gage 27) has a significantly lower distribution factor, as would be expected. All but one of the EDF's were slightly less than the ADF's, indicating a better load distribution than would be expected, based on AASHTO. This improved distribution will lead to a higher load rating. In order to evaluate this bridge correctly, each girder with different spacing will have to be taken into consideration as having a different distribution factor. Only girders with gages 1 and 19 can be averaged, yielding a value of 1.285. This value is approximately 6.2 % less than the AASHTO distribution factor value of 1.37. All distribution factor distributions and influence line graphs are located in Appendix A.4.

Table 3.5. Distribution Factors.

Gage	Lane 1	Lane 2	Lane 3	Total	EDF	ADF	% Diff
27	120	17.5	0.5	138	0.952	0.955	0.31
25	120	47.5	9.5	177	1.221	0.955	-28
3	75	75	20	170	1.172	1.235	5.1
1	27.5	120	47.5	195	1.345	1.370	1.9
19	10	67.5	100	177.5	1.224	1.370	10.7

3.4.4 End Restraints

The presence of end restraint at the supports was determined from graphs similar to that shown in Figure 3.12. This graph indicates the variation of tensile strain along the length of a girder's bottom flange, caused by a truck located at midspan.

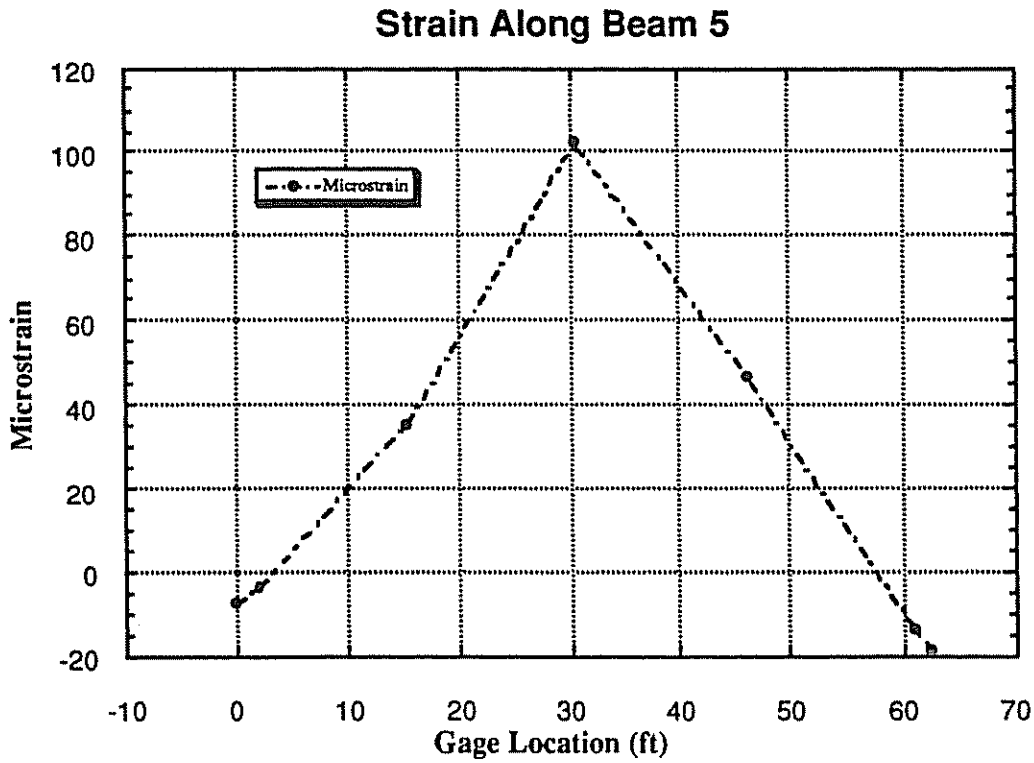

Figure 3.12. Strain Along Beam

The percent fixity (% fixity) can be determined from Figure 3.9 as follows:

$$\% \text{ Fixity} = |- \varepsilon_{end}/(\varepsilon_{pk} - \varepsilon_{end})| * 100 \qquad (3.3)$$

$$= |- (-7.5)/(102.13 - (-7.5)| * 100$$

$$= 6.8\ \%$$

Where:

ε_{end} = strain at end of beam

ε_{pk} = strain at maximum peak

The largest strain reading at the midspan is the critical one since it creates the highest moment on this system. Beams 4, 5, and 6 were evaluated for end restraint and are listed in Table 3.6. As detailed in Chapter 2, the magnitude of the strain is very important in determining the accuracy of the system's capacity.

Table 3.6. Fixity of Each Beam.

Beam # - Pier Location	Fixity
4 - Approach Pier	0 %
5 - Approach Pier	6.8 %
5 - Far Pier	15.7 %
6 - Far Pier	27.2 %

3.4.5 Axial Forces

The methods discussed in Section 2.3.5 were used to determine whether or not axial forces were being generated in the girders during the load test. In general, it was found that the location of the neutral axis along the length of a girder, due to a single truck location, did not vary. As an example, one can look at the strain distribution due to a truck at midspan, along the top and bottom flanges of beam 5 (See Figure 3.13).

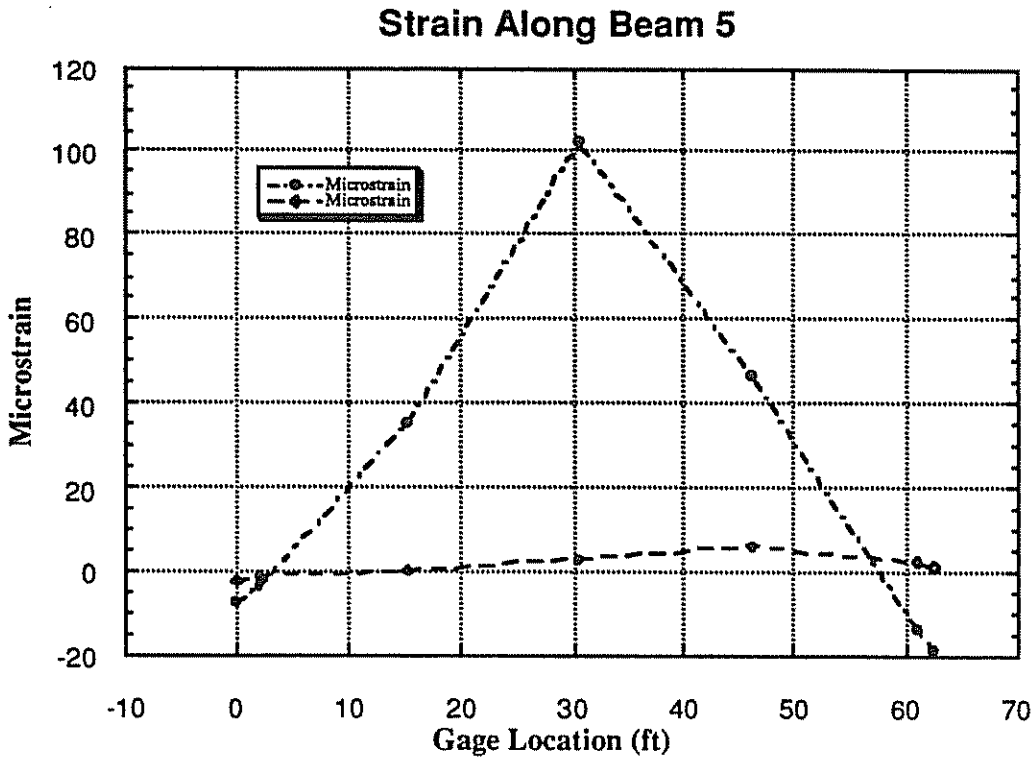

Figure 3.13. Strain Along Beam for Axial Force Determination

It can readily be seen that the gage on the top flange is located very close to the neutral axis (strain is approximately zero) at each of the five gaged locations. Based on the minimal change in neutral axis location, it will be assumed that the effects of axial forces can be neglected when evaluating this particular bridge.

3.5 Results of Analysis

A summary of values that have been determined for this bridge are listed in Table 3.7. The computed parameters are consistent with those that would be found without a field test. The slight differences in moment of inertia and distribution factors would indicate that the bridge is capable of carrying somewhat higher loads than would have been expected. More detailed tables of moment of inertia, neutral

axis location, section modulus, distribution factors, impact factors, and end restraints are tabulated in Sections 3.4.1, 3.4.2, 3.4.3, and 3.4.4, respectfully.

Table 3.7. Results of Christina Creek Bridge Test.

Bridge Properties	Field	Theoretical, AASHTO, or Plan Value
Neutral Axis Location	33.8" to 34.8"	33.4"
Concrete Strength	4 ksi	4 ksi
Effective Width	5.25' to 8.33'	5.25' to 8.33'
Deck Thickness	8.52 in	8.5 in
Moment of Inertia	22,214 in^4 to 24,227 in^4	20,620 in^4 to 22, 455 in^4
Section Modulus To Top of Deck	2364 in^3 to 2530 in^3	1936 in^3 to 2109 in^3
To Top of Beam	638 in^3 to 717 in^3	617 in^3 to 672 in^3
Impact Factor	1.30	1.27
End Restraints	0 to 27.2 %	0 %
Axial Forces	0 kips	0 kips

Chapter 4

THE DARLEY ROAD BRIDGE ON I-95

4.1 Background of the Darley Road Bridge

The Darley Road Bridge is located on I-95, near the Pennsylvania border. Only the Northbound span was evaluated, since it was determined to be under-rated for permit loads by DelDOT. The northbound bridge is a 3-span continuous, slab-and-steel-girder bridge that consists of 2 traffic lanes and one breakdown lane and carries a large amount of traffic between Philadelphia, PA and Wilmington, DE. The bridge was designed both compositely and non-compositely with the approach spans being non-composite and the center span being composite. Figure 4.1 shows the bridge in plan view. The current bridge has had only minor repairs and no major additions. The span lengths of the approach spans are identical at 35' and the span length of the center is 58'. The overall width of the bridge is 35' 10" between outer girders.

As its title indicates, this bridge passes over Darley Road, which is a two-lane rural road, located in North Wilmington.

4.2 Preparation of the Darley Road Bridge

A site survey was conducted in July of 1995 to determine what obstacles and site specifics would be encountered during the test setup and test itself. The real obstacle to gaging this bridge was how to get to the underside, which was approximately 20 ft above the road.

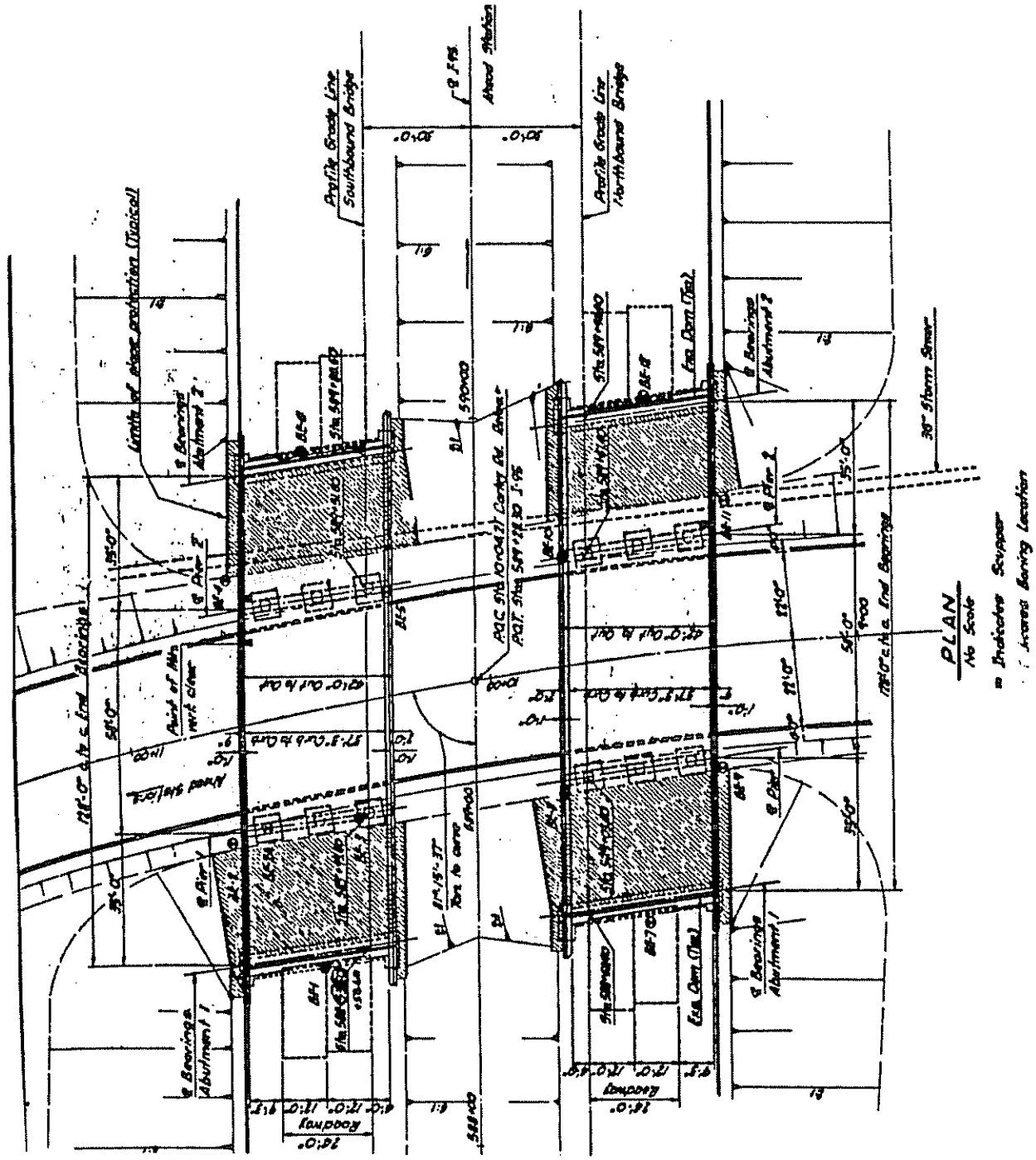

Figure 4.1. Darley Road Bridge Plan View

Another problem was that the abutments that supported the approach span were at a 30 degree angle from the ground, starting at the sidewalk and ending at the bearings. Figure 4.2 shows this obstacle. In order to deal with these problems, a caged scissor-lift was used for the instrumentation of the center span and a 20 ft ladder was used for the approach span. The bottom of the ladder was placed closer to the bearings, while the top of the ladder rested on the diaphragms that spanned laterally from girder to girder. Figure 4.2 shows the ladder configuration used for gaging the approach span. For the center span, the scissor-lift hoisted the workers up safely and was very efficient.

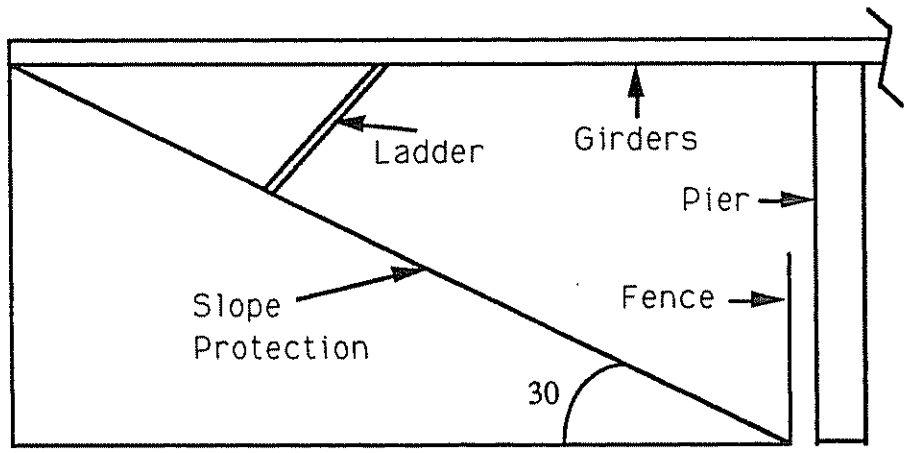

Figure 4.2. Abutment Obstacle and Ladder Configuration.

Instrumentation of this bridge was accomplished in November of 1995 using 32 strain gages to measure the top and bottom flanges of the girders. The bridge was gaged at 18 locations with emphasis placed on the midspan locations of the approach and center sections. The span itself was at an 8 degree skew. Figure 4.3 details the layout.

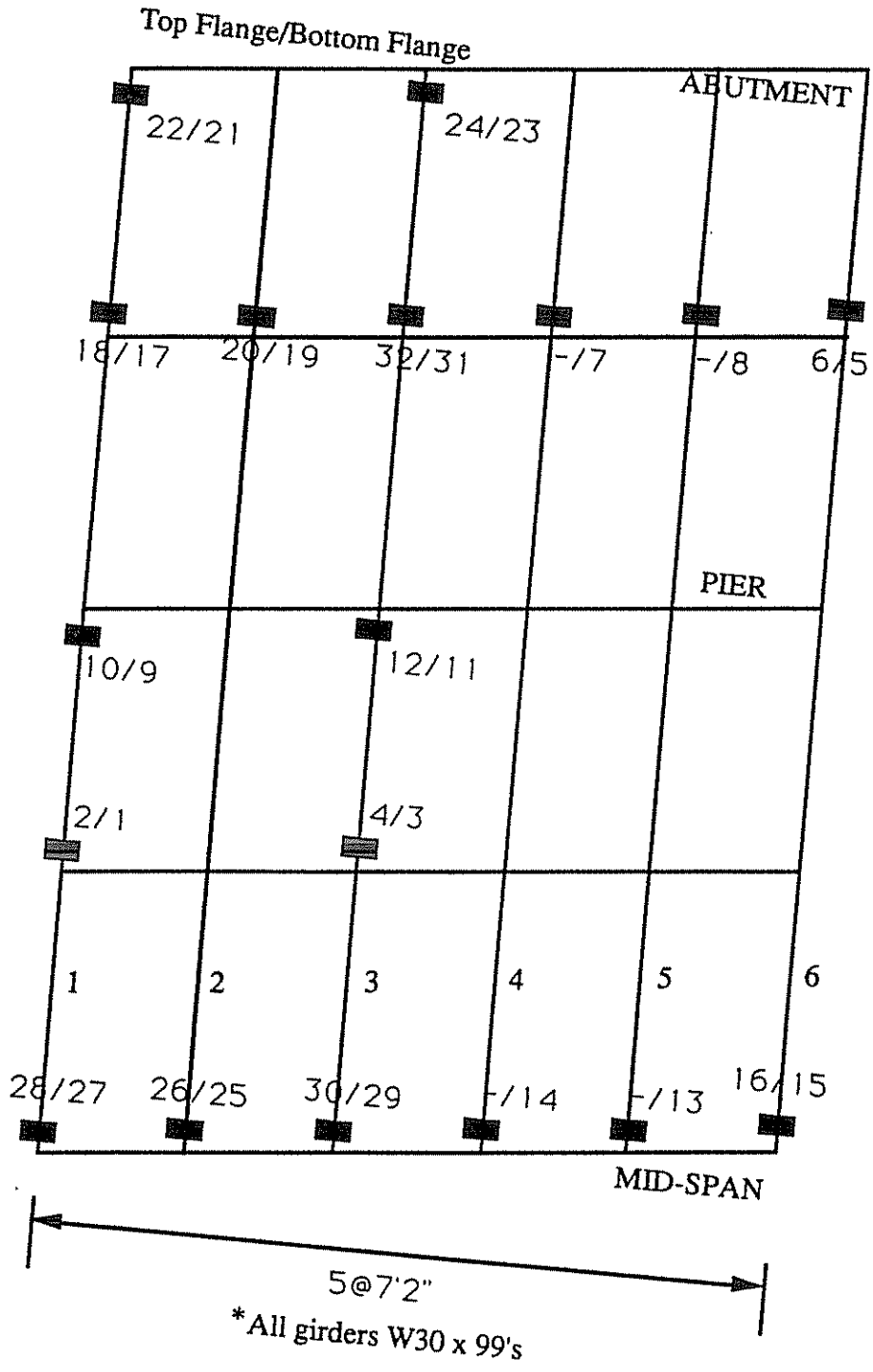

Figure 4.3. Gage Layout

Girders 4 and 5 were only gaged on the bottom flanges, while the rest were gaged at both top and bottom flanges. The top flange gages are only needed for neutral axis determination and not necessary for evaluating load distribution under positive bending. This was done due to equipment constraints.

The girders were gaged with midspan emphasis so longitudinal load distribution factors could be determined, as well as to see the behavior of the spans as the truck passed. Gages were also placed along the 1st and 3rd girders from the eastern-most side at the quarter points of the center span, as well as the end points of the center-span and the approach-span. This approach was taken to quantify longitudinal load distribution and assumed to be adequate to measure the important points on both spans. The instrumentation process took approximately 3 hours.

4.3 Load Test of the Darley Road Bridge

The load test for this bridge was conducted immediately following the gaging of the span. Typically, one would use a vehicle loaded to the legal limit if the bridge being tested had no load restrictions. In this case, a dump truck weighing 67.75 kips was used to load the bridge along various longitudinal paths, enabling substantial strain data to be collected (same truck load as used for the Christina Creek bridge). The truck load used was limited by the amount of sand that could fit in the back of the truck. Figure 4.4 details the wheel spacing and weight distribution.

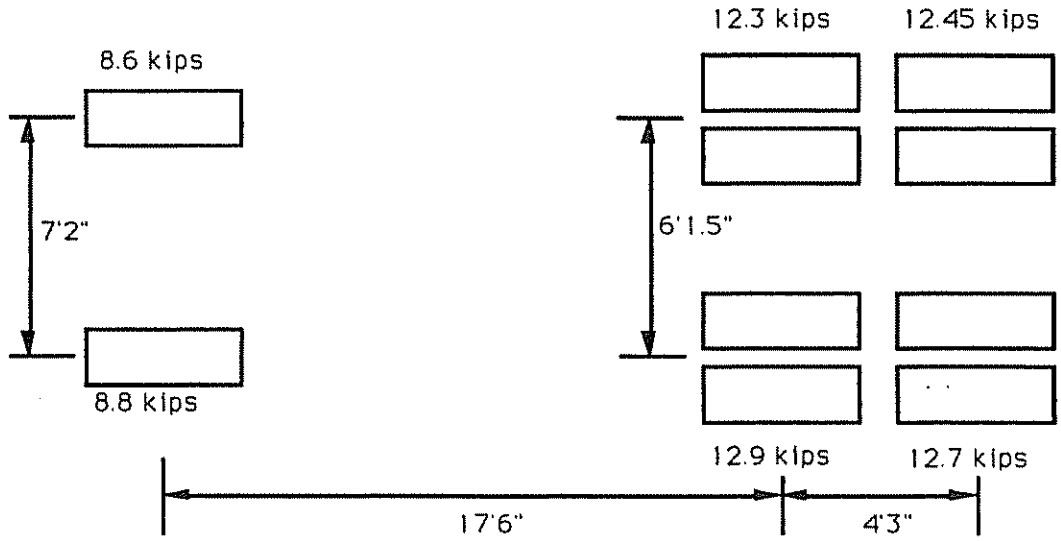

Figure 4.4. Truck Weight Distribution Detail.

Three longitudinal load paths were established using existing traffic lanes. One was located 8 feet, 5 inches from the eastern edge of the bridge, the second at 19 feet, 6 inches from the eastern edge, and the third at 31 feet, 6 inches from the eastern edge. Path A corresponded to the truck moving with the driver-side wheels on the 8' 5" painted line, Path B corresponded to the truck having its driver-side wheels on the 19.5 foot line, and Path C occurred with the truck's driver-side wheels at the 31.5 foot line. The load paths are detailed in Figure 4.5. These paths were chosen since they provided easy paths to follow and were where the actual lanes were painted on the bridge. Since the purpose of this evaluation was to determine the operating capacity, the actual lanes represented some of the critical load paths.

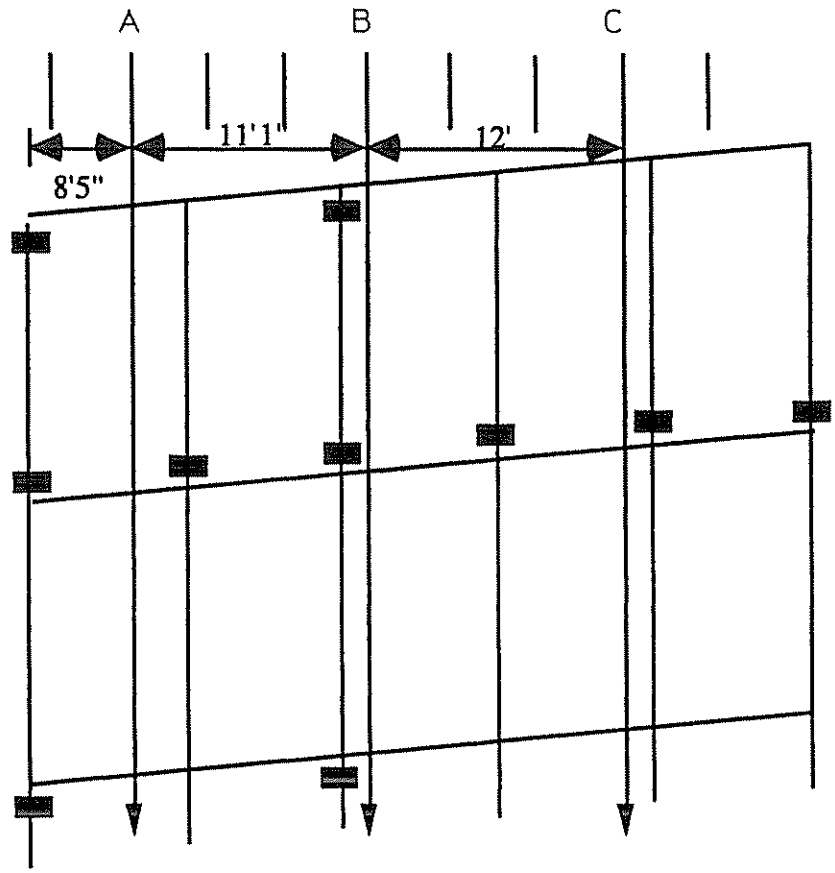

Figure 4.5. Truck Load Paths.

Starting at a datum that was roughly 10 feet before the beginning of the approach span, chalk lines were marked every 10 feet along the two painted lane lines. These marks were used to identify the longitudinal location of the truck in the strain-data, time-history record. Since the truck moved at a relatively constant speed of 5 mph, these location indicators allow the data to be converted from strain vs. time to strain vs. distance. As the truck passed along the span, a remote hand sensor was pressed at the specific markings. A total of 8 passes were made, 6 of which were semi-static tests with the truck speed at 5 mph and 2 at 55 mph for dynamic tests. Table 4.1 details the pass number, location, and speed. The reason for duplicating passes under

the semi-static condition was to ensure accurate readings were being measured. During the run of these tests, I-95 traffic was controlled by DelDOT through the use of a rolling road block. The entire test took approximately 2 hours.

Table 4.1. Truck Pass, Location, and Speed.

Pass	Location	Speed
1	A	Semi-static
2	B	Semi-static
3	C	Semi-static
4	C	Semi-static
5	B	Semi-static
6	A	Semi-static
7	B	Dynamic
8	B	Dynamic

4.4 Analysis of Data

There are several areas that were considered to be most important during the data analysis phase of this project. These areas included impact factors, distribution factors, axial forces, end restraints, and section properties; such as neutral axis location, moment of inertia, deck thickness, and effective width of the concrete slab. Through finding these, the presence of composite action was also determined. Since the techniques that are being considered require this type of information, these

parameters are critical for the load rating phase of this project. All strain-time histories are located in Appendix B.1.

4.4.1 Section Properties

Figure 4.6 illustrates the typical cross-section and its dimensions. When analyzing the strain data from the tests, a neutral axis value was found for each girder in the system. Figures 4.7 and 4.8 illustrate typical graphs of neutral axis location vs. time according to the data found for the approach and center spans. Similar graphs for each pass and the various gage pairs are located in Appendix B.2.

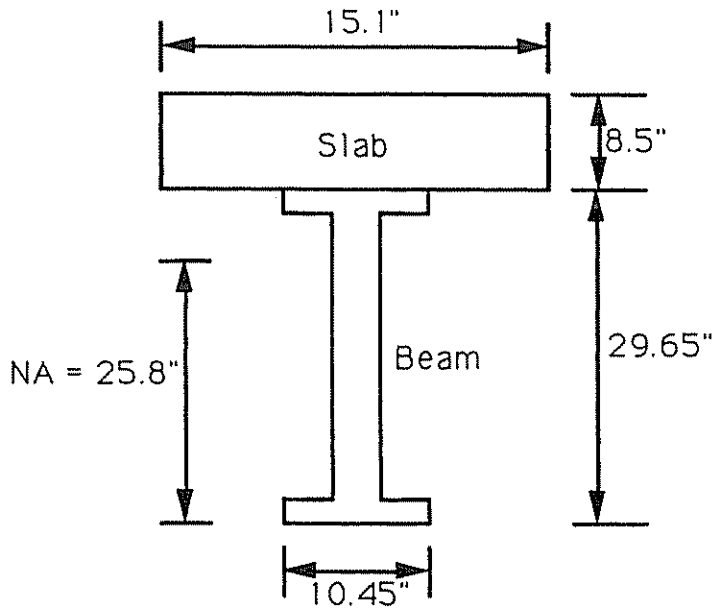

Figure 4.6. Cross - Section

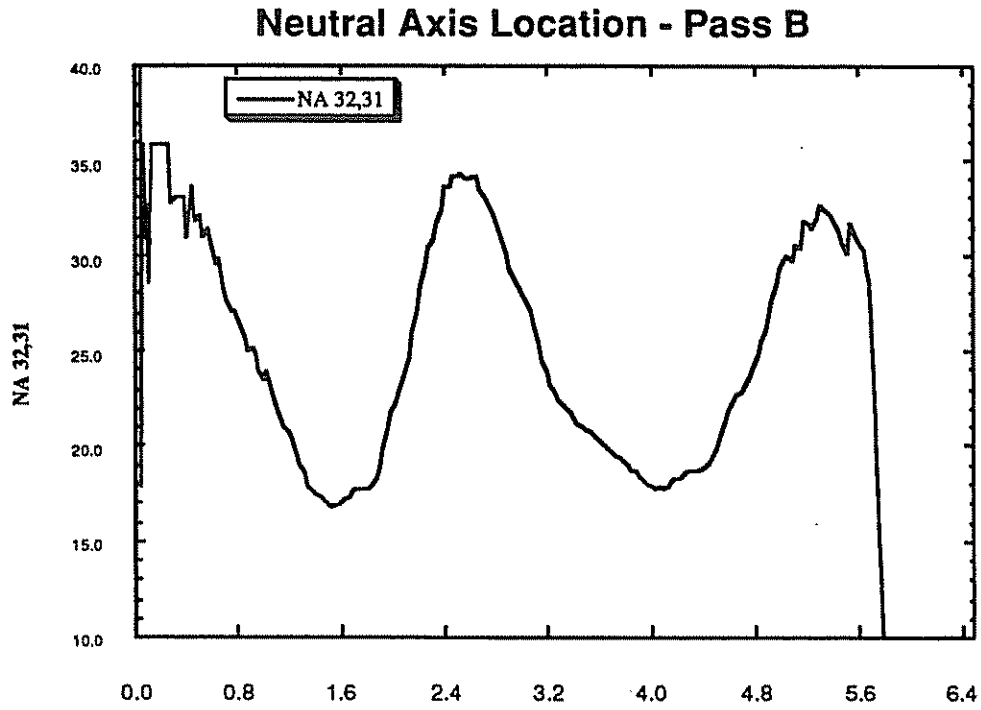

Figure 4.7. Neutral Axis Location - Approach

Most of the neutral axis graphs for the approach span did indicate the presence of composite action. Notice in Figure 4.7, however, that the approach span indicates that composite action is lost at some instances (gages 31 and 32, Pass B), while being present at others. This shows that this part of the analysis process must be very thorough in order to find any "weak" areas that would govern the overall rating of the span. The fact that most of the other gage pairs indicated composite behavior shows that even though a span may not be designed for this effect, it may exhibit characteristics of such design while in service, but may not be counted on if "weak" areas are found.

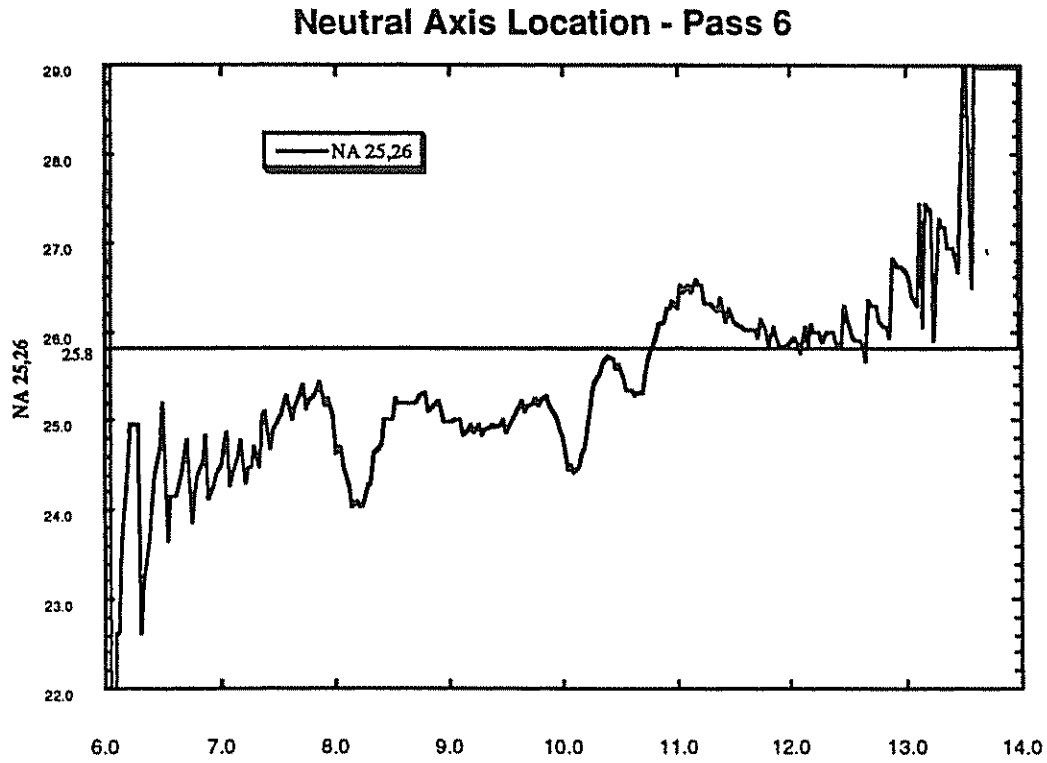

Figure 4.8. Neutral Axis Location - Center

Notice in Figure 4.8 that the center span is behaving compositely, as designed. Once graphs were made for each gage due to each pass, those gage values were plotted. On these new plots, the truck paths were drawn and the values at the points where the truck crossed the neutral axis line seemed to be average values and were taken as the neutral axis for each span, as detailed in Figures 4.9 and 4.10.

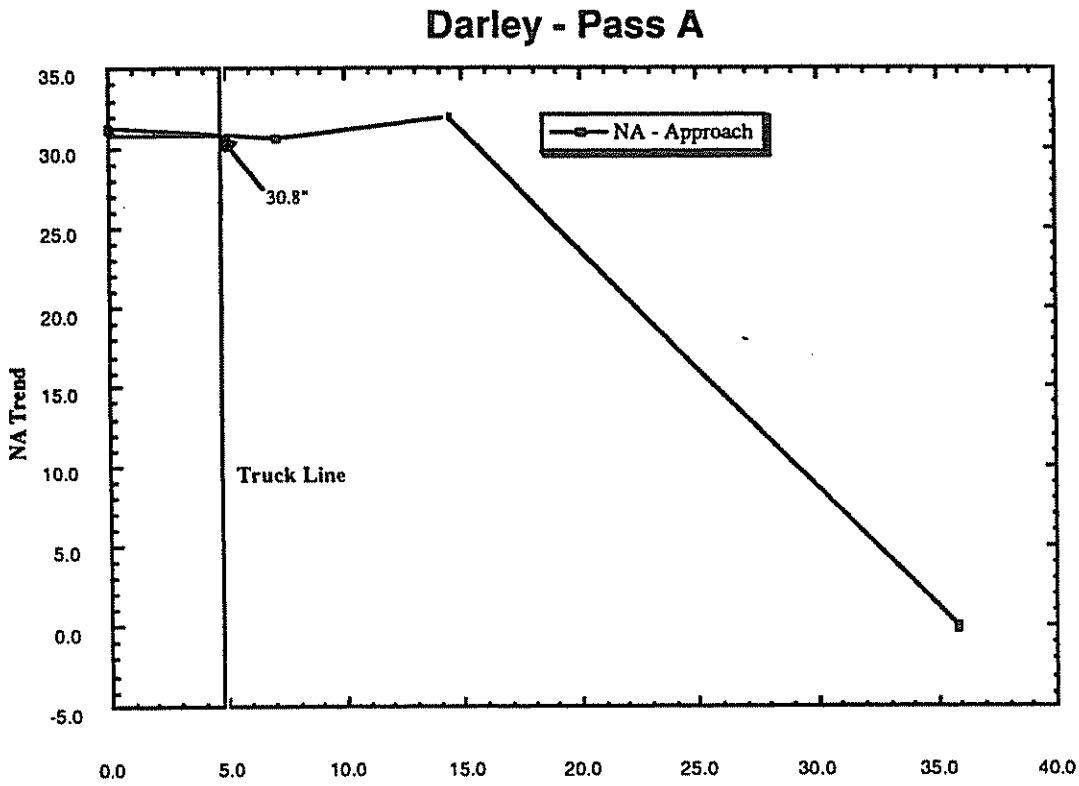

Figure 4.9. Neutral Axis Distribution - Approach

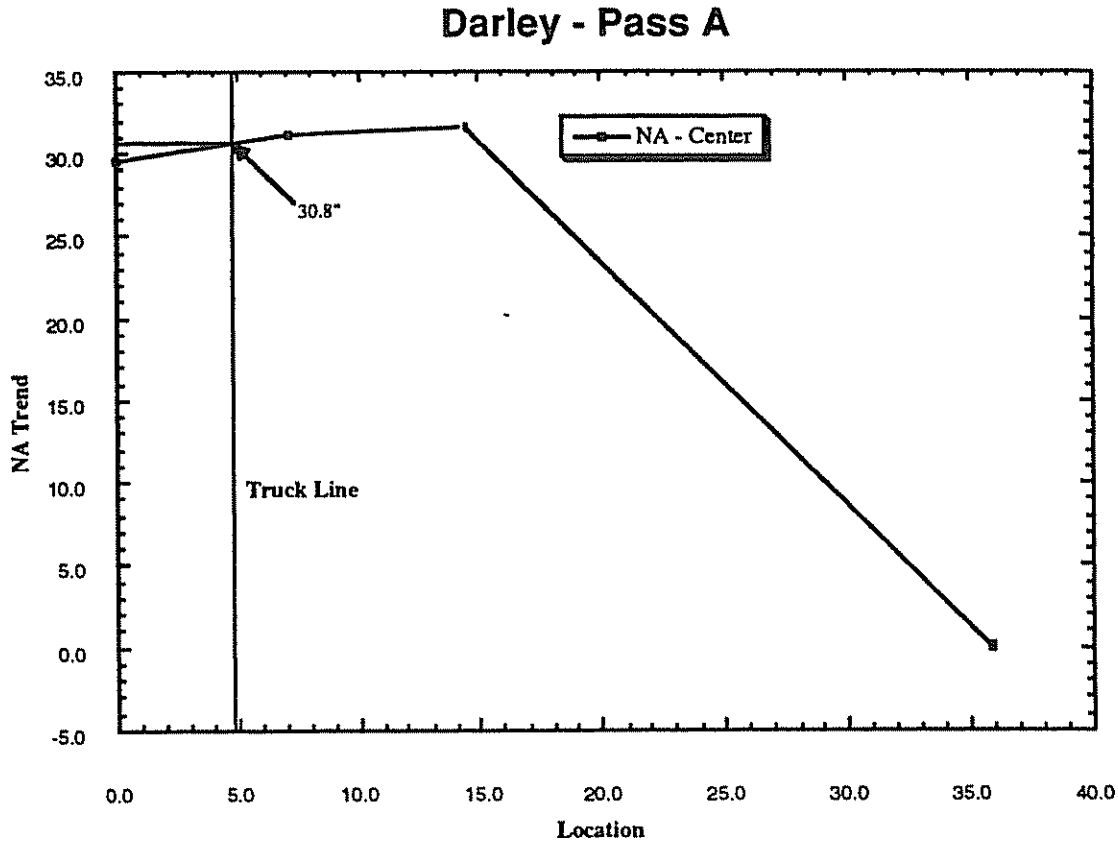

Figure 4.10. Neutral Axis Distribution - Center

Unlike the Christina Creek bridge, this bridge had an asphalt wearing surface. Since it was not evident how much overlay may have been added to the bridge, the deck thickness was taken as the unknown. With the value of the neutral axis known, the concrete strength taken as twice the initial f'c value, and the effective concrete width assumed to be the tributary area, the deck thickness was solved for using Equation 2.5. This value yielded a deck thickness of 9.08" for the girders at 7.167' spacing. As stated earlier, the plan deck thickness was 8.5", which indicates that the current deck (concrete and asphalt) is acting as if it were a solid concrete deck with a thickness 0.58" more than the original specifications. This would be consistent

with the presence of additional asphalt overlay that is not accounted for in the plans. As indicated in Chapter 2, a small change in any one variable can cause a significant change in the resulting dependent variables. Table 4.2 lists the effects of choosing different known and unknown values.

Table 4.2. Effects of Different Assumptions

Known		Unknown	I
f'c	Effective Width	Deck Thickness	13425 in^4
8000 psi	7.167'	9.08"	
f'c	Deck Thickness	Effective Width	13771 in^4
8000 psi	8.5"	8.4'	
Eff. Width	Deck Thickness	f'c	13718 in^4
7.167'	8.5"	10.5 ksi	

Notice in Table 4.2 that if the deck thickness had been equal to the initial value, either the concrete strength or effective width would be much higher than assumed. It is also worth noting that if a 4000 psi concrete strength is used with an effective width of 7.167', an unreasonably thick concrete deck results. The neutral axes, moments of inertia, and section moduli were calculated for each girder and are listed in Table 4.3. Since the neutral axis was found to be near the top flange in the center spans, composite action is taking place there. However, since some gage pairs indicated the loss of composite action for the approach span, that span will be recognized as behaving non-compositely.

Table 4.3. Neutral Axes, Moments of Inertia, and Section Moduli.

Girder #	Neutral Axis	Moment of Inertia (in^4)	Section Modulus (in^3)	
			Deck	Beam
Approach - 1,6	14.825	4933	206	333
Approach - 2,3,4,5	14.825	4933	206	333
Center - 1,6	30.8	13374	1687	434.2
Center - 2,3,4,5	30.8	13421	1692	435.8

4.4.2 Impact Factors

Figure 4.11 details the approach used to find the impact factors using the strain-time histories produced by semi-static and dynamic passes at a single gage location. In this case, the strains are from gage 23 and the truck passes are along Path B. Notice that the length of time for the semi-static pass (5 mph) is roughly 10 times the length of time for the dynamic pass (55 mph). By comparing the strain responses, it is evident that the faster vehicle had a different affect on the system than the semi-static one. By selecting the peak strains from the two time-histories, the following equation can be used to determine an impact factor:

$$I+1 = \frac{\varepsilon_d}{\varepsilon_s} \qquad (3.1)$$

Where:

I = impact factor

ε_d = maximum strain for dynamic pass

ε_s = maximum strain for semi-static pass

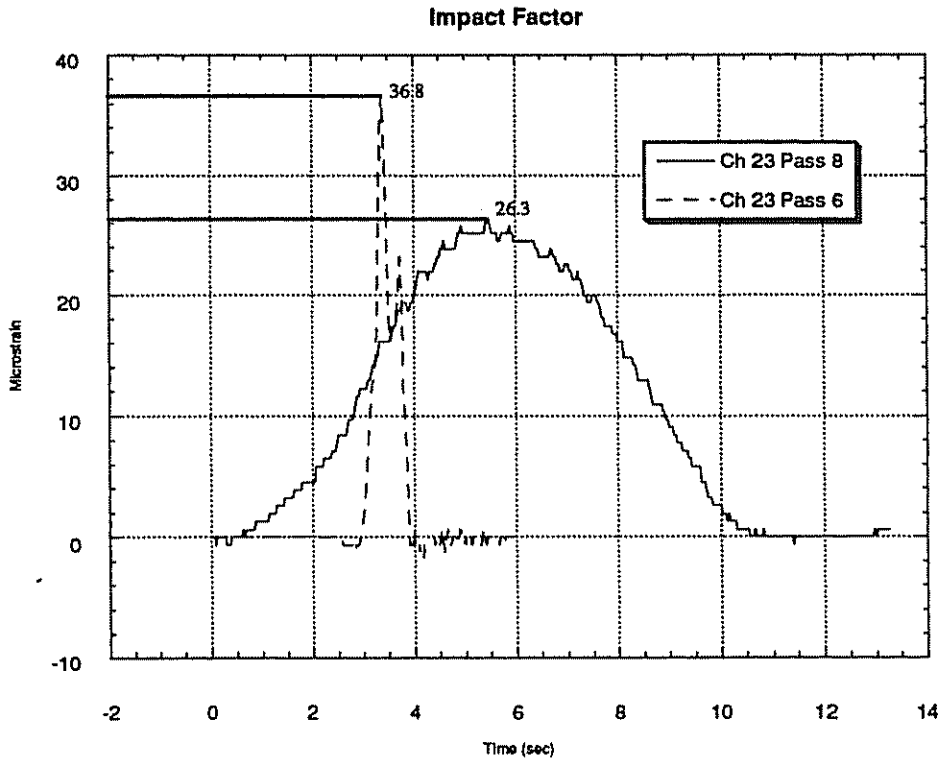

Figure 4.11. Impact Factor Strain Graph.

Similar graphs for other passes and gages are located in Appendix B.3. This same procedure was used for all bottom flange (tension) gages and applicable passes. Because it was believed that the magnitude of peak strain recorded at a gage may affect the amount of dynamic amplification, a plot of impact factors vs.

magnitude of peak strain was made (see Figure 4.12). The graph indicates that as the peak strain magnitude increases, the impact factors become more consistent. All of the impact factors for this bridge are listed in Table 4.4. This table lists values for all of the gages due to the pass locations where static and dynamic loads were applied. The final impact factor for this bridge was determined to be 1.26 for both the center and approach spans, as compared to AASHTO[3] values of 1.27 and 1.31 for the center and approach. For strains greater than 50 microstrain, 1.26 seemed like a conservative upper bound. The fact that a location that experiences low-level strains may have a higher impact factor than 1.3 is not critical in the load rating procedure.

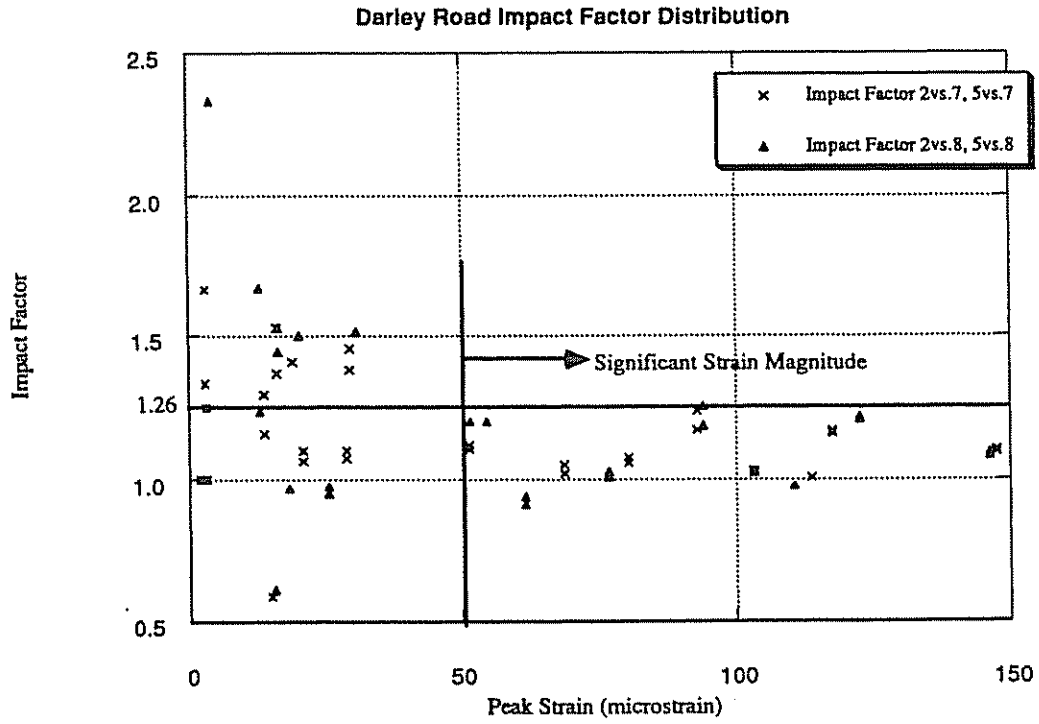

Figure 4.12. Impact Factor Value Distribution.

Table 4.4. Darley Road Impact Factors.

	Pass 2 (b-stat) vs. Pass 8(b-dyn)	Pass 2 (b-stat) vs. Pass 7(b-dyn)	Strain Range	Pass 5 (b-stat) vs. Pass 8(b-dyn)	Pass 5 (b-stat) vs. Pass 7(bdyn)	Strain Range
Ch. 23	1.5	1.409	10 to 25	1.5	1.409	10 to 25
Ch. 21	1	1	0 to 5	1	1	0 to 5
Average	0.75	0.705	***	0.75	0.705	***
Highest	1.5	1.409	***	1.5	1.409	***
Ch. 5	2.333	1.666	0 to 5	2.333	1.333	0 to 5
Ch. 8	1.515	1.455	20 to 35	1.515	1.382	20 to 35
Ch. 7	1.254	1.238	75 to 95	1.186	1.171	75 to 95
Ch. 31	0.978	1.005	110 to 115	0.978	1.005	110 to 115
Ch. 19	0.913	1.019	60 to 70	0.94	1.05	60 to 70
Ch. 17	1.67	1.368	10 to 20	1.235	1.529	10 to 20
Average	1.444	1.292	***	1.365	1.245	***
Highest	2.333	1.666	***	2.333	1.529	***
Ch. 11	0.615	0.59	15 to 30	0.615	0.59	15 to 30
Ch. 9	1.001	1.001	0 to 5	1.25	1.25	0 to 5
Average	0.808	0.796	***	0.933	0.92	***
Highest	1.001	1.001	***	1.25	1.25	***
Ch. 3	1.021	1.021	100 to 105	1.028	1.028	100 to 105
Ch. 1	0.967	1.064	15 to 25	0.967	1.1	15 to 25
Average	0.994	1.043	***	0.998	1.064	***
Highest	1.021	1.064	***	1.028	1.028	***
Ch. 15	1.529	1.294	10 to 20	1.444	1.158	10 to 20
Ch. 13	1.2	1.104	45 to 55	1.2	1.12	45 to 55
Ch. 14	1.217	1.168	100 to 125	1.21	1.16	100 to 125
Ch. 29	1.083	1.093	135 to 150	1.093	1.103	130 to 150
Ch. 25	1.008	1.056	75 to 85	1.025	1.074	75 to 85
Ch. 27	0.951	1.073	25 to 30	0.975	1.1	25 to 30
Average	1.165	1.131	***	1.158	1.119	***
Highest	1.529	1.294	***	1.444	1.158	***
Pass AVG	1.032	0.993		1.041	1.011	
Pass High	2.333	1.666		2.333	1.592	

4.4.3 Distribution Factors

The first step in determining the distribution factors for this bridge was to add all of the tensile strains at midspan due to the truck being located at midspan, for each pass. Figures 4.13 and 4.14 graph the strains felt at each gage at midspan vs. the transverse location for the approach and center spans. The total values of strain across the midspan ranged from 251 με to 287 με for the approach span and from 330 με to 395 με for the center span (these totals are indicated on the graphs). Once all of these strains were added, they were averaged to get a normalized total strain value of 264 με for the approach and 356 με for the center. These values were assumed to be the maximum amount of strain caused by a truck in a single girder. To get the value for one wheel line, the total was divided by two to get 132 με for the approach and 178 με for the center. Figures 4.13 and 4.14 also show that the amount of strain experienced by a girder depends on the location of the truck passes. It should be noted that it appears that the curb and barrier found at the edges of the bridge seem to be taking some load, as the sum of the strains is lower for passes near the edge of the bridge.

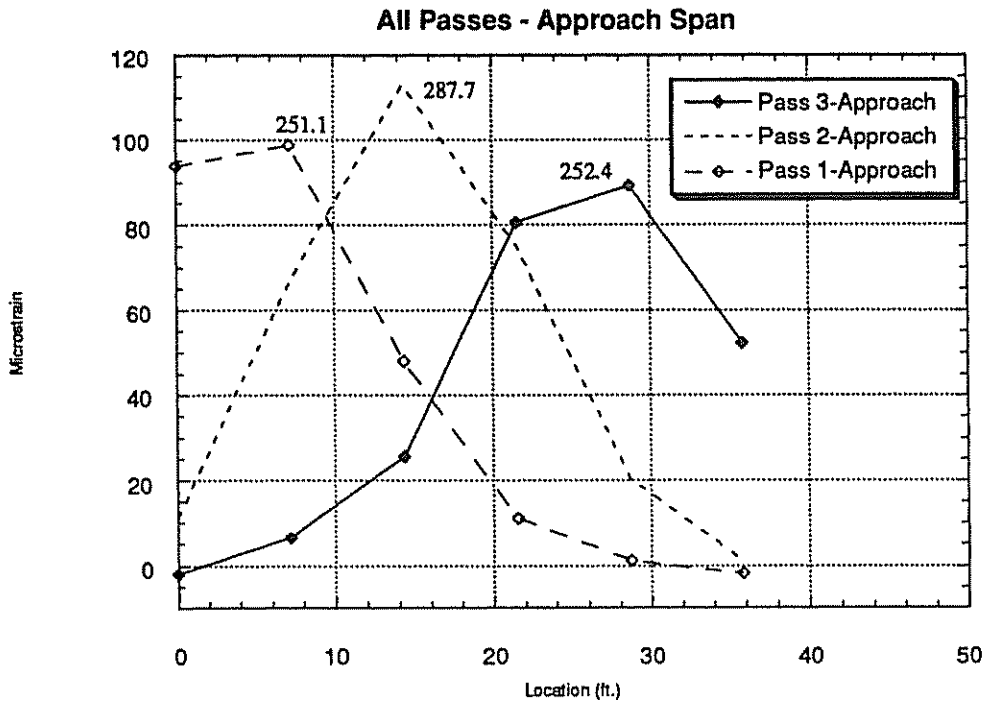

Figure 4.13. Total Strains Due to All Passes - Approach Span

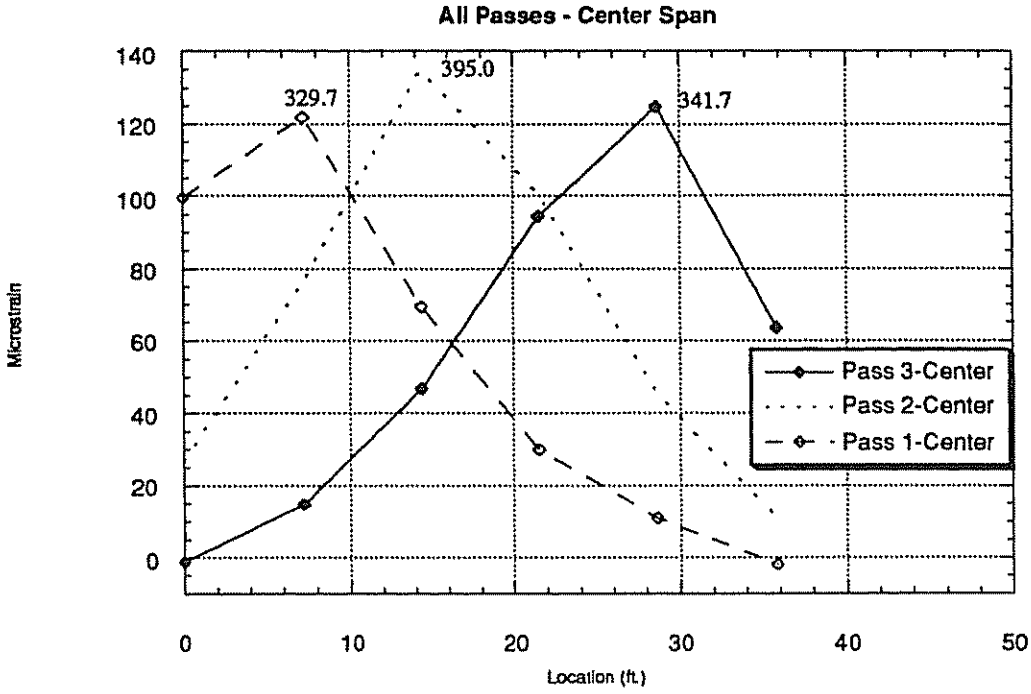

Figure 4.14. Total Strains Due to All Passes - Center Span

Influence lines for bottom flange gages across the midspan were drawn for each gage due to all of the passes for the situation when the truck was located at midspan. Because of the limited number of truck paths (three), each influence line consists of only three actual data points. Since the location of truck paths does not necessarily lead to a loading that would cause a maximum strain, assumed values were selected. After looking at strain values recorded where the truck did pass close to directly over a girder, a value of 115 με was chosen as the maximum strain for the approach span and 140 με was chosen as the maximum strain for the center span. A more complete influence line was generated by assigning this value of strain on the

influence line at a location corresponding to a hypothetical truck pass, directly over the gage that the influence line was being plotted. Next, according to the AASHTO Guide on Bridge Design[4], lanes were measured every 12 feet from the edge of the bridge to the center, resulting in a total of 3 lanes for the width measured. Within these 12 ft lanes, 6 ft vehicle widths were placed, keeping a 2 ft clearance from each of the 12 ft lane ends, so the vehicle would produce the most strain on the girder for which the influence line was drawn (values based on center line of truck were used). Figure 4.15 details an influence line graph and the lane spacing. All of the resulting influence lines exhibited consistent behavior, suggesting that reasonable values for maximum strains were used.

For each vehicle center line, the corresponding value on the influence line graph was recorded. These strain values for the three lane locations dictated by AASHTO[4] were added together and divided by the maximum strains due to one wheel line, as shown previously and found to be 132 με for the approach and 178 με for the center. The following exercise exhibits this step for the outer girder on which gage 17 was placed:

$$\text{E.D.F.} = \frac{I_\varepsilon}{W_\varepsilon} \qquad (3.2)$$

$$\text{E.D.F.} = \frac{115\mu\varepsilon + 10\mu\varepsilon + 0\mu\varepsilon}{132\mu\varepsilon}$$

$$\text{E.D.F.} = 0.947$$

Where:

E.D.F. = Experimental Distribution Factor

I_ε = Influence line total strain

W_ε = Wheel-line strain

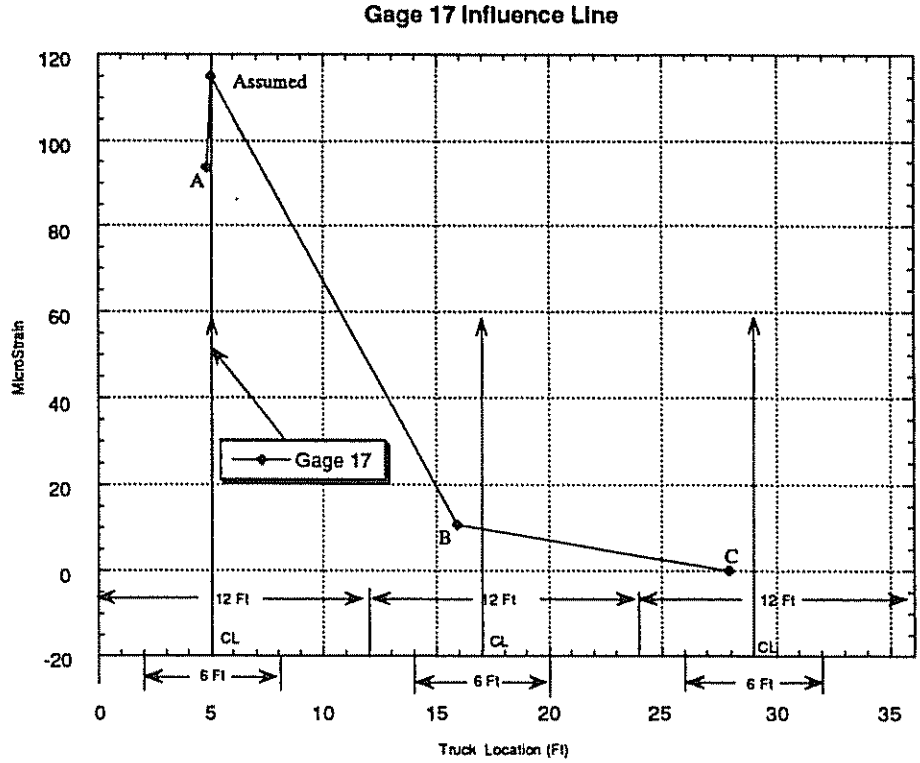

Figure 4.15. Influence Line for Gage 17.

This experimental distribution factor was compared to the value computed based on the AASHTO design code[4]. Typically, a multiple-presence factor would then be multiplied by the EDF, based on the number of load lanes available. To be conservative, multiple-presence factors will be neglected for this rating. The following exercise details the AASHTO[4] method of determining distribution factors, using the outer girder on the approach span as an example:

$$A.D.F. = \frac{S}{5.5}$$
$$A.D.F. = \frac{7.167}{5.5} \qquad (2.13)$$
$$A.D.F. = 1.303$$

Where:

A.D.F. = AASHTO Distribution Factor

S = Girder spacing

Table 4.5 lists the distribution factors for all of the girders calculated and all of the ADF's for those same girders. Note that the edge girders have a significantly lower distribution factor, as would be expected. Most of the measured distribution factors were close to the AASHTO[4] distribution factors, indicating a load distribution near expected. This improved distribution will lead to a higher load rating. For the approach span, the exterior girders had factors that were on average 23.0% less than the ADF values and the interior girders had factors an average of 3.2% more. The center span exterior girders yielded factors that were on average 31.3% less than the ADF values and interior girder factors an average of 0.2% more. These values indicate that the actual distribution factors for the interior girders are very close to that predicted by AASHTO. All distribution factor distributions and influence line graphs are located in Appendix B.4.

Table 4.5. Darley Road Distribution Factors.

Approach Span

Microstrain						
Gage	Lane 1	Lane 2	Lane 3	Total	EDF	ADF
17	115	10	0	125	0.947	1.303
19	115	60	5	170	1.290	1.303
31	62	105	18	185	1.400	1.303
7	24	98	75	197	1.490	1.303
8	5	38	115	158	1.200	1.303
5	2.5	22	115	139.5	1.060	1.303
				AVG-Int	1.345	1.303
				AVG-Ext	1.004	1.303

Center Span

Microstrain						
Gage	Lane 1	Lane 2	Lane 3	Total	EDF	ADF
27	140	22.5	-2.5	160	0.899	1.303
25	140	62	8	210	1.180	1.303
29	86	122	35	243	1.365	1.303
14	44	123	86	253	1.421	1.303
13	17	66	140	223	1.253	1.303
15	2.5	25	131	158.5	0.891	1.303
				AVG-Int	1.305	1.303
				AVG-Ext	0.895	1.303

4.4.4 End Restraints

The presence of end restraint at the supports was determined from graphs similar to that shown in Figure 4.16. This graph indicates the variation of tensile strain along the length of a girder's bottom flange caused by a truck located at midspan.

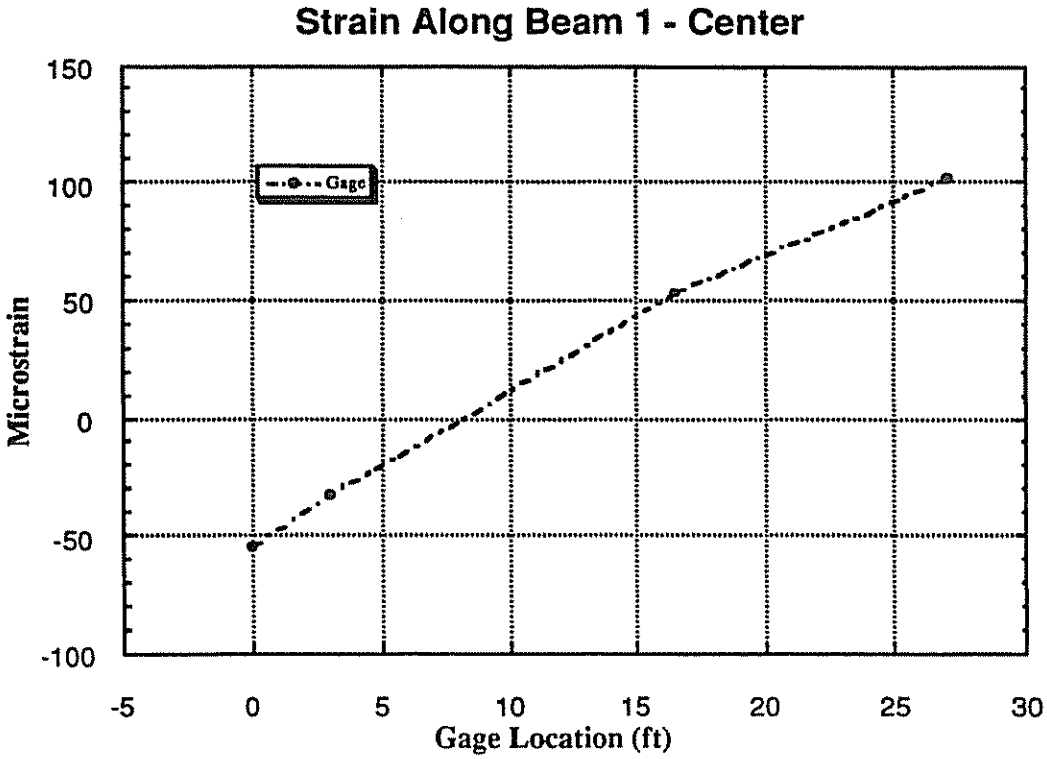

Figure 4.16. Strain Along Beam

The percent fixity (% fixity) can be determined from Figure 4.16 as follows:

$$\% \text{ Fixity} = |- \varepsilon_{end}/(\varepsilon_{pk} - \varepsilon_{end})| * 100 \qquad (3.3)$$

$$= |- (-55)/(102.07 - (-55)| * 100$$

$$= 35.0\ \%$$

Where:

ε_{end} = Strain at end of beam

ε_{pk} = Strain at Maximum Peak

Table 4.6 lists the percent fixity found for each beam.

Table 4.6. Fixity of Each Beam.

Beam # - Span	Fixity
1 - Approach	9.4 %
1 - Center	35.0 %
3 - Approach	4.2 %
3 - Center	1.8 %

4.4.5 Axial Forces

As was done for the Christina Creek Bridge, the strain variation along the length of the girders was used to indicate whether or not the neutral axis location was shifting significantly. Like the previous bridge, the top flange gages appear to be located close to the neutral axis (see Figure 4.17).

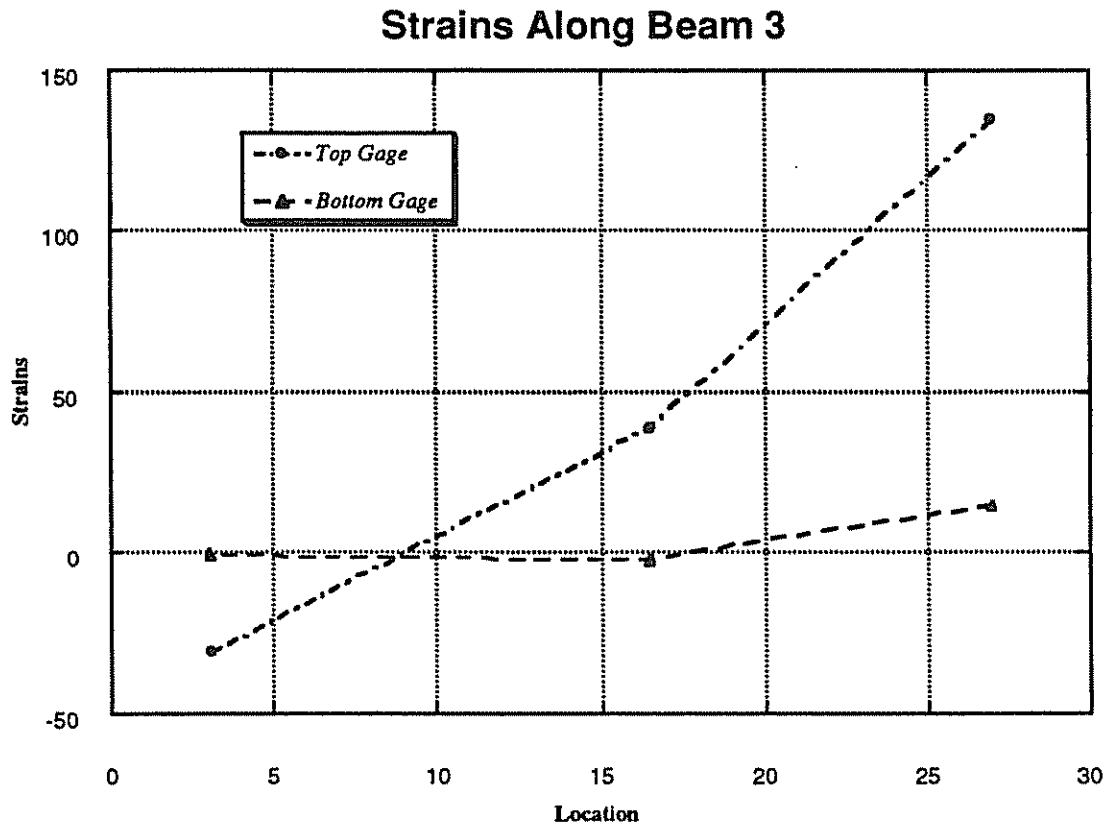

Figure 4.17. Strain Along Beam 3 for Axial Force Determination

While there is clearly some variation in strain (-2με to 15με), the slight shift in neutral axis location would represent a minimal axial force. As a result, it was concluded that the effects of axial forces can be neglected in the bridge evaluation.

4.5 Results of Data Analysis

A summary of values that have been determined for this bridge are listed in Table 4.7. Again, computed values seem reasonable and would indicate a small increase in bridge capacity, based on increased moment of inertia. More detailed tables of moment of inertia, neutral axis location, section modulus, distribution

factors, impact factors, and end restraints are tabulated in Sections 4.4.1, 4.4.2, 4.4.3, and 4.4.4, respectfully.

Table 4.7. Darley Road Results of Analysis

Bridge Properties	Field	Theoretical, AASHTO, or Plan Value
Neutral Axis Location	14.825" to 30.8"	14.825" and 30.4"
Concrete Strength	8 ksi	4 ksi
Effective Width	7.167'	7.167'
Deck Thickness	9.08 in	8.5 in
Moment of Inertia (Appr.)	4933 in^4	4933 in^4
Moment of Inertia (Center)	13374 in^4 to 14976 in^4	13397 in^4
Section Modulus (Appr.) Deck	206 in^3	206 in^3
Section Modulus (Appr.) Beam	333 in^3	333 in^3
Section Modulus (Center) Deck	1687 in^3 to 1692 in^3	1608 in^3
Section Modulus (Center) Beam	364.4 in^3 to 542.9 in^3	434.2 in^3 to 435.8 in^3
Impact Factor	1.26	1.27 to 1.31
End Restraints	1.8 to 35%	0 %
Axial Forces	0 kips	0 kips

Chapter 5

LONG-TERM MONITORING OF BRIDGES

5.1 Introduction

The use and practicality of long-term monitoring has become feasible only with recent developments in micro-processing technology. With the introduction of equipment that is capable of accurately reading and storing data under severe and variable weather conditions, the application and future of this mode of analysis is becoming one of great potential. In the following sections, different possibilities of future use are examined, along with specific devices that are presently available to accomplish specific tasks. Some future considerations include the measurement and determination of composite action in bridge structures, peak strains felt by specific elements, fatigue problems, and crack growth. Although there may be many different types of equipment available to perform these tasks, only a few specific instruments will be discussed here.

5.2 Equipment Available

The field of long-term monitoring and remote sensing is growing rapidly. The data retrieval devices used in structural monitoring are usually high-speed, large volume storage devices that record strain or resistive changes over long periods of time. The measuring devices need to be capable of maintaining reliability over these same long periods to ensure accurate and comparable measurements.

5.2.1 Measuring Devices

Several measuring devices are available for use. Normal resistive-type strain gages, such as those used to evaluate the bridges in this thesis, can be used to evaluate bridges over long periods of time. One limitation to the use of these gages, however, is their tendency to drift due to fluctuations in temperature or changes in the environment. This fluctuation can cause inaccurate data measurements and lead to faulty assumptions about a bridge's performance. Therefore, these changes must be accounted for and adjustments must be made before any conclusions can be determined. Since these adjustments can prove to be very tedious, the use of such gages is not the most efficient way to monitor a bridge's performance over long periods of time.

One very reliable and stable type of gage is a vibrating wire gage. The technology behind vibrating wire gages has been present for nearly 100 years, but was not placed into practical application until 1928. A French engineer named Andre Coyne first used this type of gage to measure water pressures inside dam embankments, located throughout France and Germany[8]. Since that time, these gages have proven to give extremely reliable measurements. This is due to the use of frequency determining measurements and a zero-stability inherent in the vibrating wire mechanical system. Figure 5.1 details the cross section of a typical vibrating wire gage.

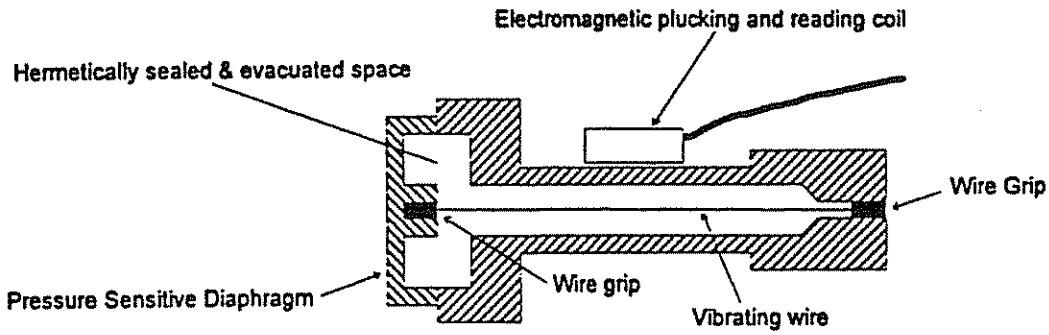

Figure 5.1. Cross-Section of Typical Vibrating-Wire Pressure Transducer.

This system is much more accurate than voltage and resistance-reliant gages found in most standard-use devices. Since frequencies can be transmitted over long cables with little signal depreciation due to cable resistance, contact resistance, and ground losses, frequency measuring greatly increases the accuracy of the measurements. To exemplify this, in the 1950's, over 3000 vibrating wire gages were installed in dam embankments throughout Europe. Of these gages, approximately 90% of them are still functioning accurately today[8]. This reliability, coupled with improvements in miniaturization and dependable sealing, have contributed to an increase in usage of this type of gage across the globe.

5.2.2 Data Retrieval and Storage Devices

There are numerous data retrieval systems available. Since these systems all operate similarly, only one will be discussed here. The SoMat Corporation offers a system that can be customized to the users needs through the addition of any of its test modules that are designed to attach to the total retrieval and storage system. The Model 2100 Field Computer System (FCS) is the most applicable to bridge monitoring, as demonstrated by Jeffrey A. Laman and Andrzej S. Nowak of the Department of Civil and Environmental Engineering at the University of Michigan[9]. They used this system to conduct Weigh-In-Motion (WIM) studies on some of Michigan's bridges to determine what truck loads were actually crossing them on a normal basis.

The SoMat FCS[10] is a portable data-acquisition system that is placed on a bridge and left to collect data, from strain gages attached to girders and other bridge components. It is a light-weight, hand-held unit with dimensions of 5"x 3" in length and width and a variable height, as dictated by the user's needs. Figure 5.2 illustrates this system. The minimum height is 2" with each optional module adding 0.41". The basic system comes equipped with the following:

Processor - 57,600 baud.

- Data collection rate of 1200 samples per second per channel.
- 32 k-byte memory; 28 k-bytes for data and 4 for program.

Power/Communications Module

- Provides regulated power to energize each module and excite strain transducers, as well as provide serial communications.

Battery Pack - Internal power of 800 milli-amp-hours of service (three 9-volt batteries).

- External power outlet for 12 VDC.

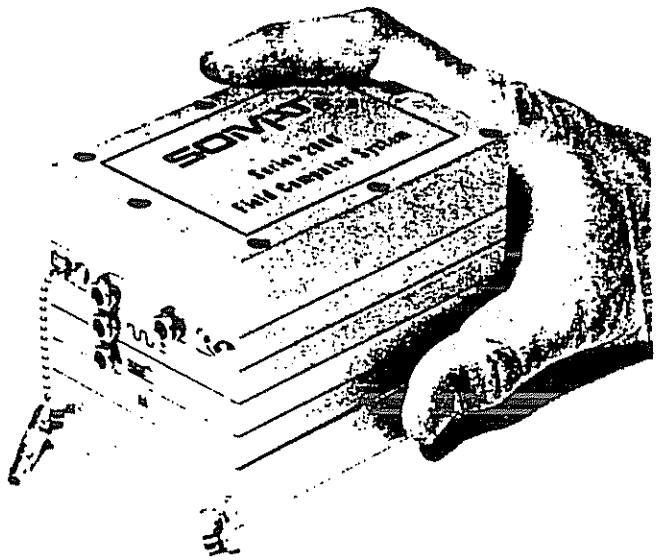

Figure 5.2. SoMat Series 2000 - Model 2100.

The system has many optional modules. Some of these include:

High Power DC-DC Converter

- Provides additional power for longer periods of operation.

1 MB Memory Module

- 1 MB of high-speed, low-power CMOS RAM.

Model 2040 Strain Gage Signal Conditioning Module

- Normalizes strain measurements.

Model 2050 Programmable Filter Module

- Low-Pass filter assembly that helps block out unwanted signals.

Model 2060 Pulse Counter

- Measures frequency and pulse width of signals.

Model 2071 Digital Module

- Used for digital signals and switch closure detection.
- Used for remote start and stop operation and event detection.

Model 2072 Status Indicator

- LED's indicate status of test conditions.

Model 2073 Parallel Transfer Indicator

- Allows uploading of large data files more efficiently.

Model 2074 Network Module

- Allows for control of two or more systems from a single PC.

All of these descriptions have been taken from the SoMat Series 2000 Technical Information Booklet[10], as provided by the corporation. There are several other modules available as well. This system seems to be a very versatile and applicable method of measuring and storing data over long time-spans. The box itself, once configured, can be mounted to the structure or nearby to avoid tampering and to minimize exposure to the weather.

5.3 Application and Capabilities

There are many applications and benefits of this type of testing. Some of these include the presence of composite action, peak strain measurements, fatigue analysis, and crack growth monitoring. The following sections discuss these benefits in further detail.

5.3.1 Presence of Composite Action

The presence of unintended composite action will cause a bridge to have a significantly higher load carrying capacity than expected. However, if the composite action is suddenly lost, the bridge capacity will immediately reduce.

Composite action can easily be identified by locating the neutral axis of girder-slab system. The neutral axis can be found by analyzing strains taken from the top and bottom flanges of a steel girder, as demonstrated in previous chapters. As daily traffic passes, strategically located pairs of gages can record strains and be used

to track the neutral axis location. If the loss of composite action occurs, it will be identified through the long-term measurements.

5.3.2 Peak Strain Measurement

Once a bridge has been field tested, peak strains recorded during long-term monitoring can be used to evaluate the condition of the bridge and the type of traffic crossing it. Gages can be placed on the girders of a bridge in the same locations as the initial field test. The strains can then be measured and processed through special algorithms to determine the highest strains read at each gage, since the last reading. After a predetermined length of time, the peak reading can be checked. Using the initial field test results as a baseline, the peak reading can be evaluated. Unexpected high readings correspond to either very heavy vehicles or a change in bridge behavior, possibly associated with deterioration. Using similar techniques, long-term bridge Weigh-In-Motion studies have been used to determine pertinent truck characteristics, such as axle weights, number of axles, axle spacing, and speed. Since this can occur without trucker knowledge, it can be extremely helpful in finding the actual size of overweight trucks, since these trucks tend to avoid weigh stations.

5.3.3 Fatigue Analysis and Crack Growth Monitoring

Fatigue analysis and crack growth monitoring are important aspects of bridge evaluation. Over the course of a bridge's life, cracks may form due to fatigue effects on initial material flaws. Figure 5.3 details the behavior of crack growth due to cyclical loading.

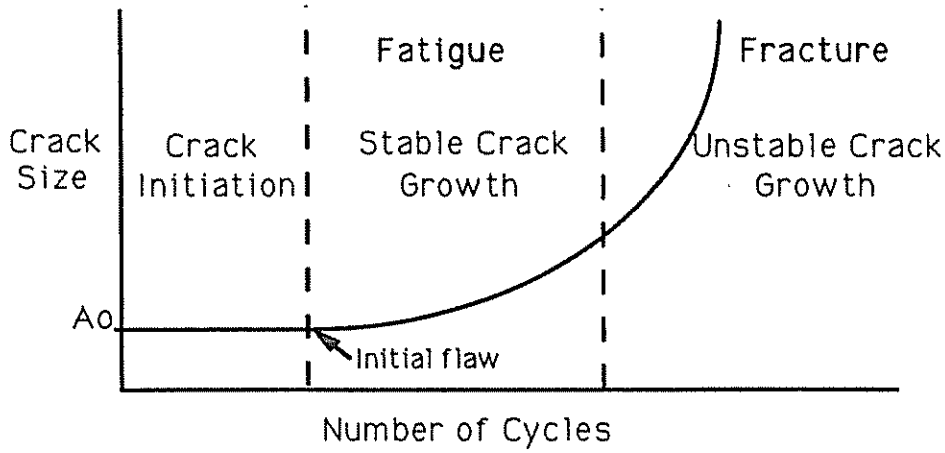

Figure 5.3. Crack Growth Effects

Cracks form from initial flaws in the material, as indicated by "A_O" on the Y-axis of the graph in Figure 5.3. Once a crack forms, it begins to grow due to repeated loading caused by normal daily truck traffic. As this growth increases, it enters a region known as "Unstable Crack Growth." This region is where failure, due to fatigue, occurs. Since crack growth normally progresses at very slow rates, vibrating-wire-crack-width gages can be useful in monitoring existing cracks. They can maintain accuracy for long periods of time, ensuring true crack growth monitoring. The ultimate goal of monitoring these cracks is to ensure they never reach unstable growth, thus preventing catastrophic failure.

5.4 Summary

Long-term monitoring of highway bridges has become increasingly important with our deteriorating infrastructure. Only recently, has there been the introduction of accurate and relatively inexpensive measuring, data retrieval, and storage devices for use over long periods of time. These devices can be instrumental in determining such characteristics as the presence of composite action, peak load characteristics, and the presence of fatigue-induced crack growth, which can lead to structural failure. The monitoring of such characteristics can provide engineers with information on daily use requirements and structural integrity, as well as help prevent catastrophes.

Chapter 6

CONCLUSIONS AND RECOMMENDATIONS

6.1 Bridge Evaluation Recommendations

The recommendations for this section are divided into sections dealing with Field Test Preparation, Gaging and Load Test, Analysis of Data, and Conclusions.

6.1.1 Field Test Preparation

When preparing for a field test, attention to details such as location, access for instrumentation, traffic volume, and how critical the highway is that the bridge supports or passes over need to be considered. If the bridge is high above the ground, the availability of equipment, such as a scissor-lift or a cherry picker, to lift personnel to the underside of the bridge should be investigated. If the bridge has any other obstacles such as rivers, gorges, or anything that rules out the use of equipment listed above, the use of a snooper truck or cable and scaffolding equipment may be needed and the availability of such equipment should be investigated, as well.

Preparation for gaging and testing is also important. Several personnel will be needed to perform the gaging task. The two tests conducted in this thesis utilized crews of 6 or more for the gaging and testing. For both gaging and testing, arrangements for traffic control must be made. Typically, either local law enforcement officials or DOT personnel will be used to ensure safety of drivers, as

well as people performing the bridge test. Personnel safety should always be given priority during the testing.

6.1.2 Gaging and Load Test

When gaging the bridge, the location of the gages is of utmost importance. For any bridge, if possible, it is recommended that gages be placed on every girder across the midspan. This is important for determining distribution factors. Midspan gages are also needed for evaluating section properties and impact factors because midspan locations typically experience the maximum strains. It is also important that several girders be gaged along their length, including gages at the beginning and end of the span (reactions). These gages are needed to establish the longitudinal load distribution that is used to evaluate the extent of unintended end restraint, as well as the presence of axial forces in the girders. The optimal girders to be gaged along their length are those that will fall directly under a selected load path. This will ensure that the magnitude of the strain being measured will be as high as possible, thus enabling more accurate bridge characteristics to be determined. Gaging at the ends of the span is important for determining the presence of end fixity and axial forces. Realizing that the number of gages available will be limited, some discretion will be required when actually selecting the location of each gage. It should be noted that not all locations require both top and bottom gages, since distribution effects are based only on tensile strain readings.

The load test of the bridge should be conducted using a vehicle that represents the maximum allowable truck loading based on the chosen truck configuration. This can be done using a dump truck loaded with sand or gravel to get it as close to the maximum allowable load (72 kips) as possible. Since load paths can

be chosen to represent normal traffic, actual traffic lanes are suitable load paths. Care must be taken when the loading is taking place to ensure that the trucks stay on a straight path. This can be done by lining the vehicle wheel up with a painted lane line. For the evaluation of distribution factors, more transverse truck locations will lead to more accurate results. At least two truck passes should be made along all load paths. This will allow the verification of acceptable data, as well as a means for determining error tolerances. To determine impact factors, several truck passes must be made at full speed (approximately 55 mph) on the same load paths used for semi-static tests.

6.1.3 Analysis of Data

It has been found that the magnitude of strain can significantly affect the values of parameters computed. For this reason, one should use strain responses that represent the maximum response observed (typically caused by the truck located at midspan or close to the gage location). It is also possible to conduct parametric studies on the effects of strain magnitude in computing bridge parameters. Those parametric studies can help to establish the magnitude of strains needed to get consistent parameter determinations.

For both the calculation of impact factors and effective deck width, the effect of using higher vs. lower strain measurements has been demonstrated. In determining individual section properties, such as neutral axis location and composite action, it is natural to base results on the more highly stressed instances. This is also true for transverse and longitudinal force distribution evaluation. For rating, it is the higher stresses that will control.

Finally, with regards to axial forces that may develop in the bridge girders, two methods for identifying whether or not axial force is present have been discussed.

6.2 Conclusions Regarding Christina Creek and Darley Road Bridges

For both the Christina Creek and Darley Road bridges, the field tests yielded bridge data that was very consistent with that suggested by AASHTO[4,5] and the original bridge plans.

For the Christina Creek bridge, some increase in the section moment of inertia of the girders was found and composite action was confirmed. Furthermore, slightly improved transverse load distribution was evident. The bearings were found to vary from being free to some having partial fixity. No axial force was believed to be developing in the girders. Impact factors were found to be close to that expected. Overall, the bridge may be able to carry slightly more load than expected.

For the Darley Road bridge, an increase in the section moment of inertia for the girders was also found. In this case, it was partially due to a buildup of the asphalt wearing surface, as well as the increase in concrete strength over time. Participation of curbs and barriers along the edges of the bridge also contributed to an increase in capacity. Transverse distribution factors and impact factors were close to values expected, according to AASHTO.[4,5] Some girders showed partial fixity, while others were functioning properly. The girders showed little effects of axial force.

Probably the most interesting result was that the approach span, although designed non-compositely, acted compositely in almost all instances. However, as discussed, there were some occurrences of non-composite behavior. For rating purposes, one would have to neglect the unintended composite behavior. The main span acted compositely, as designed. Overall, the bridge may be capable of carrying slightly more load than expected.

6.3 Long-Term Monitoring Recommendations and Conclusions

There is a growing assortment of long-term monitoring equipment available today. When deciding to perform a long-term evaluation of a bridge, detail must be given to the placement of the gages, data storage devices, and prevention of damage due to tampering and weathering. Some capabilities of this type of evaluation include determination of peak strains, identification of typical traffic loads, monitoring of fatigue-induced cracking, and the evaluation of composite action.

Vibrating wire gages were the most accurate long-term gages found in this research. Unlike traditional resistive-type gages, vibrating wire gages are not affected by temperature fluctuations and can provide accurate strain readings at a wide range of temperatures. Time also has an affect on standard gages, as their baseline value tends to drift when not closely monitored. Vibrating wire gages can provide the stability needed to account for such fluctuations and do not require close monitoring to ensure long-term accuracy.

With the introduction of high-speed, data collection and storage devices, long-term monitoring has become a feasible means of monitoring the ongoing "health" of a bridge. Devices such as those supplied by the SoMat Corporation have the capability of providing the long-term storage and retrieval requirements of such monitoring. With its numerous optional modules, it can provide the user with a site specific device to concentrate on the problems for that particular bridge.

Long-term monitoring can also be an effective tool for the preservation and rehabilitation of the infrastructure. The one-time field tests performed in this thesis can be used as a baseline for ongoing long-term monitoring results. Clearly, the field of bridge testing and evaluation can be enhanced by continued long-term monitoring.

REFERENCES

1. Wyoming Department of Transportation, Bridge Rating and Analysis of Structural Systems Computer Program, March, 1996.

2. Lichtenstein, A.G. (1995), "Bridge Rating Through Nondestructive Load Testing," Final Report, NCHRP Project 12-28(13)A.

3. New York State Thruway Authority, Final Report of Bridge Rating Through Diagnostic Testing of Two Bridges on I-84, Contract No. D211895, Lichtenstein Engineering Assoc., P.C., Consulting Engineers, New York, NY, Oct., 1995.

4. American Association of State Highway and Transportation Officials, Standard Specifications For Highway Bridges, Fifteenth Edition, 1992.

5. American Association of State Highway and Transportation Officials, Guide Specifications for Strength Evaluation of Existing Steel and Concrete Bridges, 1989.

6. Chajes, M.J., Mertz, D.R., and Commander, B., "Experimental Load Rating of a Posted Bridge," ASCE Journal of Bridge Engineering, (In Press).

7. American Concrete Institute, Building Code Requirements for Reinforced Concrete and Commentary, Sept., 1992.

8. GEOKON INC., Instruction Manual - VSM-4000 - Vibrating Wire Strain Gage, Aug., 1995.

9. Laman, J. A., "Collecting Accurate Load Data From Bridges,"*Scientific Computing and Automation,* Oct., 1994.

10. SoMat Corp., Technical Information Booklet - SoMat Series 2100, Feb., 1993.

APPENDIX C.

BRIDGE RATING BASED ON FIELD TEST RESULTS

by

Geoffrey Harlan Reichelt

A thesis submitted to the Faculty of the University of Delaware in partial fulfillment of the requirements for the degree of Master of Civil Engineering

Spring 1997

BRIDGE RATING BASED ON

FIELD TEST RESULTS

by

Geoffrey Harlan Reichelt

Approved: _____

Michael J. Chajes, Ph.D.
Professor in charge of thesis on behalf of the Advisory Committee

Approved: _____

Chin Pao Huang, Ph.D.
Chair of the Department of Civil and Environmental Engineering

Approved: _____

Stuart L. Cooper, Ph.D.
Dean of the College of Engineering

Approved: _____

John C. Cavanaugh, Ph.D.
Associate Provost for Graduate Studies

ACKNOWLEDGMENTS

I would like to express my thanks to Dr. Chajes for his advice and direction during the course of my graduate studies. I would also like to acknowledge Dennis O'Shea and the Delaware Department of Transportation who provided the funding for this project to take place as well as Jeff Schultz and Bridge Diagnostics, Inc. for providing the equipment and the instruction to perform the bridge field tests.

To those who worked hard to help get the field tests done, Jon Reid, Bill Finch, Al Meyer, Jack Demitz, and Ed Schluter, much thanks is given. Thanks to all the structural engineering graduate students for making this experience one to remember.

Special thanks to my family and Mrs. Camburn for their support in all my efforts to pursue my goals. Also I want to thank Melissa Tinney for being patient and understanding while I have worked to complete this project.

Finally, I thank God for the blessings He has given me during my graduate experience.

TABLE OF CONTENTS

LIST OF FIGURES

ABSTRACT

Engineers are faced with the responsibility of rehabilitating the rapidly deteriorating infrastructure with limited financial resources. In order to best manage these limited financial resources, engineers are searching for better ways to evaluate existing infrastructure systems.

Bridge design is a conservative process just like any other type of design. The conservatism used in the design of a bridge often can provide engineers room to find additional capacity when they may need it to keep a bridge open, or to prevent it from being posted. It then becomes a question of which structure gets priority in the bridge maintenance program.

Load evaluation of bridges helps to determine which structures require rehabilitation, which ones need total replacement, or which ones are still in adequate condition. The purpose of this research was to determine effective and efficient methods for determining the capacity of an existing bridge based on field load test results.

Chapter 1

INTRODUCTION TO LOAD EVALUATION OF BRIDGES

1.1 Introduction to Load Testing Bridges

Field testing bridges is one method for determining the strength capacity of existing bridges. It also helps engineers to understand the behavior of existing bridges. As a result of this gain in understanding, engineers can help public agencies decide which bridges to post, rehabilitate, or replace. Therefore, field testing can help prevent public monies from being unwisely spent on unnecessary repair. For example, a public agency decides to replace a well-used bridge due to findings during a visual inspection. Before they replace the bridge, they hire structural engineers to field test the bridge and determine the bridge is stronger than it appeared, and not in need of repair or replacement. Now the money can be better spent on another bridge that does need repair. In addition, the public does not have to face the inconvenience of unnecessary construction.

1.2 Nondestructive Static Load Testing Methods

Static load tests performed on bridges can be divided into two categories: proof load tests and diagnostic load tests. These methods are intended to be nondestructive. In other words, they do not cause damage to the bridge, thereby allowing the bridge to remain in service after the test has been performed. The basic procedures for both methods are discussed in the following section, however only the

diagnostic load test was performed on the bridges discussed in this paper and will therefore be discussed in greater detail in a later section.

1.2.1 Proof Load Test

Proof-load tests need careful planning since the intent is to load the bridge almost up to its limit state. A starting proof load and a target proof load are to be calculated. Monitoring equipment is chosen and installed in the appropriate locations. The bridge is slowly and incrementally loaded commencing with the starting proof load so no dynamic effects are introduced. Testing personnel must carefully watch the bridge for excessive cracking, deflecting, or settling to occur. They must also check for 10% or more nonlinearity. If any of the aforementioned behaviors take place before the target load has been reached, the test shall be terminated. If the test is terminated due to excessive cracking, deflecting, or settling, the load should be removed immediately. If the test is terminated due to nonlinearity or the target load has been reached, then the load should be removed in increments no larger than the loading increments. The bridge should then be inspected to check for damage, distressed, or displaced components [1].

1.2.2 Diagnostic Load Test

Diagnostic load testing focuses more on the instrumentation of the bridge as opposed to the loading during testing. A standard test truck for the state in which the bridge is located is used consistently throughout the test. Customarily numerous strain gages are set up at predetermined locations on the bridge girders. Strain measurements are recorded as the test vehicle is driven at a crawling speed of about 5 to 10 mph to minimize any dynamic effects. If it is so desired, data can also be recorded during high-speed passes to examine impact effects.

1.3 Bridge Capacity Evaluation

Once the load testing has been completed, it is the engineer's job to evaluate the collected data. Structural properties of the bridge can be obtained directly from the strain data as shown by Reid [2]. Those structural properties are then used in a bridge rating computer program or other analytical methods to rate the capacity of the bridge. Two methods for rating bridges using field test results are considered here. The methods are summarized below, and explained in detail in later sections.

1.3.1 BRASS

One computer program that is widely used by state agencies is called BRASS, which is an acronym for Bridge Rating and Analysis of Structural Systems [19]. Bridge engineers can use BRASS to analyze, design, or more importantly for this project, load rate a bridge. BRASS is a versatile program that can be very useful to the engineer who understands it.

1.3.2 Lichtenstein Method

As bridge load testing is becoming more widespread, engineers are devising new methods to evaluate bridges based on test data and other factors as well. Lichtenstein [3] devised a method that utilizes load test data in combination with other factors such as inspection thoroughness and frequency, structural redundancy, and fatique sensitivity. This method involves hand calculations and adjustments to the initial rating based on the test results and various factors mentioned above.

1.4 Objective of Study

The purpose of this thesis is to apply these two methods of bridge evaluation to three case studies, and make recommendations on how the procedures could be improved.

Chapter 2

A BACKGROUND OF LOAD TESTING BRIDGES

2.1 Present Load Testing Practices

At the present, load testing of bridges is being practiced worldwide as well as in the United States according to Pinjarkar *et al* [4]. The Florida DOT has specially built two tractor trailors loaded with concrete blocks to nondestructively proof test their bridges. The Ontario Ministry of Transportation and Communications has been using a very similar test set-up since 1973 [5]. Since then, Ontario has tested 225 bridges. Their tests also include dynamic, diagnostic, and ultimate load tests in addition to proof load tests. The Ontario Highway Bridge Code specifies that if a bridge's analytical evaluation is deemed unsatisfactory, a load test is to be performed.

Switzerland requires that all new and rehabilitated bridges must have a diagnostic test at service loads to calibrate and confirm analytical methods of evaluation. New Zealand will proof test restricted bridges to justify or remove existing restrictions. In general, European countries use diagnostic testing to calibrate and confirm analytical methods used to design and evaluate bridges [5].

Despite the widespread use of load tests to evaluate bridges, there is still a large lack of official provisions or guidelines to govern consistent testing procedures. Effort to fulfill the lack of general proof testing guidelines has been shown by Fu in his report, *Highway Bridge Rating By Nondestructive Proof-Load Testing For Consistent Safety* [1] for the New York DOT. Even though diagnostic load testing is

performed in the United Kingdom, they have no specific guidelines by which to test. In January of 1988, New York DOT did issue guidelines by which to establish posting ratings and evaluate the strength of state-owned bridges. As time progresses, and more people get more experience with load testing, the database will grow and more agencies will feel comfortable making guidelines to establish load testing as part of their bridge management program.

2.2 Unique Examples of Bridge Field Testing

The primary purpose of this section is to present three unique examples of bridge field testing. This will allow the reader to appreciate applications of field testing that are very much different in scope than the diagnostic tests discussed in this paper. First to be discussed is the instrumentation of the Natchez Trace Arch Bridge during construction. Next is the destructive testing of two 80-year old truss bridges. Last is the dynamic testing for the modal analysis of a bridge in Pennsylvania.

2.2.1 Natchez Trace Arch Bridge Instrumentation During Erection

The Natchez Trace Arch Bridge, located in Colorado, is a prestressed and post-tensioned concrete double arch bridge that was erected from July 21, 1992 to November 23, 1993. This case study provides interesting insight into how field testing can be used during construction. It was instrumented with 60 strain measurement devices and 20 temperature sensors during its construction so the construction engineer could compare his analytical predictions with the actual measurements [6].

A total of ten pre-cast arch segments were each instrumented at the casting yard with six vibrating wire strain gages and two Type-T thermocouples. Once the

gages and sensors were in place, measurements were taken until construction was complete. Each arch contained five of the instrumented segments.

Overall, conclusions drawn from evaluating the collected data showed that the analysis results were relatively close to those determined from the instrumentation. Analysis results had predicted somewhat larger axial deformations than what actually took place during the erection of the arch, but the deviations were nothing to be concerned with. An observation made straight from the strain readings revealed that out-of-plane bending only produced stresses of plus or minus 0.25 ksi. It was also concluded that the bridge was significantly effected by changes in temperature, and since the construction analysis did not account for temperature changes, that could explain some of the discrepancies between the predicted and experimental values. Another key factor in the discrepancies was the actual construction schedule and its modification to the originally planned construction schedule. Other details played a role in the behavior of this bridge during erection which can be found in the referenced document.

Some times the construction process is the most critical time for a bridge to collapse. This testing helped to understand stress behavior during the construction of a bridge.

2.2.2 Pratt Truss Bridge Destructive Testing

Another interesting area of bridge evaluation is the use of destructive testing on bridges that are taken out of service.

Many of the steel truss bridges built before the 1930's are still being used today [7]. Unlike the slab on steel girder bridges built close to that time period, many steel truss bridges do not exhibit extra capacity during a load test. This is mostly due

to fatique damage or excessive corrosion of critical members in the truss. Therefore efforts are being made to better assess the strength of deteriorated steel truss bridges. The example presented here illustrates truss behavior during nondestructive diagnostic testing and destructive proof load testing [7].

The bridge for this example was an eight-panel Pratt throught truss bridge. It spanned 152 feet and carried a 20 ft. roadway. Built-up riveted members composed the truss members. The bridge deck consisted of a timber floor supported by 30 inch deep transverse girders and 18 inch longitudinal stringers. Rollers and hinges on reinforced concrete abutments faced with sandstone provide bearing for the bridge.

An arms-length inspection was performed prior to testing to confirm the shop drawings and identify any deterioration or damage and retrofits. Corrosion had severely damaged the exterior stringers and nearly 100% of the webs of the stringers at both ends of the panels were gone. Even though the interior stringers were in good condition, many of them were not resting on the abutment walls at both ends. accumulated rust around the bearing rollers had caused them to cease functioning for a number of years.

At least 150 transducers were used to capture global and local effects during loading. Diagnostic testing was performed and then retrofits were made to some of the girder-to-truss connections. The retrofits were made because those connections were predicted to have premeaturely failed due to the highly concentrated load induced by the actuator to execute the destructive proof load test. Conclusions from the tests were that an accurate capacity prediction could not be made without the destructive testing of the steel truss bridge. The retrofits did perform well under loading which proved that similar retrofits on existing steel truss bridges would most likely be successful.

2.2.3 School House Road Bridge over PA-283 Spectral/Modal Analysis

While the previous two tests still focused on determining capacity or behavior under loading, this last example investigates the use of a modal analysis to detect certain flaws in a bridge [8].

As one can imagine, it would be difficult to find a bridge to test before and after a natural flaw occurred within a reasonable time period. Therefore, a bridge with a bolted splice was needed so a flaw could be simulated without permanently damaging or sacrificing the integrity of the structure. That is why the bridge carrying School House Road over PA-283 between Harrisburg and Lancaster, Pennsylvania was chosen for the test. It was chosen also for its typical composite construction, and low traffic volume. The test bridge is a two-span continuous bridge measuring 71.37 m (234 ft.) long with each span measuring 35.67 m (117 ft.). It is 14.64 m (48 ft.) wide with seven welded steel plate-girders placed at 2.19 m (7 ft. 2 in.) on centers supporting the reinforced concrete deck with 0.76 m (2 ft. 6 in.) overhangs.

The connection that was disconnected is located 7.63 m (25 ft.) from the center pier on the first interior girder next to the west fascia girder of the north span. Nineteen rows of bolts in the web and four rows of bolts in the top and bottom flange plates hold the connection together. To simulate a fatique fracture crack through the bottom flange and 15% of the web depth, all four rows of the bottom flange splice bolts and the bottom three rows of the web splice bolts were removed on one side of the connection.

Sixteen test points were evenly distributed along the centerline of the test girder. The ninth test point counting from the abutment was chosen for the reference point, and an accelerometer was mounted there. A 17th testing point was placed on

the middle of the sixth girder from the west fascia girder. This was done to differentiate flexural mode shapes from torsional mode shapes.

Once the test points were determined and the accelerometer mounted, a test was performed with the splice connection intact. Then the specified splice connection bolts were removed and a second test was performed. There was no traffic on the bridge or under the bridge during testing.

Each test consisted of a roving hammer striking each test point. The data acquisition system collected frequency data for four seconds after each strike.

Spectral/modal analysis indicated that the mode shapes of the bridge did change due to the simulated fatique crack. Research in this area is still in progress.

Chapter 3

BRIDGE LOAD RATING

3.1 Bridge Load Rating Categories

The ultimate goal of a field test is to determine the load rating of a bridge at its present state. Load rating means determining the load capacity of a bridge. There are three different load ratings assigned according to three different types of load intensities. They are the inventory, operating, and posting rating. All three ratings are discussed below.

Bridges are rated according to the weight of standard trucks. Each standard truck has a different axle loading and configuration. Delaware uses seven standard trucks. Because each truck loads a bridge differently, the ratings will vary for each standard truck.

AASHTO [10] uses a standard truck called an HS20. This vehicle is a three-axle tractor-trailer with the first two axles spaced at 14'-0". The trailer axle is varied from 14'-0" to 30'-0" from the rear truck axle to find which spacing gives the worst loading case in the analysis. The total vehicle weight is 72,000 lbs. with 8,000 lbs. on the front axle and 32,000 lbs. each on the trailer and rear truck axle.

Any component of the bridge, such as a connection or the deck can be load rated. It is generally assumed that the rating of bending moment in the girders is the critical rating so the other components are not typically rated [9].

3.1.1 Inventory Rating

According to the American Association of State Highway and Transportation Officials, AASHTO, bridges are rated using an upper and a lower range of performance [10]. Inventory rating captures the lower range of bridge performance. It represents, "a load level which can safely utilize an existing structure for an indefinite period of time [10]." Quite naturally, the factor of safety for this rating level is relatively large. In simple terms, one might say this rating indicates the bridge's performance under the loading of the large quantity of everyday traffic.

3.1.2 Operating Rating

Just as the inventory rating captures the lower range of bridge performance, the operating rating captures the upper range of bridge performance. Occasionally a bridge may need to handle an abnormally large live load. If that load were to repeatedly pass over the bridge, the bridge's life would be shortened; but nonetheless, it needs to be determined if the bridge can carry that load on infrequent occasions. Thus, according to AASHTO, the operating rating represents "the absolute maximum permissible load level to which the structure may be subjected [10]."

3.1.3 Posting Rating

The posting rating is a rating used for the legal purposes of each particular state. Each state has a legal load limit for each axle configuration of the predominant trucks that operate in that state. If a truck is over the load for its axle configuration when it pulls into a weigh station, it is ticketed and impounded until it is unloaded.

Each state determines how it wants to compute its posting ratings. In Delaware, the posting rating is found by adding two-thirds of the inventory rating to one-third of the operating rating. If a bridge presents a posting rating lower than one

(i.e. the ratio of capacity-to-standard truck weight is less than one) then the allowable weight of that truck is posted on the bridge so no trucks will overstress the bridge in its present condition. That does not mean the truck is overloaded, but rather that the bridge condition has deteriorated so it cannot handle even the legal load limit.

3.2 Bridge Load Rating Methods

Just as there are different methods used in the design of structures, there are different methods by which one load rates a structure. In fact, there are three methods for rating a bridge. They are, the Allowable Stress rating method, the Load Factor rating method, and the Load & Resistance Factor rating method.

3.2.1 Allowable Stress Rating

Allowable Stress rating utilizes 55% of the yield stress (i.e. allowable stress) of the critical member for computing the inventory rating of a structure. To obtain the operating rating, one takes the maximum load which produces 75% of the yield stress. As will be seen in the examples of the next section, the formula used is a reverse of the Allowable Stress Design formula. This method is relatively easy for steel and timber structures. However, this method is quite involved when it is used to rate a concrete structure or element.

When one rates a structure according to this method, one simply finds the allowable maximum moment based upon the allowable stress designated by the inventory and operating limits. Then the dead load effects are determined and subtracted from the calculated capacity. Next the live load capacity is divided by the maximum live load effects plus impact. Impact is based on the bridge span length. The result is the rating factor for the structure. The Allowable Stress rating equation is given by:

$$RF_{i \text{ or } o} = \frac{\text{Capacity - Dead Load}}{\text{Live Load } (1 + I)} \qquad (3.1)$$

Once the two rating factors are determined, one multiplies the loading vehicle by each rating factor to obtain the inventory and operating ratings in units of weight. Please see the example in Section 3.3.1 for an illustration of the Allowable Stress rating procedure.

3.2.2 Load Factor Rating

The AASHTO *Interim Specifications for Bridges* describes what is probably the simplest of the three accepted rating methods. This method applies a factor to the dead load and the live load in the rating equation. It is then assumed that the structure can reach ultimate capacity according to the design guidelines for the particular material in question. From there on, the Load Factor procedure is the same as the Allowable Stress procedure. In this case, the inventory rating factor would be calculated as such:

$$RF = \frac{\text{Capacity - 1.3(Dead Load)}}{1.3(5/3)(\text{Live Load})(1 + I)} \qquad (3.2)$$

And the operating rating factor would be:

$$RF = \frac{\text{Capacity - 1.3(Dead Load)}}{1.3(\text{Live Load})(1 + I)} \qquad (3.3)$$

An example is provided in Section 3.3.2.

3.2.3 Load & Resistance Factor Rating

The most recent rating procedure is outlined in the *Guide Specifications for Strength Evaluation of Existing Steel and Concrete Bridges* [12]. It is known as

the Load & Resistance Factor method. As the equation below shows, there is a factor applied to the resistance (or capacity) as well as the loads.

$$RF = [\phi R_n - \mu_d D] / [\mu_L L(1 + I)] \qquad (3.4)$$

More importantly, though, this method considers more factors involved with the rating of a bridge. In this procedure the impact effect is determined by the condition of the deck surface instead of just the span length. The values for impact effect are 0.1 for good or fair condition, 0.2 for poor condition, and 0.3 for critical condition. This makes more sense in reality because a deck in good condition will realize relatively little impact effect despite how short it may be. If the dead load is measured and known for sure then μ_d is 1.2 but is 1.4 if the overlay depth is uncertain. The average daily truck traffic, ADTT, is used to determine the value of μ_L. If the ADTT < 1000 with control of overloads then μ_L is 1.3, or μ_L can be as high as 1.8 if ADTT > 1000 without effective enforcement resulting in significant overloads. Finally, the resistance factor, ϕ, varies from 0.95 for a well conditioned, carefully inspected, and vigorously maintained bridge to 0.55 for a heavily deteriorated, non-redundant, roughly inspected, intermittently maintained bridge. As one can see, this method takes into consideration more parameters that pertain to the capacity and safety of the bridge.

An example is presented in Section 3.3.3.

3.3 Bridge Load Rating Examples

In order for the reader to better understand how a bridge capacity is rated, three examples are included in this section. All three examples are performed on the same concrete slab-on-steel girder bridge. The first example illustrates allowable stress rating while the second example illustrates load factor rating. Finally, the third

example demonstrates load and resistance factor rating. All three example are taken from White, Minor, and Derucher [13].

The bridge used in all three examples is a simple supported steel girder bridge with a noncomposite reinforced concrete deck. The span, center to center of bearings, is 25 ft. There are six W24X68 beams spaced at 7'-10" center to center. The yield stress, F_y, for the steel is 33,000 lbs/in^2. Typically the deck, overlay, and beams will weigh between 1 and 2 thousand pounds (kips) per linear foot. Therefore, for these problems, assume the weight (dead load) for the structure is 1.5 kips/ft per beam.

3.3.1 Allowable Stress Rating Example

We will rate the bridge considering an HS20 vehicle.

Span, c-c bearing, L = 25 ft

Beams = 6-W24X68

F_y = 33,000 lbs/in^2

Spacing of beams, c-c = 7'-10", or 7.83 ft.

Dead load, w_d = 1500 lbs/beam, or 1.5 kips/beam

Rating vehicle = HS20

1. Total Moment Capacity, M_t, per beam.

$M_t = (1/12) \times F_b \times S_x$

where S_x = 154 in^3, F_{bi} (inventory rating stress) = $0.55F_y$,

F_{bo} (operating rating stress) = $0.75F_y$, and 1/12 converts in. to ft.

$F_{bi} = 0.55(33{,}000) = 18{,}150$ psi or rounded to 18,000 psi

M_{ti} = (1/12)(18,000)(154)/1,000 = 231 ft-kips/beam (inventory)

F_{bo} = 0.75(33,000) = 24,750 psi

M_{to} = (1/12)(24,750)(154)/1,000 = 317.6 ft-kips/beam (operating)

2. Dead Load Moment, M_d, per beam.

$M_d = w_d L^2/8 = (1.5)(25)^2/8 = 117.2$ ft-kips

3. Available Live Load Moment, M_L.

$M_{Li} = M_{ti} - M_D = 231.0 - 117.2 = 113.8$ ft-kips (inventory)

$M_{Lo} = M_{ti} - M_D = 317.6 - 117.2 = 200.4$ ft-kips (operating)

4. Required Live Load Moment Capacity, M_r.

Determine moment, M_{HS}, from a simple statical analysis for a HS20 vehicle on a simple supported, 25 ft span. The impact adjustment, I, is obtained by taking 50/(L + 125) where L is the span length and I is no larger than 0.3. The distribution factor, DF, is determined from the AASHTO Bridge Specifications, Art 3.23.2.2, and is found to be S/5.5 for a concrete deck on steel I-beam girders with two-lane traffic.

I = 50/(25 + 125) = 0.33, I = 0.30 Therefore, impact factor = 1.30

M_{HS} = 103.7 kip-ft/wheel line

$M_r = M_{HS}$ x 1.3 x S/5.5 = (103.7)(1.3)(7.83/5.5) = 191.9 kip-ft/beam

5. Safe Load Capacity Rating

Determine rating factor $RF_{(inv)}$ and $RF_{(opr)}$.

$RF_{(inv)} = 113.8/191.9 = 0.59$

$RF_{(opr)} = 200.4/191.9 = 1.05$

Compute the inventory and operating rating for a HS vehicle by multiplying the appropriate rating factor by the HS designation in tons.

Inventory rating = $RF_{(inv)}$(HS20) = (0.59)(HS20) = HS11.8

Operating rating = $RF_{(opr)}$(HS20) = (1.05)(HS20) = HS21.0

Using an Allowable Stress analysis, the bridge ratings for the girders of this steel bridge (based on moments) are:

Inventory:	HS11.8	Gross weight: 21.2 tons
Operating:	HS21.0	Gross weight: 37.8 tons

Note that the gross weight of the HS vehicle is 1.8 times the designation number in tons. Hence the gross weight of the HS21.0 vehicle would be 37.8 tons.

3.3.2 Load Factor Rating Example

We will now consider the simple supported steel girder bridge used in the Allowable Strength example using a Load Factor analysis as described in the *Manual for Maintenance Inspection*. [10]. Again, an HS20 vehicle will be used as the rating vehicle.

Span, c-c bearing, L = 25 ft

Beams = 6-W24X68

$F_y = 33{,}000$ lbs/in^2

Spacing of beams, c-c = 7'-10", or 7.83 ft.

Dead load, w_d = 1500 lbs/beam, or 1.5 kips/beam

Rating vehicle = HS20

The general expressions are:

Inventory Strength Analysis:

$\Phi S_u = 1.3[D + (5/3)(RF)(L + I)] \leq$ Maximum Strength

and

$\Phi S_u = [D + (5/3)(RF)(L + I)] \leq$ Serviceability Strength

Operating Strength Analysis:

$\Phi S_u = 1.3[D + RF(L + I)] \leq$ Maximum Strength

and

$\Phi S_u = [D + RF(L + I)] \leq$ Serviceability Strength

where:

Φ = Capacity reduction factor, 1.0 for steel in bending.

S_u = Maximum strength, M_u for bending,

(for steel, $M_u = F_y Z$ where Z = plastic section modulus)

1. Moment capacity of the beam, M_u.

$M_u = (1/12) \times F_y \times Z = (1/12)(33{,}000)(177)/1000 = 486.8$ ft-kips /beam

2. Dead load moment, M_{DL}.

From the Allowable Strength example, M_{DL} = 117.2 ft-kips

3. Live load moment, M_{LL}.

M_{LL} will be L, the rating moment, in the equation. The live load moment, M_{HS}, for a wheel line is found in the Allowable Strength example as 103.7 ft-kips. Also the DF = 7.83/5.5 = 1.42 and the impact factor = 1.30 as before.

$M_{LL} = M_{HS}$ x DF = (103.7)(1.42) = 147.25 ft-kips /beam

and

L = 147.25 ft-kips/beam

3. Determine rating factors, RF_o and RF_i.

$RF_o = [M_u - 1.3 \times D]/[1.3 \times l \times (1+I)]$

for a compact, noncomposite section

$RF_o = [486.8 - (1.3)(117.2)]/[(1.3)(147.25)(1 + 0.3)] = 1.34$

$RF_i = 3/5 \times RF_o = (3/5)(1.34) = 0.81$

Assume serviceability strength does not control and use $RF_i = 0.81$.

4. Determine operating and inventory ratings

Operating rating = RF_o x HS20 = (1.34)(HS20) = HS26.8

Inventory rating = RF_i x HS20 = (0.81)(HS20) = HS16.1

The ratings for this bridge, based on the bending moment, using a load factor analysis are thus:

Inventory:	HS16.1	Gross weight: 28.9 tons
Operating:	HS26.8	Gross weight: 48.2 tons

3.3.3 Load & Resistance Factor Rating Example

We will again consider the simple supported steel girder bridge with a noncomposite reinforced concrete deck used in the previous two examples. The AASHTO *Guide Specifications* [12] will be used to determine a capacity based on an HS20 loading as the rating vehicle. AASHTO girder distribution factors are to be used, and it is assumed that the bridge is on a low volume rural roadway, ADT of 1200, in a mining area far from effective enforcement. An inspection of the bridge is made every two years by a trained bridge inspection team supervised by a qualified engineer. Maintenance of the roads in the area is limited.

Span, c-c bearing, L = 25 ft

Beams = 6-W24X68

F_y = 33,000 lbs/in^2

Spacing of beams, c-c = 7'-10", or 7.83 ft.

Dead load, w_d = 1500 lbs/beam, or 1.5 kips/beam

Rating vehicle = HS20

Wearing surface condition is poor

AASHTO distribution is used

Low volume roadway, no effective enforcement of loads

Redundant structure since six girders

Superstructure condition fair

Inspection good

Maintenance intermittent

The *Guide Specifications for Strength Evaluation of Existing Steel and Concrete Bridges* [12] utilizes the rating equation:

$$\phi R_n = \mu_d D + \mu_L (RF)(L)(1+I)$$

or

$$RF = [\phi R_n - \mu_d D]/[\mu_L L(1 + I)]$$

where

I	= Impact Factor
L	= nominal live load effect
D	= nominal dead load effect
RF	= rating factor
R_n	= nominal strength or resistance
μ_d	= dead load factor
μ_L	= live load factor
ϕ	= resistance factor (capacity reduction)

1. Nominal strength or resistance, R_n, per beam.

Assume the bending moment, M_n, is the controlling strength resistance per beam for the bridge. Hence, M_n is to be determined and substituted into the above equation for R_n.

$$M_n = (1/12) \times F_y \times Z_x$$

where Z_x is the plastic modulus and is equal to 177 in^3 for a W24 x 68 section. The yield stress, F_y, is equal to 33,000 lb/in^2 for this laterally supported beam. The 1/12 converts inches to feet.

$M_n = (1/12)(33,000)(177)/1,000) = 486.8$ ft-kips/beam

2. Dead load moment, M_{DL}.

From the two previous examples, $M_{DL} = 117.2$ ft-kips/beam. This dead load moment would be substituted into the above formula for D.

$M_{DL} = 117.2$ ft-kips/beam

3. Live load moment, M_{LL}.

Again from the two previous examples, $M_{LL} = 147.25$ ft-kips/beam.

4. Determine rating factor, RF.

The above equation is utilized to determine the rating factor , the terms ϕ, μ_d, μ_L and I are determined from the tables given in the AASHTO Guidelines.

ϕ = 0.9 for a redundant structure in fair condition that has had a careful inspection but only intermittent maintenance.

μ_d= 1.2 for a wearing surface that has been measured.

μ_L= 1.65 for low volume road, significant sources of overloads without effective enforcement.

I = 0.2 for poor condition wearing surface.

There is no reduction for live load due to the number of lanes and no correction for the distribution factor .

$$RF = [\phi R_n - \mu_d D]/[\mu_L L(1 + I)]$$

$$RF = [(0.9)(486.8) - (1.2)(117.2)]/[(1.65)(147.25)(1 + 0.2)] = 1.02$$

5. Compute bridge rating.

Rating = RF x Rating Vehicle = (1.02)(HS20) = HS20.4

Therefore,

Rating: HS20.4 Gross weight: 36.7 tons

For more details on the factors used in this procedure, please see reference [13].

As can be seen from the examples presented, the Allowable Stress and the Load Factor methods yield both inventory and operating ratings. On the other hand, the Load and Resistance Factor method gives a single overall rating factor which takes into consideration enforcement issues, traffic volume, and inspection thoroughness. In the case presented, the Allowable Stress method results in more conservative values than the Load Factor method. In this case, the rating factor given by the Load and Resistance Factor method is not as conservative as the Allowable Stress method, but it does approximate the average of the inventory and operating rating given by the Load Factor method.

Chapter 4

A COMPLETE BRIDGE LOAD TEST EXAMPLE

4.1 Description of Delaware Bridge #138

During the summer of 1994, the University of Delaware performed its first diagnostic field test on a bridge near Wilmington, Delaware. This test was part of a project called "Evaluation of Posted Bridges" that the University of Delaware conducted for the Delaware Department of Transportation. The purpose of the project was to investigate posted bridges in Delaware and to determine whether or not the restrictions could be removed. Bridge Diagnostics Inc. (BDI) from Boulder, Colorado helped with the field test.

The bridge that was tested is known as Bridge #138 over the Red Clay Creek. It carries traffic from the much traveled Lancaster Pike. This bridge is a skewless, non-composite slab-on-steel-girder bridge built in 1939. Its three spans are simply-supported and non-composite as shown in Figure 4.1. The bridge's dimensions in plan and elevation views are also shown in Figure 4.1. As can be seen, the center span contains nine girders with the two W36X194 facia girders being fully encased in concrete. The seven interior girders are W36X170. All girders were imbedded into the deck (underside of flange flush with the deck). Because it was the controlling span for the posting rating, only the center span was tested.

Inspection reports on Br-138 indicated that corrosion (and associated loss in section) has played a major role in causing the bridge to be posted. Cover plates were welded onto the flanges of some of the diaphragms due to extensive corrosion.

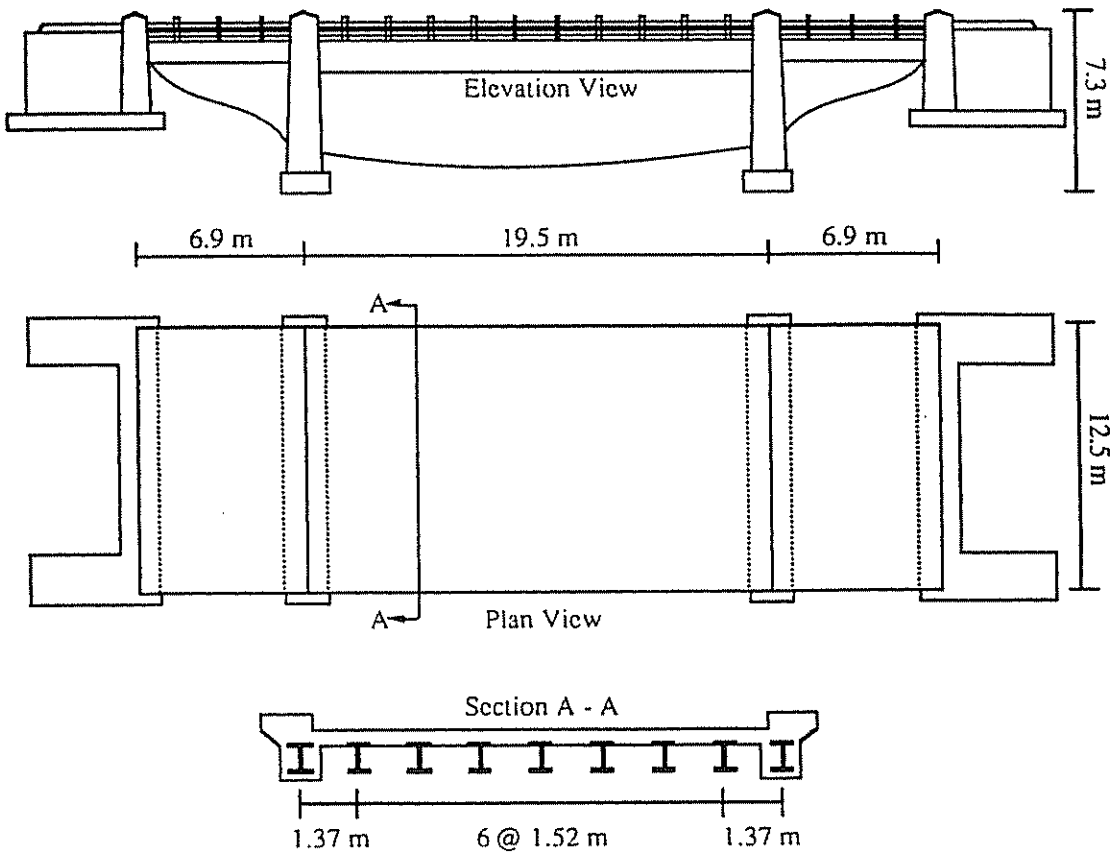

Figure 4.1 Lancaster Pike Bridge Plan and Elevation
Source: [18]

One of the main span girders showed corrosion around one of its supports. Another repair was also made in which the ends of the main span girders were welded to their supports, thus restricting longitudinal movement. As a result of the longitudinal movement restriction, the piers below the two support locations showed several cracks. Other concrete deterioration included spalling of the parapet wall tops until the reinforcing steel became visible. The bridge had recently been repainted to help

The bridge had recently been repainted to help prevent further corrosion. Inspection reports also indicated that nearly 11 inches of asphalt overlay had been applied and accumulated over the life of the bridge.

It was mentioned above that corrosion had occurred on a few of the girders at one of their supports. When the bridge was evaluated for posting, the interior girders were assumed to have 0.125 of an inch loss in section around the entire cross-sectional area for the entire length of the girder (due to the corrosion). In a more careful inspection, it was found that nearly all of the corrosion loss occurred near the supports, and not at midspan where the moment is largest. Therefore, the posting rating calculated according to the above assumption was likely quite conservative. The field test results helped determine how conservative that assumption was.

4.2 Field Test of Delaware Bridge #138

A semi-static diagnostic load test was then performed on the bridge in July of 1994. The bridge was completely instrumented and tested in approximately five hours. The instrumentation and the testing procedure will now be described.

4.2.1 Instrumentation and Testing

Since the center span controlled the bridge rating, it was the only span instrumented. A total of 32 re-usable strain transducers were installed. The strain transducers all measured 76.2 mm (3 in.) except for the 4 transducers attached to the concrete-encased fascia girders. They measured a total of 381.2 mm (15 in.) with the addition of a 305 mm (12 in.) extension. The shorter transducers are sufficient to monitor strains in steel and compressive strains in concrete, but they cannot provide accurate strain readings for concrete in tension if cracking occurs. Longer transducers

allow an average strain to be taken over a longer gage length thereby minimizing the effects of the high localized strains resulting from tensile cracking.

All nine girders were instrumented at midspan. Four of the girders were also instrumented at a location approximately 3.18 m from the girder end, which was about halfway between the girder end and a diaphragm. All locations, except for one, contained two transducers, one on the girder's top flange and another on the girder's bottom flange. The exception was the one location at the midspan of one fascia girder where four transducers were attached along the depth of the concrete-encased fascia girder. Figure 4.2 shows the instrumentation plan where "T" and "B" denote top flange and bottom flange respectively.

Attaching the transducers to the girders, whether on steel or concrete, was relatively easy. The bottom transducers were installed by using two c-clamps to clamp them onto the bottom flange. Attaching the transducers to the girder's top flange was a little more involved since the flange was flush against the deck bottom. Once the transducer location was identified, the paint in the vicinity of the transducer mounting tabs was ground off down to bare steel with a disc grinder. A quick-setting (about 10 seconds) adhesive was then used to mount the transducer. The same process was performed for the transducers mounted on the concrete, except the concrete surface had to be cleaned with the grinder for proper adhesion. After the transducers were attached at their proper locations, sets of four transducers were connected to a junction box which in turn was connected to the digital data acquisition system.

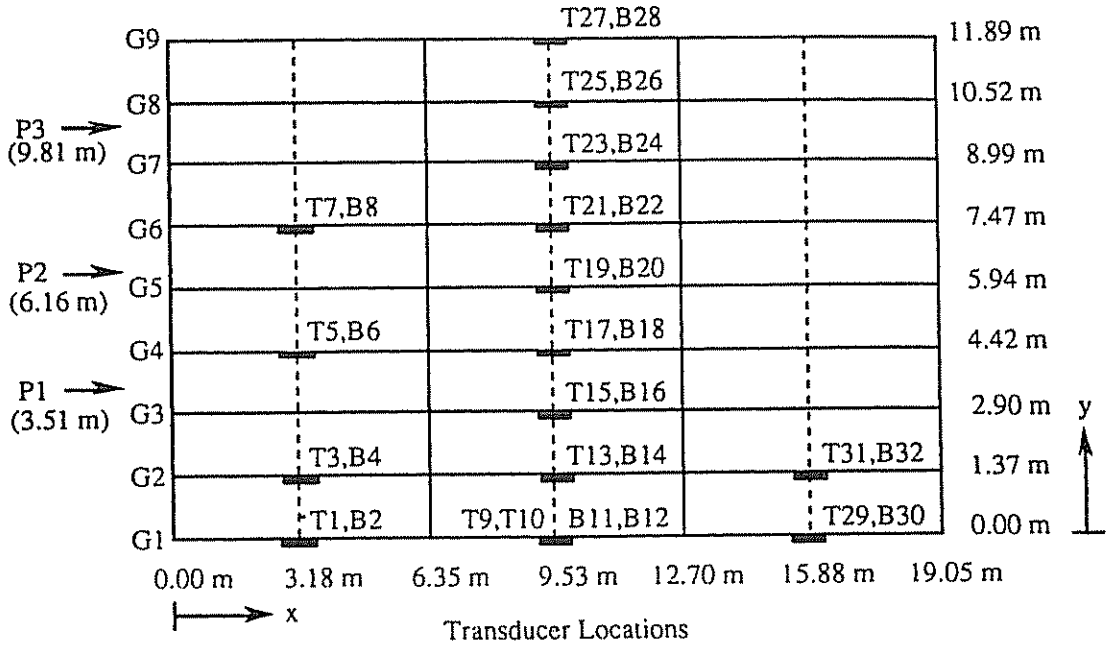

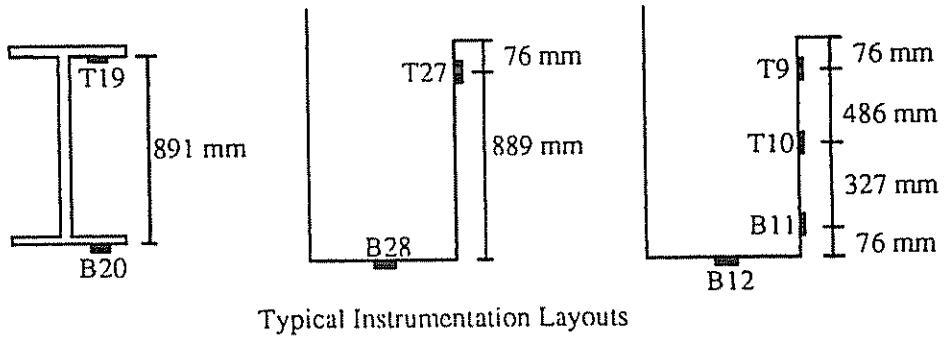

Figure 4.2 Gage Layout and Truck Pass Locations
Source: [18]

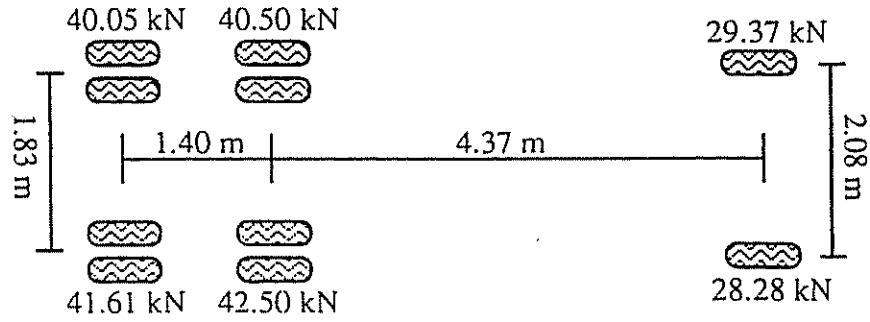

Figure 4.3 Test Truck Weight Distribution
Source: [18]

Therefore, the total instrumentation set-up consisted of 32 strain transducers connected to eight junction boxes which connected to the data collection system.

4.2.2 Test Loading

The test vehicle configuration used to load the bridge is shown in Fig. 4.3. This vehicle is a three-axle, single unit truck with a total weight of 223 kN (25 tons). When choosing the test vehicle weight, it is important not to stress the bridge beyond its linear-elastic range. For a three-axle configuration this bridge had a posting rating of 231 kN (26 tons) which was a little more than the actual test vehicle. To verify that the bridge response remained in the linear-elastic range, all of the strain responses were checked to make sure they went back to zero after each unloading.

In order to lay out the truck paths and the increment markers, a point of origin on the bridge must be chosen. For this particular bridge, the lower left corner of the plan view of the center span was chosen to be the origin. From this origin point, three load path locations were chosen according to the driver's side front wheel as shown in Figure 4.4. A temporary chalk layout along each load path indicated 10 ft.

increments. While the vehicle driver drove along the longitudinal chalk path at approximately 8 km/hr (5 mph), one of the testing personnel rode on the truck and clicked his position indicator when the front wheel passed over each 10 ft. increment marker. The position indicator sent a signal to the data acquisition system so it would record the data at that moment. This procedure allowed personnel to know the location of the truck in relation to the collected strain data. All three passes were repeated to check for consistent results. Since each pass took only about one minute, traffic was disrupted only briefly.

4.2.3 Test Results

After the test had been completed, examination of the data revealed that a maximum strain of 73 microstrain was recorded. It occurred at transducer 16 during the loading of pass P1 (see Figure 4.2).

A strain of 73 microstrain corresponds to a live load stress of 14.5 MPa (2.1 ksi), which is well below the allowable total live plus dead load stress value of 227.9 MPa (33ksi) for aged A36 steel. Discused below are some of the bridge properties that contributed to making the above measured stress lower than might be expected according design and analysis.

4.3 Properties Determined from Load Test Data

As a result of the diagnostic test performed on this bridge, a few significant properties of the bridge were determined. These properties included the lateral distribution factor, the support restraint, and the extent of unintended composite action. Three different load paths were utilized so that a lateral distribution factor could be computed. Some evidence of support restraint was displayed by the

longitudinal strain distribution along the girders. A look at the strain distribution along the depth of the girders showed definite composite action. All three of these findings are discussed below. Their derivation is not discussed in great detail because the focus of this thesis is the derivation of bridge load ratings once these properties have been determined. A more detailed discussion can be found in references [2] and [18].

4.3.1 Lateral Distribution Factor

If one independent girder is loaded, that lone girder carries the whole load itself. There are no other members to help support the load and relieve some of the stress in that girder. On the contrary, when that girder is part of a bridge span, the bridge deck interacts (as long as the girder spacing is no wider than 14 ft.) to distribute the load out to the other girders. There are many factors that affect how much distribution actually takes place. These factors include such things as the type of deck, stringer spacing, secondary member spacing, primary member stiffness, bracing detail and size and position of loads [14]. AASHTO [10] suggests simple formulae to estimate the distribution effects. These formulae incorporate the type of deck and stringer spacing. In general, the formulae tend to be conservative.

The transverse distribution factor for this multiple lane bridge according to AASHTO is the girder spacing divided by 5.5 (S/5.5). Therefore, the AASHTO distribution factor is 0.91. It was determined that the distribution factor was more like 0.71 according to a finite element model. Instead of the girders each having to carry 0.91 times the truck wheel loads (one half of the total truck weight) according to design, they are actually feeling only 71% of the truck wheel loads. This improved

transverse load distribution will lead to a higher computed bridge capacity since the load is being transversely distributed more than it was originally assumed

It is desirable to have an easier method than FEM analysis. Another simpler way to compute a distribution factor based solely on the measured strains, was devised. When the load test was performed, the bridge was loaded with a single truck. The distribution factor calculated using the strains from the test data is for a single lane loading. Looking at Figure 4.4 on the following page, half (one wheel line) of the sum of the strain values along the midspan are:

$$[7.5 + 15.7 + 49.5 + 53.1 + 38.3 + 35.9 + 14.5 + 7.9 + 1.0]/2 = 111.7$$

The single lane DF is then found by dividing the peak tensile strain (53.1 in this case) from the test and dividing it by the 111.7. This load path yielded a DF of 0.48. A single vehicle distribution factor of 0.52 was determined when all three load paths were averaged for this bridge. This compares to 0.71 determined using the AASHTO [10] formula of S/7.0 for single lane loading. Therefore, the load test data shows a 27% increase in lateral load distribution.

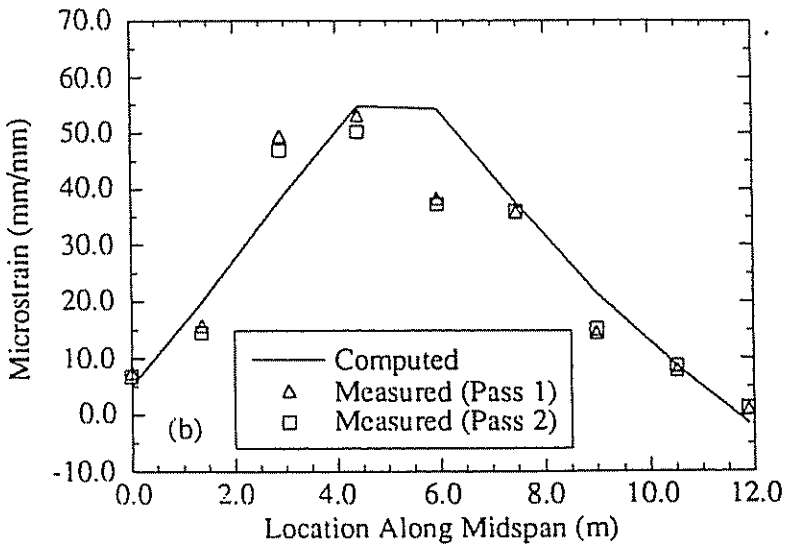

Figure 4.4 Transverse Strain Distribution
Source: [18]

Using multiple lane loading, which involved utilizing a sophisticated finite element model, a 28% increase in lateral distribution was indicated. The reader will see later in the BRASS analysis of this bridge that the capacity was improved by 27% using the multiple lane loading distribution factor. This example demonstrates that the single lane distribution gives a reasonable estimate of the difference in transverse load distribution as compared to using more complicated multiple lane loading analysis. Based on this hypothesis, within a couple hours after a bridge test, one should be able to determine a reliable influence on the bridge capacity due to the actual transverse load distribution.

4.3.2 Bearing Rotational Stiffness

A bridge is designed with the assumption that there is no rotational stiffness at the bearings of a simply-supported span. According to Bakht [15], one test showed evidence of enough elastomeric bearing restraint force developed "to reduce the applied load moments at midspan by a significant margin." Such was the case within this bridge as well. While bridge 138 did not have elastomeric bearings, its girders were welded to their bearing plates as mentioned earlier. A look at the longitudinal strain distribution along each girder reveals that some moment restraint is present at the girder ends. It was assumed that moment restraint was due to the welding of the bearing plates. Further analysis of the strain data along with the relationship of the end-to-midspan moment ratio to the rotational spring stiffness led to an end rotational stiffness of 18,325 in-kips/deg. While end restraint was found, it was not used in the rating of the bridge because the bearing supports were deteriorated too much to rely on future rotational [18].

4.3.3 Girder/Deck Composite Action

Many bridges that were built before 1950, such as this one, were built with no shear connectors between the primary steel girders and the concrete deck. For that reason, those bridges are not expected to act compositely. However, due to friction, chemical bonding, and some unforeseen mechanical interlock, many of these bridges do exhibit unintended composite action. "Unintended composite action is the most frequent and often largest source of unexpected capacity in concrete slab and steel girder bridges [16]." The following section discusses how one can determine if unintended composite action exists, and what its effect on the girder/slab cross-sectional properties are.

4.3.3.1 Neutral Axis Location

The location of the neutral axis (NA) in the steel girder is the key indicator as to whether or not the bridge is indeed acting compositely. Locating the neutral axis from a load test is a relatively simple procedure. One takes the location and magnitude of the top and bottom strain readings and by making use of the assumption that plane sections remain plane, can locate the location of zero strain (i.e. NA). For a thorough and illustrated explanation see Reid [2]. It was determined for this bridge that the neutral axis was located at an average of 31.9 inches from the bottom of the tension flange. Since the total depth of a W36X170 girder is 36.16 inches, it is fairly obvious that the bridge deck is acting compositely with the girder.

4.3.3.2 Effective Concrete Slab Thickness

A neutral axis location associated with a composite section also enables one to determine an effective concrete deck thickness. This is done by balancing the compressive forces in the deck with the tensile forces in the girder. For this bridge, the effective concrete slab thickness was determined to be 11 inches. Again, refer to Reid [2] for a detailed explanation of the effective concrete slab thickness. Knowing the effective concrete slab thickness is useful in modeling programs such as BRASS and STAAD.

4.3.3.3 Composite Section Properties

Once that the effective concrete slab thickness and effective width (taken to be one half the girder spacing) is known, it is possible to find the moment of inertia of the girder/slab section by using transformed areas. The average moment of inertia for section of this bridge were found to be 30,300 in^4 for the interior girders and

54,600 in^4 for the concrete-encased fascia girders [18]. A detailed analysis of finding the composite moment of inertia is also found in Reid [2].

Chapter 5

EVALUATING BRIDGE CAPACITY USING LOAD TEST DATA

5.1 Bridge Analysis

The previous chapter discussed how bridge properties can be determined from a load test. While it is useful to know those properties, the real challenge is how to use those properties to rate a bridge. For this project, the properties determined from the load test were used in conjunction with a bridge analysis program called BRASS as well as a bridge rating procedure devised by A.G. Lichtenstein, P.E., Dr. Eng [3].

5.2 BRASS

BRASS stands for Bridge Rating and Analysis of Sructural Systems. The BRASS program was developed by the Wyoming Department of Transportation with sponsorship provided by the Federal Highway Administration [19]. One of the main purposes of BRASS is to obtain inventory and operating ratings according to the *Manual for Maintenance Inspection of Bridges* [10].

BRASS allows a wide variety of structures and materials to be analyzed. Structures can include continuous beam bridges, rigid frame bridges, slant leg structures, and rigid-frame box culverts. Materials can include reinforced concrete, prestressed concrete, structural steel, or timber. In addition to determining ratings, BRASS also enables one to design and review bridge decks and girder sections, as well as perform a structural analysis of the bridge.

The methods of analysis used vary according to the type of structure. A column analogy is used for beam type structures. Cell structures and slant leg frames are analyzed by the slope deflection method. Deflection is calculated by virtual work. BRASS uses a Gauss-Jordan method to invert the resulting matrices for solution of the governing equations.

5.2.1 Using BRASS

BRASS users can supply the as-built information and/or design information according to their needs in a command file. In general, such things as the span descriptions, cross-section properties, end conditions (fixities, springs), dead loads, and live loads are entered in the command file. Depending on the needs of the user, BRASS can perform a rating, design, or analysis of a bridge. Also BRASS is capable of using either Allowable Stress Design or Load Factor Design as. Work is currently in progress to make Load & Resistance Factor Design available.

Information is entered with the bridge being modeled as a single beam. An example of a typical BRASS file is shown in Figure 5.1. Afer the title and type of analysis is chosen, the typical beam cross-section is described and designated to a particular span. Along with each series of commands for each span is a command to describe the end restraints. Once the structure is laid-out, the loads are entered. Typically the load input starts with the dead loads and ends with the live load information. The live-load command is where the distribution factor is entered. If live-loads are to be applied, then the next set of commands describe what vehicles or what axle loading and configurations are to be applied. Next the type of design and rating factor variables are entered. At the end of the command file, the locations on the spans where the bridge is to be rated are input. For example, it is obvious on a

simple span bridge that the mid-span is the critical section for rating the bridge according to moment. Discussion of some output from BRASS is in the following section.

```
TITLE          BRIDGE NO. 1-138, RD.237(SR48), SOUTH OF WOODDALE, OVER RED CLAY CREEK
TITLE          STEEL BEAM CONC. NON-COMPOSITE, BUILT IN 1940, Ct#673
COMMENT          3-SPAN BR.,MIDDLE BEAM ON MIDDLE SPAN ANALYZED
ANALYSIS         1,0,4
XSECT-A          1,33
XSECT-B          0.68, ,12.027, ,1.10,1.10
XSECT-C          60.0,11.0,-1.0,0.0,0.0,0.0
SPAN-A           1,62.5,1,36.17,36.17
SPAN-C           1,62.5,1
FIXITY           0,1,0,1,1,0
COMMENT FIS                , ,219900, , ,219900
PROPERTIES-ST1   , ,2.5
PROPERTIES-ST2   10.2, ,33
COMMENT          SLAB=531 LBS/FT     W.S.=750 LBS/FT    PARAPET=190 LBS/FT
DEAD-LOAD        1,0.562,.940
LDE              1, , ,DIAPHRAM DEAD LOADS
POINT-DL         0,.274,1,0.0
POINT-DL         0,.274,1,20.83
POINT-DL         0,.274,1,41.66
POINT-DL         0,.274,1,62.5
LIVE-LOAD        3,0.71, ,50
TRUCK-CODE1      H520T,S335
DESIGN           3,0
INVENTORY        0.55,0.4,0.55
OPERATING        0.76,0.55,0.75,
COMMENT          POSTING LEVEL 2
POSTING          0.62,0.45,0.617,
STEEL-1          104,4
STEEL-1          105,4
```

Figure 5.1 Sample BRASS Command File

5.2.2 Evaluating Br-138 Using BRASS

Not only can BRASS be used to design a bridge or rate a bridge according to its design parameters, it can also be used to rate a bridge according to its present condition. Properties that have been determined from load testing can be used for the appropriate parameters in the command file. Table 5.1 shows the effects of different parameters on the posting rating of the Lancaster Pike Bridge using BRASS. The particular parameters that were changed from design based on the testing were the

section moment of inertia (composite and non-composite), the DF, and the support restraint. The largest benefit in terms of load carrying capacity came from the support restraint. Because it was determined that the support restraint was due to plates being welded on by the maintenance crew and the test results showed some level of uncertainty, it was decided not to count on this benefit. The next largest added benefit was due to a better distribution factor. A study of the strain distribution across the bridge by Chajes [18] concluded with an improvement of the distribution factor from 0.91 to 0.71 using the FEM model analysis. An improvement of 35.7% of the total benefit was made due to just the distribution factor benefit. The final beneficial effect was due to the presence of unintended composite action which signified a larger moment of inertia for the girder/slab section. There was no evidence throughout the testing of the composite action being lost. Therefore it was decided to rely on this benefit as well. Combining the benefits of the distribution factor and the unintended composite action yielded a 46% increase in the posting rating from 0.74 to 1.08.

Table 5.1 Benefits Received from Varying BRASS Parameters

FIELD VARIABLES IN BRASS FILES	POSTING RATING	BENEFIT	PERCENTAGE OF IMPROVEMENT
1. Original DelDOT	0.74	N/A	N/A
2. w/ Moment of Inertia	0.85	14.90%	19.70%
3. w/ Distribution Factor	0.94	27.00%	35.70%
4. w/ Non-Composite Action	0.42	-43.20%	N/A
5. w/ Support Constraint	0.99	33.80%	44.60%
6. w/ #2,#3, & #5	1.41	90.50%	N/A
7. w/ #2, #3, & No Support Restraint	1.08	45.90%	N/A
8. w/ #2, #3, #4, & #5	0.88	18.90%	N/A
9. w/ #2, #3, #4, & No Support Restraint	0.53	-28.40%	N/A

Using this method allows the bridge engineer to understand where any increase or decrease in load rating is coming from. For example, of the three parameters that were found to change from original design values, the unintended composite action (increase in I), improvement in load distribution (DF), and unintended support restraint comprise 19.7%, 35.7%, and 44.6% of the total increase in capacity respectively.

Some things that might be worth studying by others could be looking into more detail at the stages of loading and how the different factors come into play at those stages. This would mean understanding more on how BRASS operates and considers each loading stage in comparison to the actual history of the structure. It could be possible some of the modeling using BRASS is not fully accurate but the author is confident any variation does not amount to any significant change.

5.3 Lichtenstein Method

Lichtenstein [3] has devised a method for "modifying the analytical load rating for a bridge based on the results of a diagnostic load test." This method uses the maximum strain or corresponding stress measureduring the diagnostic load test and compares it to the strain or stress predicted theoretically. Any benefit received from a lesser than expected strain is then decreased by factors which consider circumstances surrounding the load test, the type and frequency of inspection the bridge receives, and the redundancy of the bridge structure as well as fatique sensitivity. Below is an example of the Lichtenstein method as it was used on Br-138. To cover the full detail of this procedure is not within the scope of this paper. For the reader to get a full understanding of this procedure, please see the referenced document [3]

5.3.1 Evaluating Br-138 with the Lichtenstein Method

Br - 138, Lancaster Pike Bridge

F_y = 36 ksi

f'c = 4 ksi

Length = 64 ft.

c-c spacing = 5 ft.

Test vehicle width = 6 ft. - 5 in.

The distribution factor is determined by using simple statics and geometry of the loading vehicle at the point where it created the highest strain.

D.F. = 3.0/5.0 + 0.58/5.0 = 0.716

By loading the bridge with the actual test truck, the maximum theoretical moment is:

M_{max} = 664.71 ft-kips

$(M_{max})(D.F.) = (664.71)*(0.716) = 475.9$ ft-kips

During testing, maximum strain recorded in the bridge was 73 microinches which corresponds to a stress of 2.1 ksi (recall that the bridge behaved compositely). Using a section modulus of 580 in^3 for the non-composite section yielded a stress of 9.8 ksi based on the maximum theoretical moment of 5710.8 in-kips. Assuming the section is fully composite yields a section modulus of 812.67 in^3. Full composite action would theoretically demonstrate a stress of 7.03 ksi (strain of

244 microinches). Notice the maximum strain read during testing is considerably lower than even what a full composite section would predict. Therefore, an effective section modulus of 2719.4 in^3 was calculated based on the 2.1 ksi.

Next the value for K_a is determined:

$$K_a = 7.03/2.1 - 1 = 2.33$$

Using the knowledge gained from the prior evaluation (Section 5.2), one realizes that this value reflects the benefit the bridge exhibits without the effect of unintended composite action.

Based on values found in the tables in Ref. [3], the value for K_b was calculated as 0.64. This means only 64% of the benefit received from all factors will be utilized in the final rating. In our case, this means that only 64% of the increase in load carrying capacity due to load distribution, or rotational fixity at the bearings, and a larger moment of inertia due to the 11 inches of asphalt overlay will be counted on. The K_b factor accounts for such things as the inspection frequency and redundancy of the bridge structure. Those values lead to a value of:

$$K = 1 + K_a K_b = 1 + (2.33)*(0.64) = 2.49$$

Thus according to the Lichtenstein method, the rating factor for this bridge can be improved by a factor of 2.5.

5.4 Analytical Modeling

If one chooses, a bridge can be modeled using a finite element analysis. By using plate elements for the bridge deck and beam elements for the girders, finite element analysis can determine the lateral distribution factor and the rating factor for a bridge based on the properties determined from the load test. Finite element models are great for detailed analysis, but they are time consuming and sometimes cumbersome to work with. It is the emphasis of this paper to determine an accurate ways to evaluate a bridge without having to formulate a sophisticated model. With the increase in demand for bridge testing, it is becoming more necessary to devise a straightforward yet accurate method to quickly assess the capacity of bridge.

Chapter 6

BRIDGE TESTING AND EVALUATION CASE STUDIES

6.1 Delaware Bridge 704 - Christina Creek Bridge

On October 30, 1995, the University of Delaware load tested the Christina Creek bridge. The Christina Creek bridge is located just south of Newark, Delaware. It provides crossing over the Christina Creek for traffic heading south on I-95 just north of the Maryland state line. DelDOT chose this bridge for testing due to limited capacity for overload vehicles.

The Christina Creek bridge is a three-span simply-supported bridge built on a 13 degree skew. It was designed compositely with shear connectors between the steel girders and concrete deck. Since its original construction, it has had three rehabilitations with each one expanding the bridge width by two more girders. At its present state, it is 80'-10" wide from centerline to centerline of the outside girders. The approach spans are each 24'-7" while the main span is 63'-2".

6.1.1 Load Test of Christina Creek Bridge

A total of eight passes were made by one three-axle dump truck weighing a total of 34 tons. Six of the passes were semi-static. Four different paths were used. Two of those passes were duplicated to check data redundancy. The last two passes were dynamic, meaning the truck's speed was approximately 55 mph as it crossed the bridge. Data was recorded by 32 strain gages mounted at approximately half and quarter point locations as well as a couple of spots where diaphragms were located.

Due to the bridge spanning a body of water and making girder accessibility difficult, the total field time involved in the test was one full day.

6.1.2 Evaluation of Christina Creek Bridge

The Lichtenstein and BRASS methods were used to evaluate Christina Creek bridge. According to the Lichtenstein method, based on the field test this bridge rating can be increased by a factor of 2.5. The author feels this value is a bit high and warrants more research in the future. Reid [2] found that most of the bridge properties were very similar to the AASHTO [12] design values so there were no obvious properties to change in a BRASS analysis except the distribution factor. The single lane DF was computed to be 0.68, while the AASHTO single lane DF was 1.07. This represents a 36% improvement. Applying this percentage increase to the multiple lane DF from 1.52 to 0.96, leads to an increase in the rating of 122%. This increase was similar to that found for Lancaster Pike bridge.

6.2 Delaware Bridge 791 - Darley Road Bridge

On October 31, 1995, the University of Delaware load tested the Darley Road bridge. It is a three-span, steel girder, continuous bridge with a composite main span and non-composite approach spans. The approach spans each measure 35'-0", and the main span measures 58'-0". The overall width from centerline to centerline of the exterior girders is 35'-10". The bridge provides crossing over Darley Road, a two lane rural in northern Wilmington, DE, for traffic heading northbound on I-95 close to the Pennsylvania state line. Again, DelDOT chose this bridge for testing due to limited capacity for overload vehicles.

6.2.1 Load Test of Darley Road Bridge

A total of eight passes were made by the same testing vehicle used to test the Christina Creek bridge the previous day. Six of the eight passes were semi-static. Three load paths were chosen with each path being tested twice for the test of data redundancy. The last two passes on this bridge were dynamic as well with the truck maintaining a speed of approximately 55 mph. A total of 32 strain gages were used to collect data at various locations on the main span and the approach span. Testing of this bridge took a total of six hours to complete.

6.2.2 Evaluation of Darley Road Bridge

Like before, the Lichtenstein and BRASS methods were used to evaluate the bridge. For this bridge, the Lichtenstein method gave an increase of 1.5 times the original rating factor. That value seems to be more in the vicinity of the capacity improvement found for the other bridges. One of the main reasons the Lichtenstein method provided a more moderate increase for Darley Road bridge as compared to the Christina Creek bridge was that the Lichtenstein method substantially reduces any improvement when the bridge is fatique sensitive, as was the case with the Darley Road bridge. Just like Christina Creek bridge all properties except the distribution factor were found to be consistent with AASHTO values. The single lane DF was computed to be 0.74, while the AASHTO single lane DF was 1.02. This represents a 27% improvement. Applying this percentage increase to the multiple lane DF from 1.30 to 0.94, leads to an increase in the rating of 76%.

Overall, these two bridges seem to have a capacity at least 76% better than originally calculated according to design values. The author personally does not feel

totally comfortable with the values determined by the Lichtenstein method, and would like to see more tests done for comparison.

Chapter 7

CONCLUSIONS

7.1 Conclusions

The objective of this research was to develop a simple, rational method for utilizing load test results to rate bridges. Two methods were investigated: the Lichtenstein method and the BRASS based method. Both methods were used for bridges Br-138, Br-704, and Br-791. The Lichtenstein method indicates increases in ratings of 2.5, 2.5, and 1.53 respectively for the three bridges are warranted. When the BRASS based method was used, increases in ratings of 1.46, 2.22, and 1.77 were indicated for the three bridges respectively.

It should be noted that when the BRASS based method was used, not all of the measured effects were counted on for the final rating. For example, for Br-138, the effects due to unintended support restraint were not considered because it was felt that they may be lost in the future. This can explain some of the difference between the Lichtenstein and BRASS values. For the other two bridges, the only significant parameter that was found to change from design values was the load distribution. This effect was incorporated into the BRASS ratings, and would also have been incorporated in the Lichtenstein method.

Both methods have some beneficial attributes. The Lichtenstein method is simple and uses limited strain data. It accounts for inspection, fatique, redundancy, and test validity. However, it does not attempt to quantify the phenomena leading to

the change in behavior from that predicted theoretically. On the other hand, the BRASS based method utilizes parameters that are computed from the test results. Therefore the change in behavior from predicted is better understood and tied directly to the particular phenomena responsible. The method does not, however, account for inspection, fatique, redundancy, or test validity. As indicated above, the method has the desirable feature of allowing the rating engineer to include only the effects they are comfortable with.

It is the author's opinion that future work should focus on combining the beneficial attributes of the two methods to create a single more optimal procedure.

REFERENCES

1. Fu, G., (1995)."Highway Bridge Rating By Nondestructive Proof-Load Testing For Consistent Safety." Research Report 163, Transportation Research and Development Bureau, New York State Department of Transportation.

2. Reid, J.S., (1996). "Bridge Evaluation and Long-Term Monitoring." Master Thesis, University of Delaware, Newark, DE.

3. Lichtenstein, A.G. (1995), "Bridge Rating Through Nondestructive Load Testing," Final Report, NCHRP Project 12-28(13)A.

4. Pinjarkar, S. G., Guedelhoefer, O.C., Smith, B.J., and Kritzler, R.W. (1990). "Nondestructive Load Testing for Evaluation and Rating." NCHRP Project 12-28(13) Final Report.

5. Tharmabala, T. (1990). "Strength Evaluations of Bridges." *Extending the Life of Bridges,* ASTM STP 1100.

6. Bridge Diagnostics, Inc. (1994). "Instrumentation of the Natchez Trace Arch Bridge." Report submitted to Finley-McNary Engineers, Inc. Bridge Diagnostics, Inc., Boulder, CO.

7. Aktan, A.E., Lee, K.L., Naghavi, R., and Hebbar, K. (1994). "Destructive Testing of Two 80-Year-Old Truss Bridges." *Preprint, TRB Paper 940255,* Transportation Research Board, 73rd Annual Meeting, Washington, D.C.

8. Biswas, M., Pandey, A.K., and Samman, M.M. (1989). "Diagnostic Experimental Spectral/Modal Analysis of a Highway Bridge." *The International Journal of Analytical and Experimental Modal Analysis,* 5(1), 33-42.

9. AASHTO, *Manual for the Condition Evaluation of Bridges,* Washington, D.C., 1994.

10. AASHTO, *Manual for Maintenance Inspection of Bridges,* Washington, D.C., 1990.

11. AASHTO, *Interim Specifications for Bridges,* Washington, D.C., 1976.

12. AASHTO, *Guide Specifications for Strength Evaluation of Existing Steel and Concrete Bridges,* 1989.

13. White, Kenneth R., John Minor, and Kenneth N. Derucher. *Bridge Maintenance Inspection and Evaluation*. New York, NY: Marcel Dekker, Inc., 1992.

14. Tonias, Demetrios E., P.E., *Bridge Engineering*. New York, NY: McGraw-Hill, Inc., 1995.

15. Bakht, B., and Jaeger, L.G. (1990a). "Bridge Testing - A Surprise Every Time." *J. Struct. Engrg.*., ASCE, 116(5), 1370-1383.

16. Edberg, W.M. (1994). "State-of-the-art Survey in Experimental Load Rating of Bridges." Master Thesis, University of Delaware, Newark,DE.

17. Bridge Diagnostics, Inc. (1994). "Load Testing and Rating: Lancaster Pike Over Red Clay Creek" Report submitted to the University of Delaware, Bridge Diagnostics, Inc., Boulder, CO.

18. Chajes, M.J., Mertz, D.R., and Commander, B., "Experimental Load Rating of a Posted Bridge," ASCE Journal of Bridge Engineering, (In Press).

19. Wyoming Department of Transportation, *Bridge Rating and Analysis of Structural Systems*. Computer Program, March, 1996.

Appendix

USING THE LICHTENSTEIN METHOD FOR BR-704 AND BR-791

Lichtenstein Method for Br-704

Br - 704, Cristina Creek Bridge

F_y = 36 ksi

f'c = 4 ksi

Length = 62 ft. - 6 in.

c-c spacing = 8 ft. - 4in.

Test vehicle width = 7 ft.

The distribution factor is determined by using simple statics and geometry of the loading vehicle at the point where it created the highest strain during the field test.

D.F. = 6.17/8.33 + 3.5/8.33 = 1.16

By loading the bridge with the actual test truck, the maximum theoretical moment is:

M_{max} = 438.79 ft-kips

(M_{max})(D.F.) = (438.79)*(1.16) = 509.0 ft-kips

During testing, maximum strain recorded in the bridge was 102 microinches which corresponds to a stress of 2.9 ksi. Assuming the section is fully composite yields a section modulus of 717.0 in^3. Theoretically, the strain would have been 294 microinches which gives a stress of 8.4 ksi.

Next the value for K_a is determined:

$$K_a = 294/102 - 1 = 1.88$$

This value gives the increase in capacity due based on theoretical versus actual strain.

Based on values found in the tables in Ref. [3], the value for K_b was calculated as 0.8. This means only 80% of the benefit received from factors such as better distribution factors is counted on due to knowledge of such things as the inspection frequency or redundancy of the bridge structure. Those values lead to a value of:

$$K = 1 + K_a K_b = 1 + (1.88)*(0.8) = 2.5$$

Thus according to the Lichtenstein method, the rating factor for this bridge can be improved by a factor of 2.5.

Lichtenstein Method for Br-791

Br - 791, Darley Road Bridge

$F_y = 36$ ksi

f'c = 4 ksi

Length = 58 ft.

c-c spacing = 7 ft. - 2 in.

Test vehicle width = 7 ft.

The distribution factor is determined by using simple statics and geometry of the loading vehicle at the point where it created the highest strain during the field test.

D.F. = 5.33/7.17 + 2.0/7.17 = 1.02

By loading the bridge with the actual test truck, the maximum theoretical moment is:

M_{max} = 239.2 ft-kips

$(M_{max})(D.F.) = (239.2)*(1.02) = 244.0$ ft-kips

During testing, maximum strain recorded in the bridge was 133 microinches which corresponds to a stress of 3.8 ksi. Assuming the section is fully composite yields a section modulus of 758.21 in^3. Theoretically, the strain would have been 244 microinches which gives a stress of 7.0 ksi.

Next the value for K_a is determined:

$K_a = 244/133 - 1 = 0.83$

Based on values found in tables in Ref. [3], the value for K_b was calculated as 0.64. This means only 64% of the benefit received from factors such as better distribution factors is counted on due to knowledge of such things as the inspection frequency or redundancy of the bridge structure. The fact that this bridge was fatique sensitive helped to reduce any increase in rating. Those values lead to a value of:

$$K = 1 + K_a K_b = 1 + (0.83)*(0.64) = 1.53$$

Thus according to the Lichtenstein method, the rating factor for this bridge can be improved by a factor of 1.53.

Delaware Center for Transportation
University of Delaware
Newark, Delaware 19716